



AN ABSTRACT OF THE THESIS OF

Jackson Keppen for the degree of Master of Science in Nuclear Engineering presented on  
June 11, 2020.

Title:

Feasibility Study of a Thermal Spectrum Thorium Breeder Reactor Without Chemical Reprocessing

Abstract approved: \_\_\_\_\_

Camille J. Palmer

Todd S. Palmer

This thesis presents a feasibility study of a thorium fueled thermal spectrum breeder-burner reactor that operates without chemical reprocessing. Materials were evaluated for their potential as moderators using standard analytical methods. These materials were then used as moderators to evaluate criticality and enrichment in an infinite fuel pin lattice. The criticality and heavy metal mass of the system as a function of burnup were then used to calculate a neutron balance for each case. The neutron balance indicated that there are insufficient neutrons available in an infinite lattice to operate in a breed-and-burn configuration. A core model was developed to confirm the results of the infinite lattice. Design bounds were developed from the lattice investigation, and used by an optimization routine to evaluate reactor cores with one-quarter symmetry. The black-box optimization program, Gnowee, coupled to the neutronics and depletion code, SCALE, was used to facilitate the process. This procedure required the development of an automated core generation tool that could read the output perturbations from Gnowee and translate that into a new input for SCALE, and a tool to read the output of SCALE to inform the objective function and constraints in Gnowee. None of the core configurations operated with breeding while remaining critical. A two-region infinite lattice using annular fuel pins with enriched breeder blankets was used to test alternative fuel swapping schemes. The two-region infinite lattice analysis indicated that fuel in an annular geometry with an enriched blanket could remain critical while breeding in a breeder-burner configuration.

©Copyright by Jackson Keppen

June 11, 2020

All Rights Reserved

Feasibility Study of a Thermal Spectrum Thorium Breeder Reactor Without Chemical  
Reprocessing

by  
Jackson Keppen

A THESIS

Submitted to:

Oregon State University

in partial fulfillment of  
the requirements for the  
degree of

Master of Science

Presented June 11, 2020  
Commencement June 2021

Master of Science thesis of Jackson Keppen presented on June 11, 2020.

APPROVED:

---

Co-Major Professor, representing Nuclear Engineering

---

Co-Major Professor, representing Nuclear Engineering

---

Head of the School of Nuclear Science and Engineering

---

Dean of the Graduate School

I understand that my thesis will become part of the permanent collection of Oregon State University libraries. My signature below authorizes release of my thesis to any reader upon request.

---

Jackson Keppen, Author

## ACKNOWLEDGMENTS

First and foremost, I would like to thank Dr. Todd Palmer and Dr. Camille Palmer for their guidance and assistance in this thesis process. It is because of them that I have been able to start this process and develop the network of people that has furthered my career. I want to thank my research group that I met through the Drs. Palmer, especially Ryan Stewart and Emory Colvin for all of their help in optimization and thesis writing.

I would also like to thank all those from NuScale Power for their roles in this endeavour. I want to thank Dr. Jose Reyes and NuScale Power for supporting this project and funding this research. I also have to give a huge thank-you to Derick Botha, who started this project and has helped to guide me through every step of the process with his unerringly accurate predictions. This project could not have happened without him. I must give a special thanks to Dr. Azat Galimov, may he rest in peace, for his assistance in writing code for Python and Linux, as well as sense of humor and pleasant company.

I must thank my dear friends and family who listened to my complaints and offered support through this process. I want to thank my mother and father, Dena and Dan, for supporting me in a myriad of ways through 18 straight years of school. I want to thank all of my friends for understanding canceled plans and stressed conversations. I have to give another special acknowledgement to Dee Hahn, my high school calculus teacher, tennis coach, and dear friend, who would be more disappointed than anyone else if I had not tried to get this degree. Finally, I want to thank my incredible wife, Hayley, who I would be utterly lost without. There are not words enough to describe how she has helped me.

Thank you all so much. This has been an incredible journey, and I am excited for what comes next.

# TABLE OF CONTENTS

	<u>Page</u>
1 Introduction	1
1.1 Thorium Fuel Cycle . . . . .	2
1.1.1 Chemical Reprocessing . . . . .	3
1.2 Reactor Physics . . . . .	3
1.2.1 Benefits of a Thorium Fuel Cycle . . . . .	13
1.3 Breeder Reactor Designs . . . . .	15
1.3.1 LWBR . . . . .	15
1.3.2 Molten Salt Reactors . . . . .	18
1.3.3 Moltex . . . . .	19
1.3.4 Fast Reactors . . . . .	19
1.3.5 Breeder-Burner Reactors . . . . .	20
1.3.6 Analytic Breeding Studies . . . . .	22
1.4 Optimization Strategies . . . . .	24
1.4.1 Optimization Methods in the Nuclear Field . . . . .	26
1.4.2 Surrogate Modeling . . . . .	27
1.5 Objectives . . . . .	27
2 Methods	29
2.1 Introduction . . . . .	29
2.2 Software . . . . .	29
2.2.1 Gnowee Optimization Code . . . . .	29
2.2.2 SCALE Transport and Depletion Code . . . . .	31
2.2.3 Coupling SCALE and Gnowee . . . . .	32
2.3 Engineering Judgments . . . . .	37
2.4 Reduction of Order Method . . . . .	39
2.4.1 Geometry and Materials . . . . .	40
2.5 Infinite Homogeneous Model . . . . .	43
2.6 Infinite Lattice Pin Analysis . . . . .	44
2.6.1 Neutron Balance Equation . . . . .	45
2.6.2 Fission Product Removal Effects . . . . .	46
2.7 Quarter-Core Analysis . . . . .	47
2.8 Two-Region Lattice . . . . .	49

TABLE OF CONTENTS (Continued)

	<u>Page</u>
3 Results	53
3.1 Introduction . . . . .	53
3.2 Reduction of Order . . . . .	53
3.3 Infinite Homogeneous Model . . . . .	54
3.4 Infinite Lattice Pin Analysis . . . . .	54
3.4.1 Fission Product Removal Effects . . . . .	55
3.4.2 Moderation Curves . . . . .	56
3.4.3 Trends for Fissile Isotope Ratio and $k_{inf}$ . . . . .	60
3.4.4 $k_{inf}$ , $^{233}\text{U}$ Enrichment, and Neutron Balance vs Burnup . . . . .	64
3.5 Quarter-Core Analysis . . . . .	82
3.6 Two-Region Lattice . . . . .	84
4 Discussion and Conclusions	89
4.1 Discussion . . . . .	89
4.1.1 Reduction of Order Study . . . . .	89
4.1.2 Infinite Homogeneous Model . . . . .	89
4.1.3 Infinite Lattice Pin Model . . . . .	90
4.1.4 Quarter-Core Analysis . . . . .	93
4.1.5 Two-Region Lattice . . . . .	95
4.2 Summary and Future Work . . . . .	95
4.2.1 Summary . . . . .	96
4.2.2 Future Work . . . . .	96
Appendices	103
A Additional Moderation Curves	104
A.1 $^{233}\text{U}$ Concentration and $k_{inf}$ . . . . .	104
A.1.1 Metallic Moderator $k_{inf}$ . . . . .	104
A.1.2 Metallic Moderator $^{233}\text{U}$ Concentration . . . . .	105
A.1.3 Metallic Moderator Neutron Balance . . . . .	105
A.1.4 Low Moderator Density Metallic Moderator $k_{inf}$ . . . . .	106
A.1.5 Low Moderator Density Metallic Moderator $^{233}\text{U}$ Enrichment . . . . .	106
A.1.6 Low Moderator Density Metallic Moderator Neutron Balance . . . . .	107



TABLE OF CONTENTS (Continued)

	<u>Page</u>
A.1.7 Graphite Moderated $k_{inf}$ . . . . .	107
A.1.8 Graphite Moderated $^{233}\text{U}$ Concentration . . . . .	108
A.1.9 Graphite Moderated Neutron Balance . . . . .	108
A.2 Two-Region $k_{inf}$ and $^{233}\text{U}$ Concentration . . . . .	109
A.3 Other Moderator Curves . . . . .	113

## LIST OF FIGURES

Figure	Page
1.1 Cross sections of $^{233}\text{U}$ and $^{232}\text{Th}$ . . . . .	4
1.2 Neutrons released from fission per neutron absorbed . . . . .	6
1.3 Comparison of moderator-fissile isotope ratio and pitch-to-diameter ratio for varying enrichment in a novel metallic moderator. . . . .	10
1.4 Comparison of moderator-fissile isotope ratio and pitch-to-diameter ratio for varying moderator density. . . . .	11
1.5 $k_{eff}$ as a function of H-fissile ratio. . . . .	12
1.6 Cross section of LWBR core . . . . .	16
1.7 LWBR conversion ratio and neutron sinks as a function of operation time . . . . .	18
1.8 Zero dimension neutron balance and $k_{eff}$ . . . . .	21
1.9 Converting pin geometry to ring geometry . . . . .	22
1.10 Maximum theoretical breeding ratio as a function of the slowing down power per fuel atom ratio for $^{233}\text{U}$ fuel at 900K . . . . .	23
1.11 Maximum theoretical breeding ratio as a function of moderator to fissile ratio . . . . .	24
2.1 A high-level flowchart describing the process that Gnowee uses to optimize a problem. . . . .	34
2.2 A high-level flowchart describing the process that couples SCALE to Gnowee. . . . .	36
2.3 A high-level flowchart describing the application of the constraint function after the objective function has been solved. . . . .	37
2.4 Top view of quarter-core model . . . . .	41
2.5 Side view of quarter-core model . . . . .	42
2.6 Core configuration with circular fuel regions of nearly equal thickness. . . . .	48
2.7 Core configuration with circular fuel regions that each contain roughly the same fuel mass. . . . .	48
2.8 Core configuration with hexagonal fuel regions of nearly equal thickness. . . . .	49
2.9 The geometry of the two-region, infinite lattice case. From the center outward, the regions are: moderator, burner fuel, a second small moderator region, and then breeder fuel. . . . .	50

LIST OF FIGURES (Continued)

<u>Figure</u>	<u>Page</u>
3.1	Criticality of control case with no fission product removal compared to case with fission product removal. . . . . 55
3.2	$^{233}\text{U}$ concentration of control case with no fission product removal compared to case with fission product removal. . . . . 56
3.3	$k_{eff}$ at BOL as a function of pitch-to-diameter ratio . . . . . 57
3.4	$k_{eff}$ at BOL as a function of H-to-fissile isotope ratio . . . . . 57
3.5	Comparison of moderator-fissile isotope ratio and pitch-to-diameter ratio for varying enrichment. . . . . 59
3.6	Comparison of moderator-fissile isotope ratio and pitch-to-diameter ratio for varying moderator density. . . . . 60
3.7	FIR at EOL for metallic moderator as a function of pitch-to-diameter ratio . . . 61
3.8	$k_{inf}$ at BOL for metallic moderator as a function of pitch-to-diameter ratio . . . 62
3.9	FIR at EOL for metallic moderator with low moderator density as a function of pitch-to-diameter ratio. . . . . 62
3.10	$k_{inf}$ at BOL for metallic moderator with low moderator density as a function of pitch-to-diameter ratio . . . . . 63
3.11	FIR at EOL for graphite as a function of pitch-to-diameter ratio . . . . . 63
3.12	$k_{inf}$ at BOL for graphite as a function of pitch-to-diameter ratio . . . . . 64
3.13	$^{233}\text{U}$ enrichment as a function of burnup in the breeder region. . . . . 66
3.14	$^{233}\text{U}$ enrichment as a function of burnup in the burner region. . . . . 67
3.15	Neutron balance as a function of burnup in the breeder region. . . . . 67
3.16	Neutron balance as a function of burnup in the burner region. . . . . 68
3.17	$k_{inf}$ for metallic moderator as a function of burnup, enrichment, and pitch-to-diameter (PD) ratio for higher enrichments. . . . . 69
3.18	$k_{inf}$ for metallic moderator as a function of burnup, enrichment, and pitch-to-diameter ratio for lower enrichments. . . . . 69
3.19	$^{233}\text{U}$ number density for metallic moderator as a function of burnup, enrichment, and pitch-to-diameter ratio for higher enrichments. . . . . 70
3.20	$^{233}\text{U}$ number density for metallic moderator as a function of burnup, enrichment, and pitch-to-diameter ratio for lower enrichments. . . . . 70

LIST OF FIGURES (Continued)

Figure	Page
3.21 Neutron balance for metallic moderator as a function of burnup, enrichment, and pitch-to-diameter ratio for higher enrichments. . . . .	71
3.22 Neutron balance for metallic moderator as a function of burnup, enrichment, and pitch-to-diameter ratio for lower enrichments. . . . .	71
3.23 $k_{inf}$ of the best breeder and burner cases for metallic moderator with low moderator density as a function of burnup, enrichment, and pitch-to-diameter ratio for higher enrichments. . . . .	72
3.24 $k_{inf}$ of the best breeder cases for metallic moderator with low moderator density as a function of burnup, enrichment, and pitch-to-diameter ratio for lower enrichments. . . . .	72
3.25 $^{233}\text{U}$ number density of the best breeder and burner cases for metallic moderator with low moderator density as a function of burnup, enrichment, and pitch-to-diameter ratio for higher enrichments. . . . .	73
3.26 $^{233}\text{U}$ number density of the best breeder cases for metallic moderator with low moderator density as a function of burnup, enrichment, and pitch-to-diameter ratio for lower enrichments. . . . .	73
3.27 Neutron balance of the best breeder and burner cases for metallic moderator with low moderator density as a function of burnup, enrichment, and pitch-to-diameter ratio for higher enrichments. . . . .	74
3.28 Neutron balance of the best breeder cases for metallic moderator with low moderator density as a function of burnup, enrichment, and pitch-to-diameter ratio for lower enrichments. . . . .	74
3.29 $k_{inf}$ for graphite as a function of burnup, enrichment, and pitch-to-diameter ratio for higher enrichments. . . . .	75
3.30 $k_{inf}$ for graphite as a function of burnup, enrichment, and pitch-to-diameter ratio for lower enrichments. . . . .	75
3.31 $^{233}\text{U}$ number density for graphite as a function of burnup, enrichment, and pitch-to-diameter ratio for higher enrichments. . . . .	76
3.32 $^{233}\text{U}$ number density for graphite as a function of burnup, enrichment, and pitch-to-diameter ratio for lower enrichments. . . . .	76
3.33 Neutron balance for graphite as a function of burnup, enrichment, and pitch-to-diameter ratio for higher enrichments. . . . .	77
3.34 Neutron balance for graphite as a function of burnup, enrichment, and pitch-to-diameter ratio for lower enrichments. . . . .	77

LIST OF FIGURES (Continued)

Figure	Page
3.35 Number of neutrons required to reach an enrichment compared to the number of neutrons produced by the enrichment. . . . .	82
3.36 Optimizing for an EOL blanket enrichment that is as large as possible, relative to the BOL driver enrichment. . . . .	84
3.37 $k_{inf}$ of the high enriched breeder two-region lattice with metallic moderator as a function of burnup and enrichment, with a fuel thickness of 2.5 cm. . . . .	85
3.38 $^{233}\text{U}$ number density of the high enriched breeder two-region lattice with metallic moderator as a function of burnup and enrichment, with a fuel thickness of 2.5 cm. . . . .	85
3.39 $k_{inf}$ of the high enriched breeder two-region lattice with metallic moderator as a function of burnup for the best case result. . . . .	86
3.40 $^{233}\text{U}$ number density of the high enriched breeder two-region lattice with metallic moderator as a function of burnup for the best case result. . . . .	87
A.1 $k_{inf}$ for metallic moderator as a function of burnup, enrichment, and pitch-to-diameter (PD) ratio. . . . .	104
A.2 $^{233}\text{U}$ number density for metallic moderator as a function of burnup, enrichment, and pitch-to-diameter ratio. . . . .	105
A.3 Neutron balance for metallic moderator as a function of burnup, enrichment, and pitch-to-diameter ratio. . . . .	105
A.4 $k_{inf}$ for metallic moderator with low moderator density as a function of burnup, enrichment, and pitch-to-diameter ratio. . . . .	106
A.5 $^{233}\text{U}$ number density for metallic moderator with low moderator density as a function of burnup, enrichment, and pitch-to-diameter ratio. . . . .	106
A.6 Neutron balance for metallic moderator with low moderator density as a function of burnup, enrichment, and pitch-to-diameter ratio. . . . .	107
A.7 $k_{inf}$ for graphite as a function of burnup, enrichment, and pitch-to-diameter ratio. . . . .	107
A.8 $^{233}\text{U}$ number density for graphite as a function of burnup, enrichment, and pitch-to-diameter ratio. . . . .	108
A.9 Neutron balance for graphite as a function of burnup, enrichment, and pitch-to-diameter ratio. . . . .	108
A.10 $^{233}\text{U}$ number density for metallic moderator in two-region lattice as a function of burnup and enrichment for 1.5 cm moderator radius and 0.5 cm thick inner fuel region. . . . .	109

LIST OF FIGURES (Continued)

Figure	Page
A.11 $k_{ing}$ for metallic moderator in two-region lattice as a function of burnup and enrichment for 1.5 <i>cm</i> moderator radius and 0.5 <i>cm</i> thick inner fuel region. . . .	109
A.12 $^{233}\text{U}$ number density for metallic moderator in two-region lattice as a function of burnup and enrichment for 3.0 <i>cm</i> moderator radius and 0.5 <i>cm</i> thick inner fuel region. . . . .	110
A.13 $k_{ing}$ for metallic moderator in two-region lattice as a function of burnup and enrichment for 3.0 <i>cm</i> moderator radius and 0.5 <i>cm</i> thick inner fuel region. . . .	110
A.14 $^{233}\text{U}$ number density for metallic moderator in two-region lattice as a function of burnup and enrichment for 3.0 <i>cm</i> moderator radius and 1.5 <i>cm</i> thick inner fuel region. . . . .	111
A.15 $k_{ing}$ for metallic moderator in two-region lattice as a function of burnup and enrichment for 3.0 <i>cm</i> moderator radius and 1.5 <i>cm</i> thick inner fuel region. . . .	111
A.16 $^{233}\text{U}$ number density for metallic moderator in two-region lattice as a function of burnup and enrichment for 4.5 <i>cm</i> moderator radius and 2.0 <i>cm</i> thick inner fuel region. . . . .	112
A.17 $k_{ing}$ for metallic moderator in two-region lattice as a function of burnup and enrichment for 4.5 <i>cm</i> moderator radius and 2.0 <i>cm</i> thick inner fuel region. . . .	112
A.18 FIR at EOL for zirconium hydride as a function of moderator to fissile ratio . . .	113
A.19 FIR at EOL for zirconium hydride as a function of pitch to diameter ratio . . . .	114
A.20 $k_{eff}$ at BOL for zirconium hydride as a function of moderator to fissile ratio . .	115
A.21 $k_{eff}$ at BOL for zirconium hydride as a function of pitch to diameter ratio . . . .	116
A.22 FIR at EOL for light water as a function of moderator to fissile ratio . . . . .	117
A.23 FIR at EOL for light water as a function of pitch to diameter ratio . . . . .	117
A.24 $k_{eff}$ at BOL for light water as a function of moderator to fissile ratio . . . . .	118
A.25 $k_{eff}$ at BOL for light water as a function of pitch to diameter ratio . . . . .	118

## LIST OF TABLES

Table	Page
1.1 Regions of Shippingport core . . . . .	16
2.1 The heuristics used by Gnowee algorithms . . . . .	31
3.1 Atom number densities ( <i>atoms/bn-cm</i> ) of $^{233}\text{U}$ , $N_U$ , in the different fuel regions at the beginning-of-life (BOL) and end-of-life (EOL) after 200 days . . . . .	53
3.2 Computation time comparison . . . . .	54
3.3 The moderating properties of the examined materials, adjusted for a Maxwellian spectrum at 1000 $K$ . . . . .	54
3.4 Comparing BOL and EOL $k_{inf}$ and $^{233}\text{U}$ number density of the control to the fission product (FP) removal case. . . . .	56
3.5 Comparing minimum $^{233}\text{U}$ enrichment required to maintain $k_{inf} \geq 1.0$ moderated by the metallic moderator. . . . .	78
3.6 Comparing minimum $^{233}\text{U}$ enrichment required to maintain $k_{inf} \geq 1.0$ moderated by the metallic moderator with low moderator density. . . . .	78
3.7 Comparing minimum $^{233}\text{U}$ enrichment required to maintain $k_{inf} \geq 1.0$ moderated by graphite. . . . .	78
3.8 Peak number of excess neutrons ( $n/cm^3$ ) as a function of pitch-to-diameter ratio and enrichment for metallic moderator. . . . .	79
3.9 Peak number of excess neutrons ( $n/cm^3$ ) as a function of pitch-to-diameter ratio and enrichment for metallic moderator with low moderator density. . . . .	79
3.10 Peak number of excess neutrons ( $n/cm^3$ ) as a function of pitch-to-diameter ratio and enrichment for graphite moderator. . . . .	80
3.11 The net number of neutrons ( $n/cm^3$ ) required to breed a fuel of starting enrichment to a new enrichment with metallic moderator. . . . .	80
3.12 The net number of neutrons ( $n/cm^3$ ) required to breed a fuel of starting enrichment to a new enrichment with low density metallic moderator. . . . .	81
3.13 The net number of neutrons ( $n/cm^3$ ) required to breed a fuel of starting enrichment to a new enrichment with graphite moderator. . . . .	81
3.14 Parameters and parameter bounds put into Gnowee. . . . .	83
3.15 Volumes and $^{233}\text{U}$ concentrations of two-region lattice. . . . .	88

# 1 Introduction

Anthropogenic climate change is an active and growing concern of the modern era, resulting from deforestation and the use of carbon emitting fossil fuels for power generation and transportation [4]. In order to reach the goals put forth in Article 4 of the Paris Agreement, anthropogenic emissions must be carbon neutral by 2050 so that a two degree Celsius increase in average global temperature, relative to pre-industrial temperatures, can be avoided [42]. Despite a lack of federal commitment to the Paris Agreement, there is still domestic pressure to adhere to the Agreement and other nations have made legally binding resolutions to abide by the Agreement [42]. Many solutions focus on the use of wind and solar power, but nuclear power is a necessary component of a carbon neutral economy [25]. Nuclear power is the second largest source of carbon-free energy in use today, after hydroelectric generation, with roughly 10% of all electrical power in the world generated from nuclear reactors [19]. Nuclear power's advantage over most renewable power sources is its capacity to generate base-load power, whereas other sources such as wind and solar are intermittent and often peak when electrical demand is lower [6]. There are a number of organizations working to bring nuclear power more prominently into the energy mix.

The World Nuclear Association (WNA) has proposed the Harmony programme with the intent of reaching the carbon targets laid out in the Paris Agreement. The goal of the Harmony programme is to have nuclear power as the source of 25% of global energy production by 2050. This would require the addition of nearly 1000  $GWe$  of nuclear power in the next 30 years [45]. For comparison, the total global capacity of active nuclear generating stations is 391  $GWe$  [30]. Facilitating the Harmony programme's goal will require cheaper reactors and fuel, as cost is one of largest barriers to building new reactors. Projected overnight capital costs for new nuclear is 5945  $$/kW$ , while combined cycle gas plants are only 978  $$/kW$  [43]. The levelized cost of electricity (LCOE), which is the sum of all costs over the plant's lifetime divided by the sum of all electricity produced over its lifetime, is also in favor of natural gas, which has an LCOE of 38.07 $$/MWh$  compared to nuclear power's LCOE of 74.88  $$/MWh$  [44]. A portion of LCOE is capital costs, but fuel can potentially be a large contributor to operating costs.

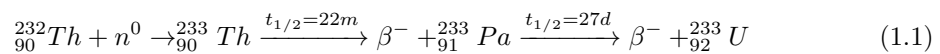
In terms of fuel cost and availability, current projections have identified over 130 years worth of uranium that is recoverable. About 25% of it is economically recoverable at a cost of \$130 per kilogram of uranium, and a further 20% is recoverable at a cost of \$260 per kilogram, which



is not economical at this time. However, these forecasts use the 2017 rate of global uranium use of 62,825 tons of uranium ( $tU$ ) annually [30]. If the WNA Harmony programme is brought to fruition using the same light water reactor (LWR) technology that most of the world’s reactors rely on today, the global demand will more than triple; fuel resources currently supply 400  $GWe$  but the Harmony programme predicts that 1250  $GWe$  are needed to achieve 25% of global power generation from nuclear. This means that there could be a significant increase in demand for fuel. It is likely that advanced reactor designs will be able to use fuel more effectively, but uranium is still a finite resource. Fuel costs are not a limiting factor at this time, but could become a cost driver if prices fluctuate high again; this happened in the recent past. During a speculative market in 2007 uranium prices peaked at nearly six times the current price: 354  $\$/kgU$  in 2007 compared to 62  $\$/kgU$  in 2017 [30]. It is therefore important to draw from other forms of nuclear fuel for the next generation of reactors to achieve better long-term stability and economic viability. One potential candidate for this application is thorium.

## 1.1 Thorium Fuel Cycle

The thorium fuel cycle utilizes the same concept as the uranium-plutonium fuel cycle;  $^{232}\text{Th}$ , a ‘fertile’ isotope, can absorb a neutron and decay into  $^{233}\text{U}$ , a ‘fissile’ isotope. A fertile nucleus can be transmuted into a fissile nucleus if it absorbs a neutron, and a fissile nucleus undergoes fission if it absorbs a neutron.  $^{233}\text{U}$  and other fissile isotopes can be used as a nuclear fuel to power a nuclear reactor. There are two intermediate isotopes between  $^{232}\text{Th}$  and  $^{233}\text{U}$ , shown in Equation 1.1 [24],



The conditions that are favorable for the  $^{232}\text{Th} + n^0$  reaction are not the same conditions that are favorable for the  $^{233}\text{U}$  fission reaction. Thorium reactors typically have multiple regions within the core to capitalize on different neutron energy conditions in different areas. The region that has more fissile material is called the ‘driver’ or ‘burner’ region, and is where most fissions occur. The region that contains less fissile material is often referred to as a ‘blanket’, as it wraps around the driver region. It is also called the ‘breeder’ region, as this region is where the majority of the fissile isotope production occurs. The breeder region should experience a net

increase in fissile material during its residence in the core [12].

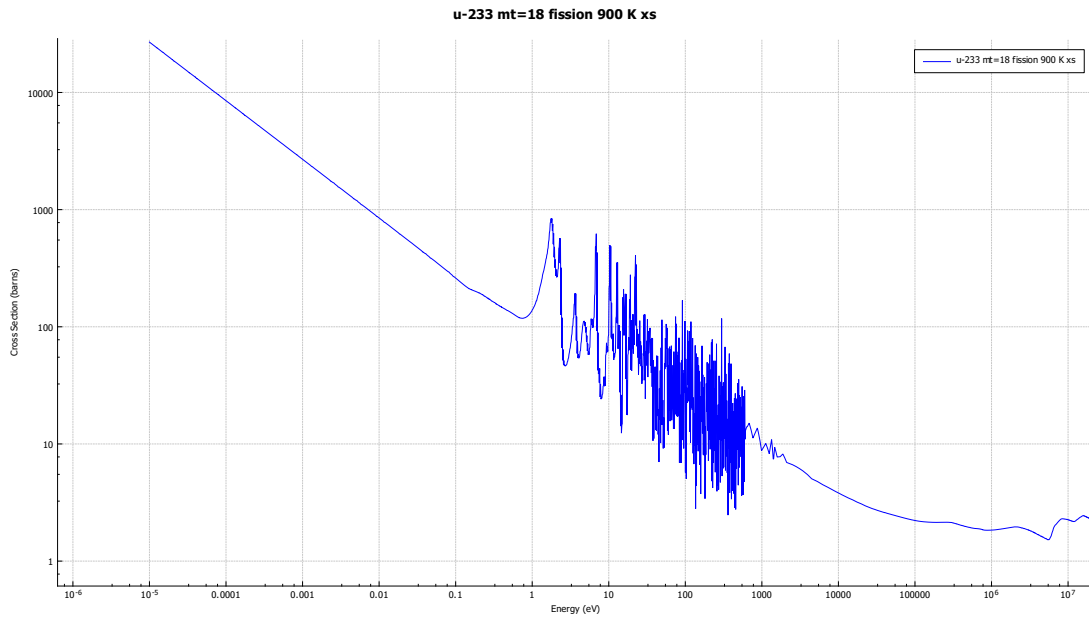
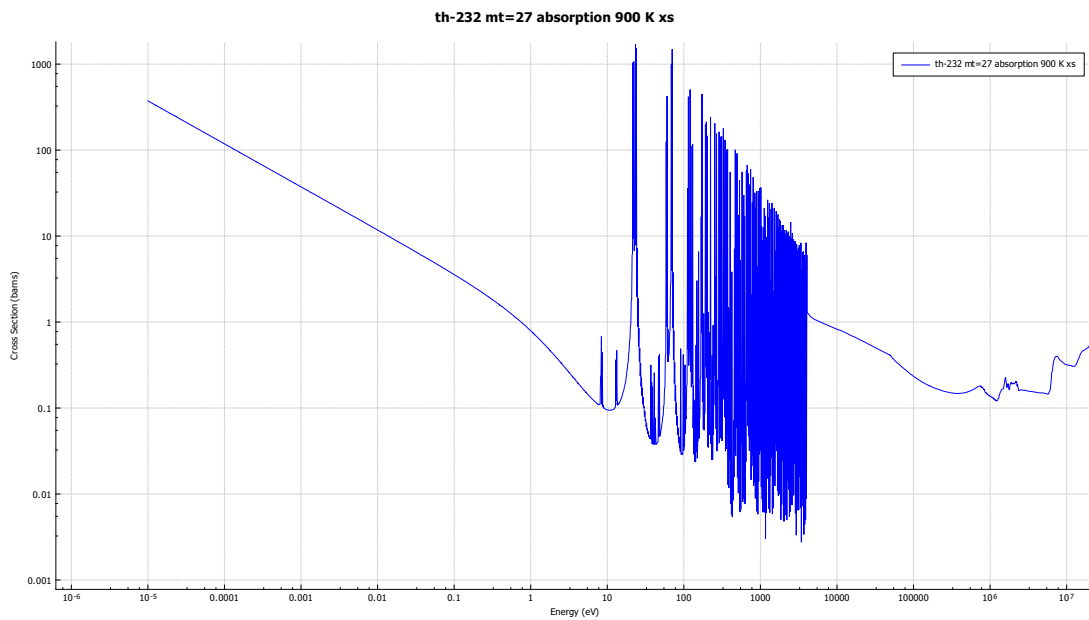
### 1.1.1 Chemical Reprocessing

There are two general fuel cycles: open and closed. An open cycle uses enriched fuel in a once-through process that burns the fuel and then transfers the used fuel into storage. A closed cycle also uses enriched fuel, but the used fuel is then chemically re-processed to remove fission products, isolate fissile isotopes, and be used again in a core. Thorium fueled reactors, especially Molten Salt Reactors (MSRs), utilize a closed cycle that chemically removes  $^{233}\text{U}$  or its precursor  $^{233}\text{Pa}$  from the breeding region and concentrates the  $^{233}\text{U}$  to be used in the burning region. Fission product poisons can also be removed during the reprocessing. Concentrating the fissile isotopes in the fuel is necessary for the operation of many reactors and improves the economics of others. The removal of the fission product poisons allows for more efficient fuel use and breeding [5]. The downsides of chemical reprocessing come down to cost. A chemical treatment plant capable of handling highly radioactive material adds significant costs to the already high capital costs of a nuclear reactor. The operations and maintenance costs of handling the fuel over the reactor's lifetime also increases because of the fuel reprocessing. A potential solution is to utilize a closed cycle that does not rely on chemical reprocessing.

## 1.2 Reactor Physics

### Neutron Reactions

The probability of a particular neutron interaction with matter is quantified through the neutron cross section. Neutrons can have several types of interaction with matter. They can scatter and transfer energy between the neutron and a nucleus, either speeding up or slowing down the neutron. Neutrons can also be absorbed by a nucleus, which can result in the emission of secondary particles or radiation, or cause a fissile nucleus to fission. The cross sections of these interactions depend on the energy of the incident neutron and the temperature of the material, and are generally divided into three neutron energy ranges: the fast region, the resonance interval, and the  $1/v$  absorption region.

(a) Fission cross section of  $^{233}\text{U}$  at 900K(b) Absorption cross section of  $^{232}\text{Th}$  at 900KFigure 1.1: Cross sections of  $^{233}\text{U}$  and  $^{232}\text{Th}$  [28]

The  $1/v$  absorption region is the lowest energy region where the the velocity of the incident neutrons is inversely proportional to the cross section. This region contains neutrons that are relatively slow moving, also called ‘thermal’ neutrons. Thermal neutrons are neutrons that have reached thermal equilibrium with the media containing them. This is the regime in which LWRs

operate due to an optimal moderator to fuel ratio.

The resonance interval is the region in which the cross section exhibits strong peaks and troughs. In this region the peaks, or 'resonances', widen as the material increases in temperature; this process is known as 'Doppler broadening' [7]. The cross sections in every region are dependent on temperature, but Doppler broadening is an important safety feature for many reactors that incorporate negative temperature coefficients and burnable poisons to control reactor power.

The fast region, which is the energy range of the fission spectrum, generally has the lowest cross sections. This is the region in which unmoderated reactors operate and is also the region which generally allows for breeding in a  $^{238}\text{U}$ - $^{239}\text{Pu}$  breeding cycle. The absorption of fast neutrons in fuel releases more neutrons on average than the absorption of thermal neutrons in fuel, where the extra neutrons facilitate the breeding process. This can be seen in Fig.1.2. Reactors operating in the fast spectrum have some disadvantages compared to thermal spectrum reactors, such as fast neutrons cause more damage to materials than thermal neutrons. The higher neutron energy results in more displacements per atom (DPA), a common metric of neutron fluence-induced damage. These displacements can cause strain and failure in the fuel, cladding, and surrounding structures [15].

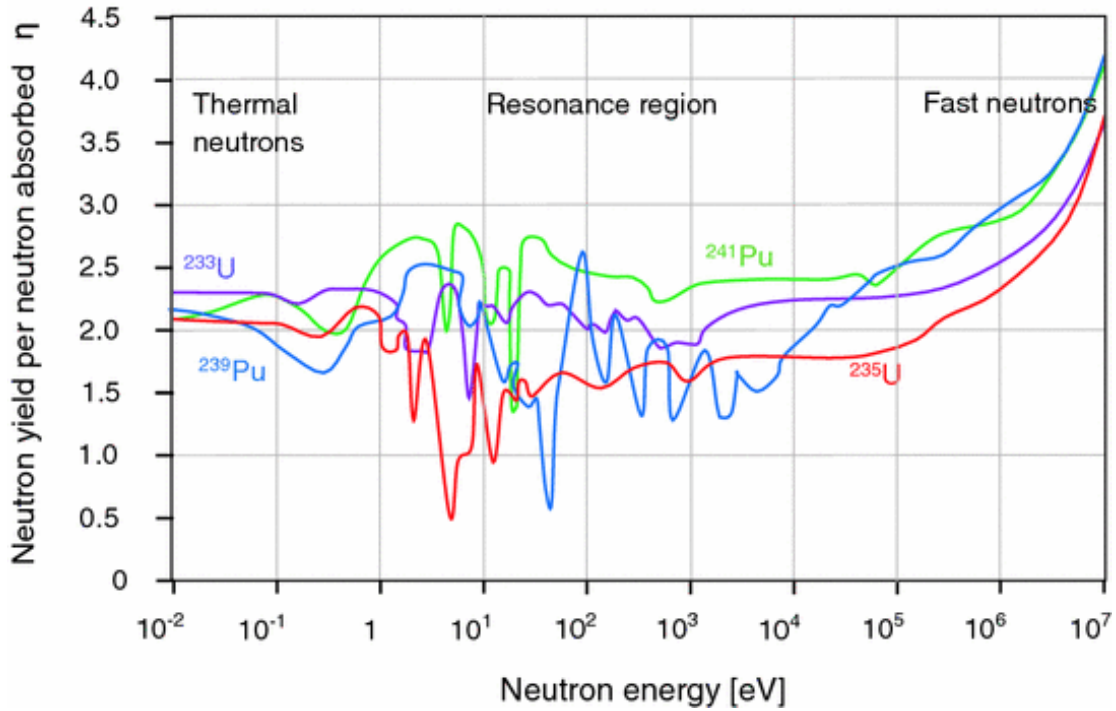


Figure 1.2: Neutrons released from fission per neutron absorbed [8]

Since the interaction of neutrons with matter is stochastic, neutrons will not all maintain the same energy; instead the flux will be composed of a spectrum of neutron energies. Neutrons that have experienced fewer scattering interactions will still retain most of their original energy. A neutron flux that is predominantly fast neutrons is called a ‘hard’ spectrum. A flux can be hardened by absorbing thermal neutrons, reducing the overall flux but shifting the average energy to a higher value.

Conversely, a neutron flux can be ‘softened’ by moderating the neutron flux and reducing the average neutron velocity. High energy neutrons that have several scattering interactions with nuclei will lose much of their original energy and slow down. This process is called ‘thermalization’ as the average neutron energy will approach the energy associated with the ambient temperature of the material in which they are scattering. In thermal equilibrium, a Maxwellian distribution can be used to describe the density of particles per unit energy ( $N(E)$ ), which takes the form

$$N(E) = \frac{2\pi N}{(\pi kT)^{\frac{3}{2}}} E^{\frac{1}{2}} \exp(-E/kT) \quad (1.2)$$

where  $N$  is the total particle density,  $k$  is the Boltzmann constant equal to  $8.617E - 5 \text{ ev/K}$  and  $T$  is the temperature in Kelvin [24]. The average energy of a neutron in this distribution is given by

$$E_{ave} = \frac{3}{2}kT \quad (1.3)$$

### Cross Sections and Moderator Qualities

There are two common metrics used for evaluating the effectiveness of a moderator: the slowing-down power represents the effectiveness of the moderator to slow down a neutron and the moderating ratio describes the likelihood of parasitic absorptions instead of scattering events. The moderator power, or slowing-down power, is defined as

$$SDP = \zeta \Sigma_s \quad (1.4)$$

and the moderating ratio is defined as

$$MR = \zeta \frac{\Sigma_s}{\Sigma_a} \quad (1.5)$$

where  $\Sigma_s$  is the macroscopic scattering cross section,  $\Sigma_a$  is the macroscopic absorption cross section, and  $\zeta$  is the mean lethargy gain per collision. The value of  $\zeta$  depends on the mass of the target nuclei,

$$\zeta = \log\left(\frac{E_i}{E_f}\right) = 1 - \frac{(A-1)^2}{2A} \log\left(\frac{A+1}{A-1}\right) \quad (1.6)$$

where  $E_i$  is the initial energy of the neutron,  $E_f$  is the final energy of the neutron, and  $A$  is the atomic weight of the target nuclei [2]. In general, a higher slowing-down power and higher moderating ratio indicate that a material is a better moderator. These values can be used as figures of merit to compare the qualities of different moderator materials.

### Criticality

A nuclear reactor operates by facilitating and controlling a chain reaction of fissioning atoms. When a fissile atom absorbs a neutron, it has a high probability of splitting, or fissioning, which

releases heat and 2 to 3 neutrons. The heat of this reaction is used as the heat source for a power cycle and the neutrons are used to cause more fissions. A reactor that maintains a neutron balance in which the number of fissions and neutrons generated is not growing or diminishing is called ‘critical’. A reactor that is not able to sustain the chain reaction is called ‘subcritical’, while a reactor that is growing in power or neutron population is called ‘supercritical’. The criticality of a reactor can be described by the dominant eigenvalue of the system called ‘ $k_{eff}$ ’, or the effective criticality of the system.  $k_{eff}$  is also referred to as the multiplication factor, or the factor by which the neutron population grows in each successive generation [7].

There are a number of ways  $k_{eff}$  can be defined. The most straightforward description is that  $k_{eff}$  represents neutron production divided by neutron loss. A critical reactor has a  $k_{eff}$  of exactly 1, while subcritical and supercritical reactors have  $k_{eff}$  values of less than or greater than 1, respectively.  $k_{eff}$  can be broken down further into its constituent parts using the six-factor formula,

$$k_{eff} = \eta f p \epsilon P_{FNL} P_{TNL} \quad (1.7)$$

where

- $\eta$  is the average number of neutrons produced per absorption in the fuel;
- $f$  is the thermal utilization, which is the probability that an absorbed thermal neutron is absorbed by the fuel;
- $p$  is the resonance escape probability, which is the probability that a neutron slows from the fast spectrum into the thermal spectrum without being absorbed;
- $\epsilon$  is the fast fission factor, which is the contribution of neutrons due to fast fission reactions;
- $P_{FNL}$  is the probability of fast non-leakage, which is the likelihood that a fast neutron does not leak out of the system; and
- $P_{TNL}$  is the probability of thermal non-leakage, which is the likelihood that a thermal neutron does not leak out of the system.

Criticality safety is an important consideration in reactor design. There are several associated requirements for modern reactor designs, such as having both active and passive criticality

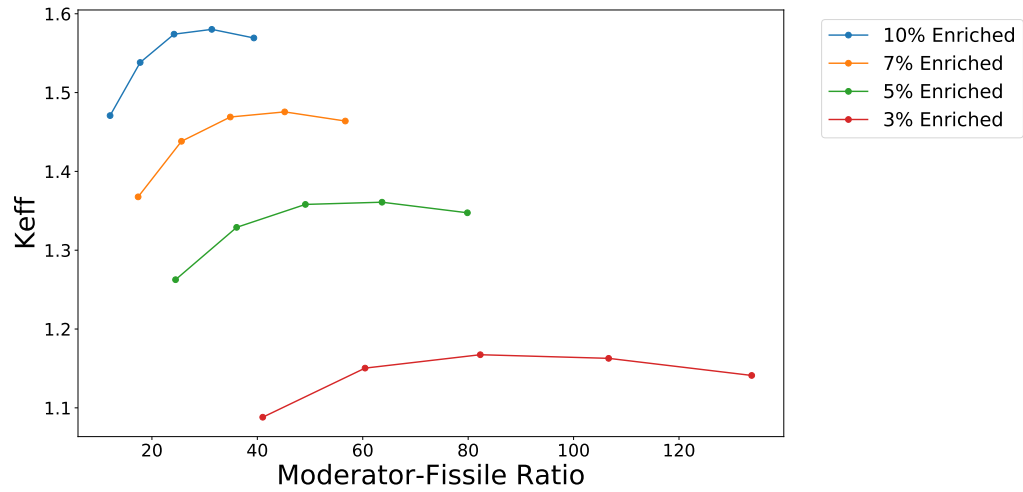
control. This means that there must be a reactivity control mechanism that is directly controlled, e.g., control rods and boric acid, as well as passive reactivity control. Passive reactivity control generally comes in the form of negative temperature coefficients that ensure the reactor will reduce its reactivity as temperature increases. A positive temperature coefficient means that as the reactor increases in temperature, it also increases in reactivity. This is a positive feedback loop that can result in severe accidents; the RBMK-type reactor of the Chernobyl disaster had an inherent positive temperature coefficient, contributing to its meltdown [20]. A positive reactivity feedback coefficient is untenable in terms of modern licensing as it is a violation of 10 CFR 50.A.1.11, otherwise called general design criterion (GDC) 11, which requires that a reactor core shall be designed so that the inherent characteristics of the reactor compensate for rapid increases in reactivity. There have been many designs that utilize the breeding potential of fertile isotopes that are safe to operate; notable designs include the Light Water Breeder Reactor (LWBR), breeder-burner (B&B) reactors, and molten salt reactors (MSRs). These concepts give key insights into trends and favorable designs for breeder reactors. These concepts of criticality, flux spectrums, and moderation dictate the materials and geometries that are suitable for a given reactor type.

### **Reactor Geometries**

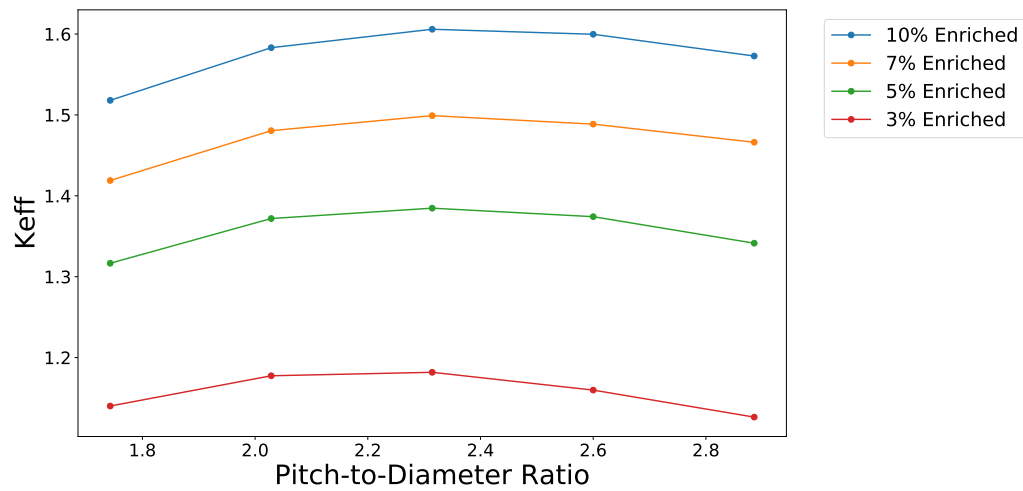
For a typical fuel-pin-based core, a ratio of the fuel pin pitch to the fuel pin diameter (pitch-to-diameter ratio) is used as a design value. The physics behind the pitch-to-diameter ratio can be better understood by recognizing that the pitch-to-diameter ratio correlates to the ratio of the number of atoms of moderator to the number of atoms of fissile material. This ratio is called the moderator-fissile ratio, or for moderators that use hydrogen this can be called the H-fissile ratio. These two values do not always trend together and one may be more valuable than the other in some cases. For example, the moderator-fissile ratio shows a trend more clearly than the pitch-to-diameter ratio in Fig. 1.4, in which the moderator density is changing and in turn disrupting the pitch-to-diameter trend. In a similar way, the pitch-to-diameter ratio preserves its trend as enrichment increases, while the moderator-fissile ratio peak shifts. This can be seen in Fig. 1.3 where the moderator-fissile peak shifts down as enrichment increases. Fig. 1.3 and Fig. 1.4 were generated for a hypothetical metallic moderator of interest to NuScale. Pitch-to-diameter ratio or moderator-fissile ratio can be used as an independent variable to find ideal values for



dependent variables. Care must be taken to ensure that the conclusions drawn account for the behavior of the independent variables.



(a)  $k_{eff}$  as a function of moderator-fissile ratio.



(b)  $k_{eff}$  as a function of pitch-to-diameter ratio.

Figure 1.3: Comparison of moderator-fissile isotope ratio and pitch-to-diameter ratio for varying enrichment in a novel metallic moderator.

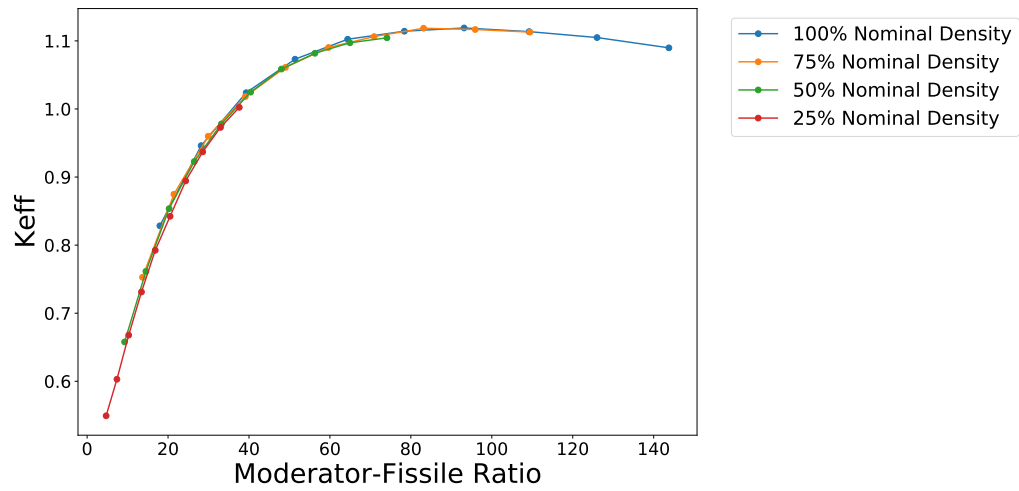
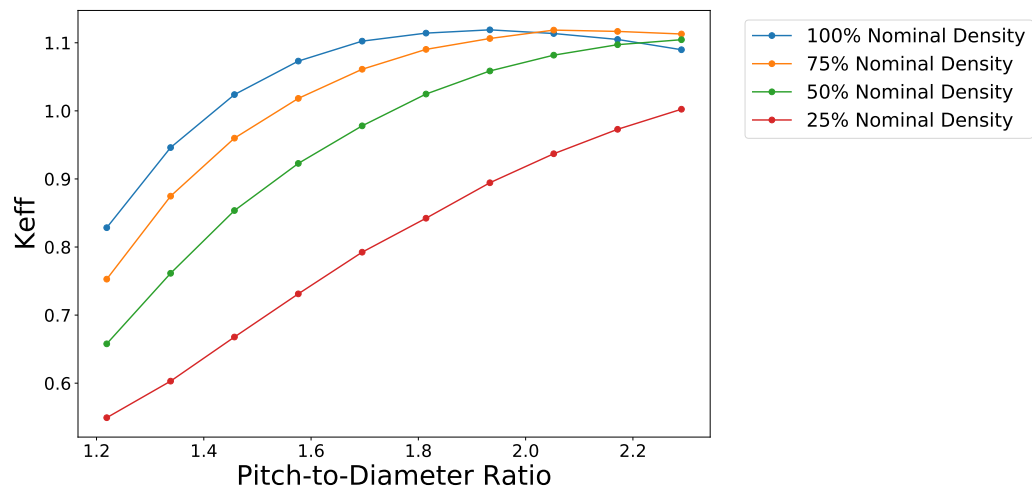
(a)  $k_{eff}$  as a function of moderator-fissile ratio.(b)  $k_{eff}$  as a function of pitch-to-diameter ratio.

Figure 1.4: Comparison of moderator-fissile isotope ratio and pitch-to-diameter ratio for varying moderator density.

A metric to compare the performance of a pitch-to-diameter ratio could be the criticality of the core, described by  $k_{eff}$ . The criticality of a system typically increases with increasing pitch-to-diameter ratio, up to a point. After this peak, the losses due to parasitic absorption within the moderator exceed the gains to fission yields. A ratio less than the value corresponding to the peak means the system is under-moderated, and a ratio greater indicates that the system is over-moderated. This can be seen in Figure 1.5. Modern reactors are required to have a negative

moderator coefficient of reactivity, which means that increases in moderator temperature will reduce the reactivity of the system [31]. This means that reactors such as LWRs are required to be under-moderated so that heat addition, void formation, and loss of coolant and/or moderator do not increase the reactivity of the system.

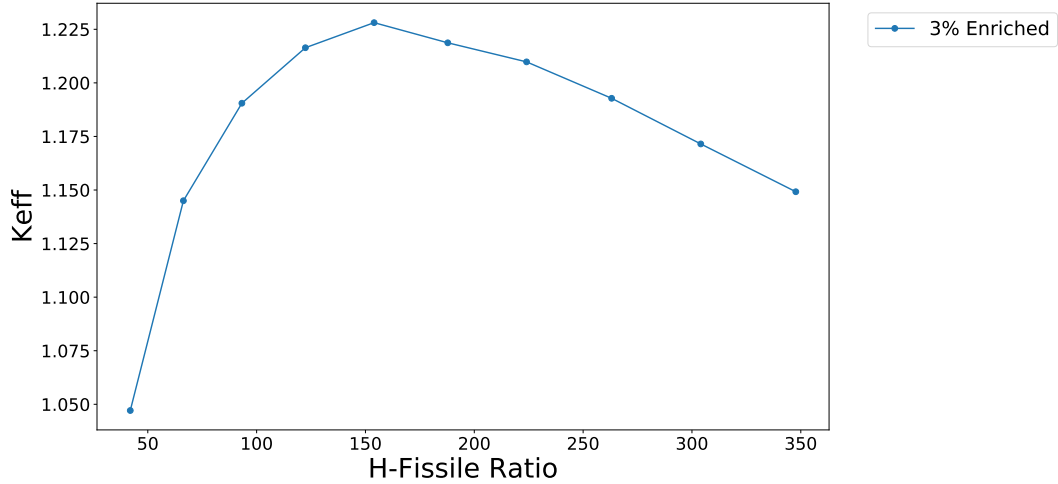


Figure 1.5:  $k_{eff}$  as a function of H-fissile ratio.

The ratios could also be used as independent variables to determine trends in the capacity for breeding, described by the fissile isotope ratio (FIR). FIR is a common value used to compare the net breeding of fissile material over time and is simply the number of fissile atoms at end-of-life (EOL) divided by the number of fissile atoms at the beginning-of-life (BOL). The breeding ratio is another important quantity that is often used. The breeding ratio can be described by

$$BR = \eta\epsilon - 1 - L \quad (1.8)$$

where  $BR$  is the breeding ratio,  $\eta$  is the neutrons produced per neutron absorption in fuel,  $\epsilon$  is the fast fission factor, and  $L$  is the neutrons lost per absorption in the fuel.

The breeding ratio, also known as the conversion ratio, can be described by the parameter  $C$  [24]. If a number of atoms,  $N$ , are consumed then  $NC$  fertile atoms are converted to fissile isotopes. If the produced fissile isotope is the same as the isotope that produced it, such as  $^{233}\text{U}$  fissions producing more  $^{233}\text{U}$ , the new nuclei will in turn be used to convert more fertile nuclei. This relationship has the form  $NC * C = NC^2$ , and this trend continues in an infinite series

which yields

$$NC + NC^2 + NC^3 + \dots = \frac{NC}{1 - C}.$$

Every nuclear power plant in the United States uses LWR technology to produce heat and steam for electricity generation. These reactors have a value of  $C$  that is less than one [18]. This means they use more fuel than they produce and thus are named ‘burners’. A reactor that has a  $C$  value of exactly one has no net change in its fuel inventory, and is called a ‘converter’. A reactor with a  $C$  value of greater than one, in which there is a net gain in fuel, is known as a ‘breeder’ reactor. Another parameter of importance is the ‘breeding gain’,  $G$ , defined as

$$G = C - 1$$

which represents the net increase in the number of fissile atoms per fuel atom consumed [24]. However, these quantities need additional specification in the case of a reactor that does not utilize chemical reprocessing. A breeder reactor that uses reprocessing only needs to enrich the fuel to the point at which the losses due to reprocessing do not cause the net change in fissile isotopes to be negative. A reactor without reprocessing will need to breed the fuel to an enrichment that is sufficiently high that it can maintain criticality and be used as a source of neutrons to breed the next batch of fuel. A different ratio is proposed for reactors without chemical reprocessing: the enrichment ratio. It is simply the effective enrichment of the driver at the beginning-of-life divided by the effective enrichment of the blanket at end-of-life. An enrichment ratio of one or less indicates that the blanket fuel could be swapped into the driver region of the core to continue the cycle.

### 1.2.1 Benefits of a Thorium Fuel Cycle

#### Isotopics

A thorium based fuel cycle has many advantages compared to a uranium based fuel cycle. Thorium is between three and four times as abundant as uranium and is widely distributed in nature. This allows for longer-term sustainability of fission based nuclear power when used alongside uranium reactors [5]. Traditionally, the thorium fuel cycle is considered more proliferation re-

sistant than the uranium fuel cycle due to the formation of  $^{232}\text{U}$  from (n,2n) reactions with  $^{233}\text{U}$  or the decay of  $^{233}\text{Pa}$ . The most common decay chain of  $^{232}\text{U}$  begins with a 5 *MeV* alpha particle followed by a series of short-lived, strong gamma emitters such as  $^{212}\text{Bi}$  and  $^{208}\text{Tl}$ . The proliferation of used fuel from the thorium cycle would require shielding and remote handling beyond what would be needed for the proliferation of uranium-based fuel. There are several contributing factors to this, such as lower end-of-life enrichment, higher heat generation, and increased radiation hardness and uniqueness due to  $^{232}\text{U}$  [5]. These factors make diversion easier to detect and clandestine reprocessing more difficult. The thorium fuel cycle also does not require enrichment except for the starting fissile load, which simplifies the production process and reduces the long-term need for centrifuges that could have weapons applications. This reduces potential points for proliferation, as well as eliminates the need for centrifuges and other enrichment facilities in non-weapons states. However, reactor designs that utilize thorium in a liquid fuel, such as molten salt reactors (MSRs), often have on-line chemical reprocessing that can be a site of diversion of nuclear fuel. In particular, the  $^{233}\text{U}$  precursor,  $^{233}\text{Pa}$ , can be chemically removed from the solution and will decay into high-purity  $^{233}\text{U}$  [5].

Availability and proliferation resistance are not the only potential benefits of a thorium fuel cycle; thorium has long-term radiological advantages over uranium as a nuclear fuel. The  $^{232}\text{Th}$ - $^{233}\text{U}$  fuel cycle produces a smaller quantity of plutonium and other long-lived actinides compared to the  $^{235}\text{U}/^{238}\text{U}$ - $^{239}\text{Pu}$  cycle. A thorium and uranium fuel could produce 80 to 85 *kg* of plutonium per *GW – yr* compared to a typical LWR reactor fuel which produces 270 *kg* of plutonium per *GW – yr* [41]. This reduces the long-term radiotoxicity of the spent fuel, though the thorium fuel cycle still has some long-lived radioisotopes such as  $^{231}\text{Pa}$  and  $^{229}\text{Th}$  [5].

## Neutronics

In addition to the isotopic benefits, the  $^{232}\text{Th}$ - $^{233}\text{U}$  cycle has neutronic advantages over the  $^{235}\text{U}$  and  $^{238}\text{U}$ - $^{239}\text{Pu}$  cycles. The absorption cross section of  $^{232}\text{Th}$  is nearly three times that of  $^{238}\text{U}$ , allowing for a higher conversion rate to the fissile isotope. The  $^{238}\text{U}$ - $^{239}\text{Pu}$  cycle can only breed in a fast flux spectrum which causes the materials to experience more neutron damage and structural strain [15]. A fast flux is required because there must be more than two neutrons per fission in a breeder reactor: the first neutron is absorbed by a fertile isotope and decays into a fissile isotope, and then the second neutron fissions the fissile isotope. There are always losses

due to leakage, poisons, and parasitic absorptions, so more than two neutrons are required. The average number of neutrons released per absorption of a neutron in fuel is typically characterized by the symbol  $\eta$ . It is dependent on the energy of the neutron that caused the fission and the fissile isotope. The value of  $\eta$  for  $^{233}\text{U}$  from thermal neutrons is around 2.3, while the thermal  $\eta$  of  $^{235}\text{U}$  and  $^{239}\text{Pu}$  is between 2.0 and 2.1. The  $\eta$  values for  $^{235}\text{U}$  and  $^{239}\text{Pu}$  from thermal neutrons are too low to allow for breeding, but the  $\eta$  of  $^{233}\text{U}$  is sufficiently high to allow breeding.

Since  $^{232}\text{Th}$  on its own is not fissile, thorium fuel needs to be doped with a fissile isotope or supplied with a source of neutrons to generate  $^{233}\text{U}$  within it. The latter is usually an accelerator driven source (ADS) and the system behaves as a subcritical reactor that can be used for breeding fuel or burning actinides [29]. A reactor fueled by thorium enriched in  $^{233}\text{U}$  operated during the Light Water Breeder Reactor (LWBR) project that took place in the Shippingport reactor from 1977 to 1982. After five years of operation, the core fissile isotope ratio was found to be 1.01, or a one percent increase in the amount of fissile isotopes in the core compared to the beginning-of-life fuel loading [32].

## 1.3 Breeder Reactor Designs

Breeder reactors are reactors that operate with a conversion ratio greater than one, meaning that the fuel inventory increases over time. Most successful breeder reactors operate with a fast neutron spectrum and convert fertile  $^{238}\text{U}$  into fissile  $^{239}\text{Pu}$ . However, these fast reactors come with their own problems, primarily higher enrichment requirements for the fuel and increased strain due to high neutron fluence. Another problem is that many breeder reactors utilize, or planned to utilize, chemical reprocessing to extract the fissile isotopes from the fuel [14]. There are a number of designs that aim to work around these limitations.

### 1.3.1 LWBR

The LWBR was a light water cooled and moderated core that went into the vessel of the original Shippingport reactor [32]. The fuel rods were made of a blend of thorium oxide (thoria) and  $\text{UO}_2$  with zircaloy cladding. The  $\text{UO}_2$  was enriched to 98wt%  $^{233}\text{U}$ . The cross section of the core, seen in Fig 1.6, shows the different regions. The concentration of uranium varied based on the location in the core. The highest concentration of uranium was in the movable seed region

<i>Region</i>	<i>Enrichment Equivalent (wt%)</i>	<i>Fuel Diameter (in.)</i>
I - Movable Seed Region	3.8	0.3063
II - Standard Blanket Region	1.8	0.5717
III - Power Flattening Blanket Region	2.1	0.5274
IV - Reflector Rod Region	0	0.8323

Table 1.1: Regions of Shippingport core [32]

labeled 'I', with less fuel in each region going outwards until reaching the reflector region which contained no initial loading of  $^{233}\text{U}$ , shown in Table 1.1. The 'Enrichment Equivalent' in Table 1.1 is the  $^{233}\text{U}$  wt% of the heavy metal in that region.

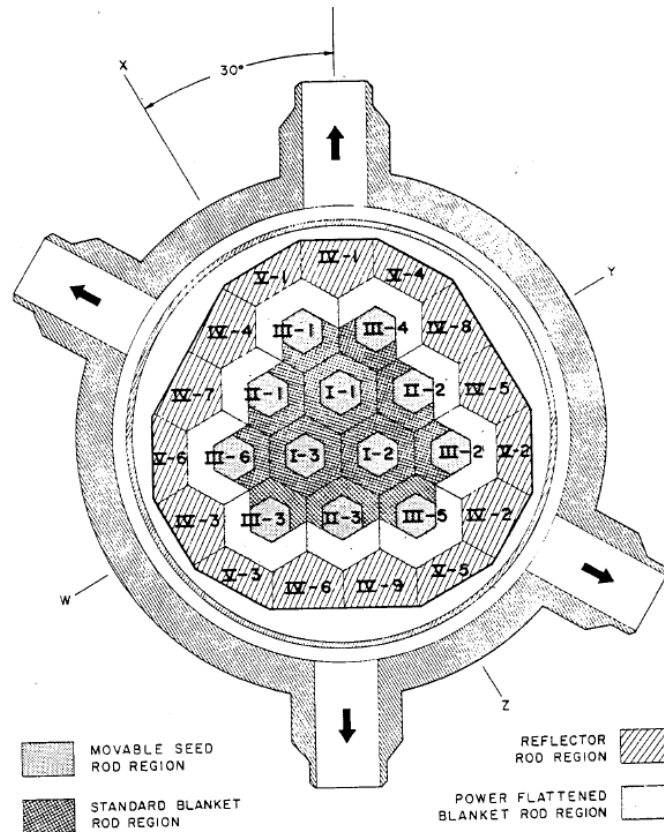


Figure 1.6: Cross section of LWBR core [32]

The pitch-to-diameter ratio of the pins stayed within the range of 1.1 to 1.2 over the whole core, but the diameter of the rods was smallest in the seed region, larger in the standard blanket and power flattening regions, and largest in the reflector blanket. This was intentionally done to harden the neutron spectrum in the blanket regions to fall within the resonance absorption

region of  $^{232}\text{Th}$ .

There are a number of design features of the LWBR that optimized it for breeding, despite light water being a less optimal moderator for breeding conditions when compared to low-absorption moderators such as graphite and heavy water [17, 36]. The layout of the core played a key role in the ability to breed. As previously described, each region contained different amounts of fissile material and different sized rods. This encouraged fission in the seed and standard blanket regions, and breeding in the reflector region. The large amount of thorium in the reflector region also reduced the neutron leakage, improving the overall neutron economy [17]. Part of the unique design is that none of the reactivity control mechanisms used neutron poisons. This eliminated any parasitic absorptions by the control rods, which typically consume about four percent of the neutrons produced in an LWR system [17]. Instead, the seed regions were inserted into the core to increase reactivity and removed to reduce it. The moving seed regions increased the leakage when they were removed, allowing the blanket regions of the core to absorb the excess neutrons. To further improve the neutron economy, all of the structural metal in the core was made of low-hafnium Zircalloy to minimize parasitic structural absorptions. Zircalloy was used due to the unfavorable high-temperature properties of aluminum, and the relatively large absorption cross section of steel in the thermal and resonance regions. The result of these features is that the reactor was able to operate with a net gain in fissile isotopes, as seen in Fig. 1.7.

The design features of the LWBR are important factors in the consideration of future designs because it is one of the few thorium reactors that has demonstrated breeding outside of simulations. These parameters and values are important as they can be used as guidance for the analysis of other thermal spectrum breeder reactors.



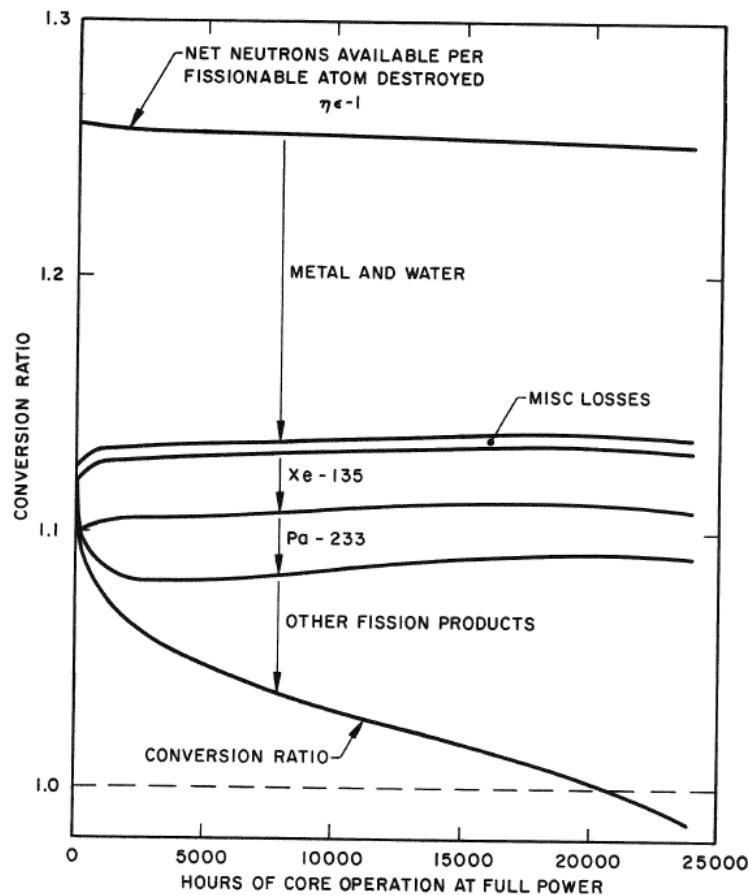


FIGURE 12.

Figure 1.7: LWBR conversion ratio and neutron sinks as a function of operation time [17]

### 1.3.2 Molten Salt Reactors

Molten Salt Reactors (MSRs) are liquid salt cooled reactors that dissolve fuel into the coolant. One type of MSR that has been gaining attention is the liquid fluoride thorium reactor (LFTR) which uses thorium fuel mixed in a fluoride salt coolant. Proponents of these reactors point to appealing properties such as inherent safety, low fuel costs, and proliferation resistance [16]. These reactors are intended to have online refueling and chemical processing to remove fission products and add additional fuel. These capabilities allow for a more efficient neutron economy and reduce the source term of the fuel salt. Typically the cores are wrapped in a fertile blanket that breeds fuel that can be re-introduced into the core.

A successful example of an MSR is the Molten Salt Reactor Experiment (MSRE) that op-

erated at Oak Ridge National Laboratory from 1965 to 1969. The design used a graphite moderator and the core was intended to be surrounded by a thorium blanket to capture neutrons and breed uranium. However, in order to properly test the reactor the thorium blanket could not be installed, so net breeding could not be achieved. The MSRE was originally fueled with  $^{235}\text{U}$ , which was later substituted by  $^{233}\text{U}$ . It demonstrated the ability to remove noble gases online and maintain the other fission products in the fuel salt [16].

### 1.3.3 Moltex

The Moltex Energy Stable Salt Reactor (SSR) is a fast reactor fueled by spent fuel currently going through the licensing process in Canada. It has the unique design of liquid fuel contained within a solid tube. This gives it the benefit of liquid fuel such as lack of neutron damage to the fuel matrix and fission product venting. It also has the benefit of fuel rods, which increase proliferation resistance by making it easier to keep track of fuel inventory (a bundle with a serial number instead of a flowing volume of liquid) as well as keeping the fuel contained.

Although the designers claim it had breeding potential [27], the SSR is generally considered incapable of breeding [40]. The coolant salt is too absorptive in the fast spectrum, which limits the breeding potential of plutonium. The reactor is unmoderated, which reduces the potential of thorium as a viable breeding fuel. This shows the importance of proper coolant and moderator selection to improve breeding capability.

### 1.3.4 Fast Reactors

Fast breeder reactors (FBRs) are a class of reactor that are cooled by liquid metal, usually sodium, lead, or lead-bismuth eutectic. FBRs operate in the fast spectrum and have the neutronic surplus associated with fast fission reactions. FBRs do not experience the same number of parasitic absorptions as thermal reactors due to the lack of moderator material, but the leakage of neutrons out of the core is generally higher for FBRs and neutron damage can be more severe [3]. To make up for the less-optimal fission cross sections in the fast region, the enrichment of FBR fuel must be greater than thermal reactor fuel; 20% is the minimum enrichment of most FBRs. FBRs, when compared to LWRs, are unique in their ability to utilize far more of the energy available in the fuel. More of the fissile material is consumed and more of the

fertile material is converted into fissile material. This phenomenon is what allows FBRs to use depleted uranium coming out of LWRs in the blanket region of the reactor [14].

Many FBRs have been built in the United States and internationally, including two iterations of the Experimental Breeder Reactor (EBR). Despite successful demonstration reactors, FBRs never became the standard reactor around the world; this is mostly a matter of cost. FBRs could not economically compete with light water technology, but also had inherent reactivity safety problems and proliferation concerns associated with highly enriched fuels and plutonium production [3]. The fate of FBRs is important to consider in the modern world: a ‘better’ reactor loses its edge if it is not cost competitive.

### 1.3.5 Breeder-Burner Reactors

A breeder-burner (B&B) reactor is a nuclear reactor that generates its own fuel through the breeding of fissile fuel from fertile feedstock. B&B reactors typically operate in the fast spectrum and therefore are also a type of fast breeder reactor. While there are many benefits to breeding a reactor’s fuel within itself, there are some substantial drawbacks. The fertile fuel in B&B reactors has a minimum burnup that it must reach in order to tip over from net-absorber of neutrons to net-producer of neutrons. This tip-over point is usually on the order of 10% fissioned initial heavy metal atoms (FIMA). Neutronically, this is achievable; however, the fuel and structural material have limits to the dislocations per atom (DPA) that can accumulate before large stresses form in the cladding and cladding failure is likely. B&B reactors are especially susceptible to this due to both the high burnup required and increased DPA per collision from fast neutrons. The peak DPA of the fuel can be reduced by limiting the peak burnup.

The design of a B&B reactor can include the movement of fuel around the core to reduce the peak burnup in the fuel, as well as take advantage of different neutron energy spectrums at different locations [15, 14, 23]. In general, the goal of a B&B reactor is that little to no chemical reprocessing is done and that the fuel can be moved from region to region directly. Regions of the core that have a faster neutron spectrum are typically better for breeding than lower energy neutron spectra, while the regions with a lower energy neutron spectrum are better at efficiently using the fuel [14]. Fuel can be swapped from one region to the other to take advantage of the neutron spectrum unique to each region.

B&B reactors can be analyzed using a neutron balance to determine the minimum burnup

required for fuel to transition from a net neutron sink to a net neutron source. An example of a neutron balance is in Fig. 1.8, and the equation is described in Section 2.6.1. The fuel of a typical high enriched, fast spectrum B&B reactor is able to transition from breeding to burning without having to change geometry, though they can swap fuel to reduce the peak burnup. Thorium reactors are more likely to be obligated to swap due to breeding and burning occurring best in different flux spectrums, as thorium fueled B&B reactors suffer a significant reactivity penalty compared to uranium fueled reactors [21]. The minimum point in the B&B neutron balance curve corresponds to the criticality of the system transitioning from subcritical to critical, and the maximum point corresponds to the criticality of the system transitioning from critical to subcritical.

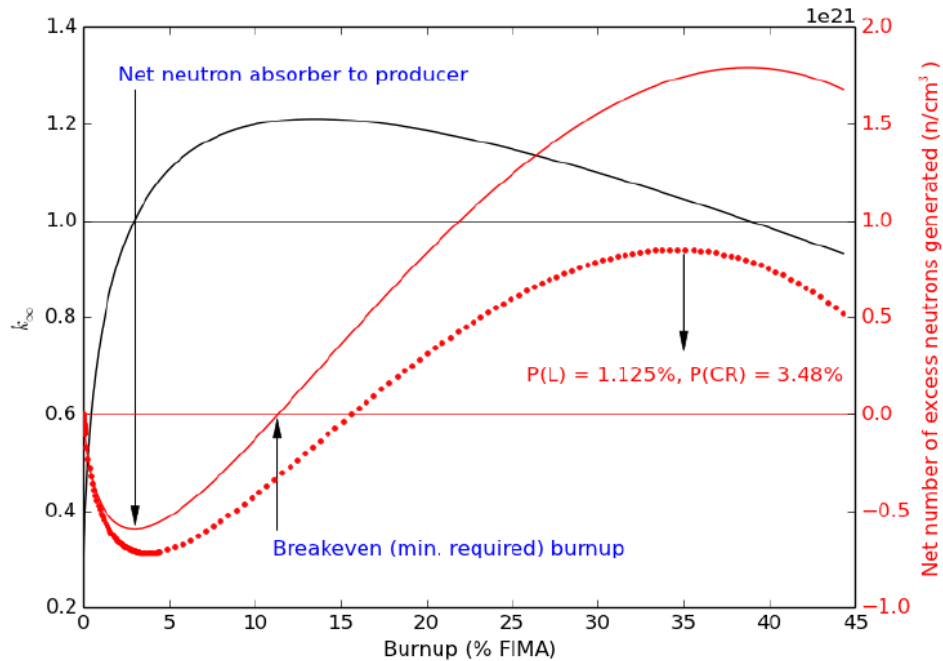


Figure 1.8: 0D neutron balance and  $k_{eff}$  [14]

Fast spectrum thorium fueled B&B reactors have been evaluated before, and have consistently been found to under-perform in terms of sustainable criticality and burnup duration, relative to  $^{238}\text{U}$  fueled fast reactors [13].

### Improvements to Computational Time

A homogenization method to decrease computational time and memory usage was used by Greenspan et. al that applied well to B&B reactors [14]. The arrangement of pins in the core can be grouped into rings (also called R-Z geometry), as shown in Fig. 1.9. According to Greenspan et. al, the pin and R-Z geometry showed ‘good agreement’, and the R-Z geometry ran six to seven times faster than the hexagonal pin geometry. However, the reactor modeled was an unmoderated fast reactor, so a similar justification will have to be made if this same method is applied to a thermal reactor. There is potential that similar methods applied to a thermal reactor could reduce the computational time required for each case..

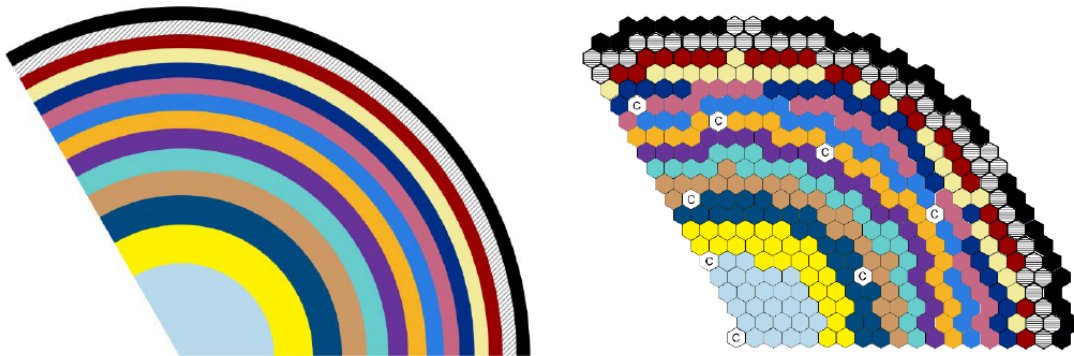


Figure 1.9: Converting pin geometry to ring geometry [14]

#### 1.3.6 Analytic Breeding Studies

Analytic and semi-analytic solutions exist that show the performance of many different moderators in a breeder reactor [35, 36]. A crucial part of breeder reactor design is the choice of moderator. A neutron balance can be used to determine the potential breeding ratio as a function of the moderator stopping power, cross section, and number of fissile isotopes. The maximum breeding ratio of a moderator has been calculated before, and can be used as an indicator for a moderators viability for breeding. Fig 1.10 shows the potential for over-moderation as well as the importance of using  $^{233}\text{U}$  compared to  $^{239}\text{Pu}$ , which performs relatively poorly in the moderated environment [36].

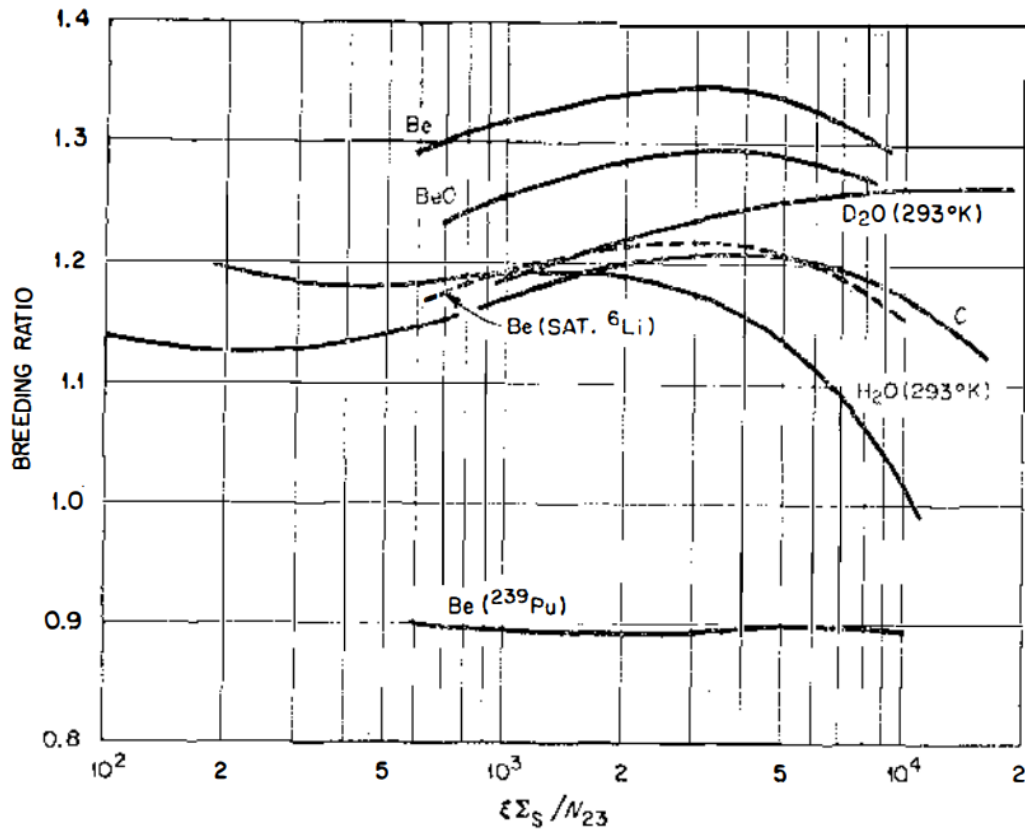


Figure 1.10: Maximum theoretical breeding ratio as a function of the slowing down power per fuel atom ratio for  $^{233}\text{U}$  fuel at 900K [36]

A study from Oak Ridge National Laboratory showed that for a two region graphite moderated core, the net breeding can be slightly higher than unity [36]. The theoretical breeding the system could have achieved is shown in Fig 1.11. However, the authors noted that losses due to fission product poisons and reprocessing were significant. Another large source of loss was the parasitic absorptions by  $^{233}\text{Pa}$ , which represents the loss of both a neutron and a fissile isotope. At steady state, the ratio of absorptions in  $^{233}\text{Pa}$  to absorptions in  $^{232}\text{Th}$  was around  $\frac{1}{2}\%$ . The losses to  $^{233}\text{Pa}$  were large due to the high power density that the authors used in an attempt to have a short doubling time [35]. Throughout the report, it is shown that the breeding potential for thorium fuel is highly dependent on both the moderator material and the moderator-to-fuel atom ratio. This is an important consideration for the design.

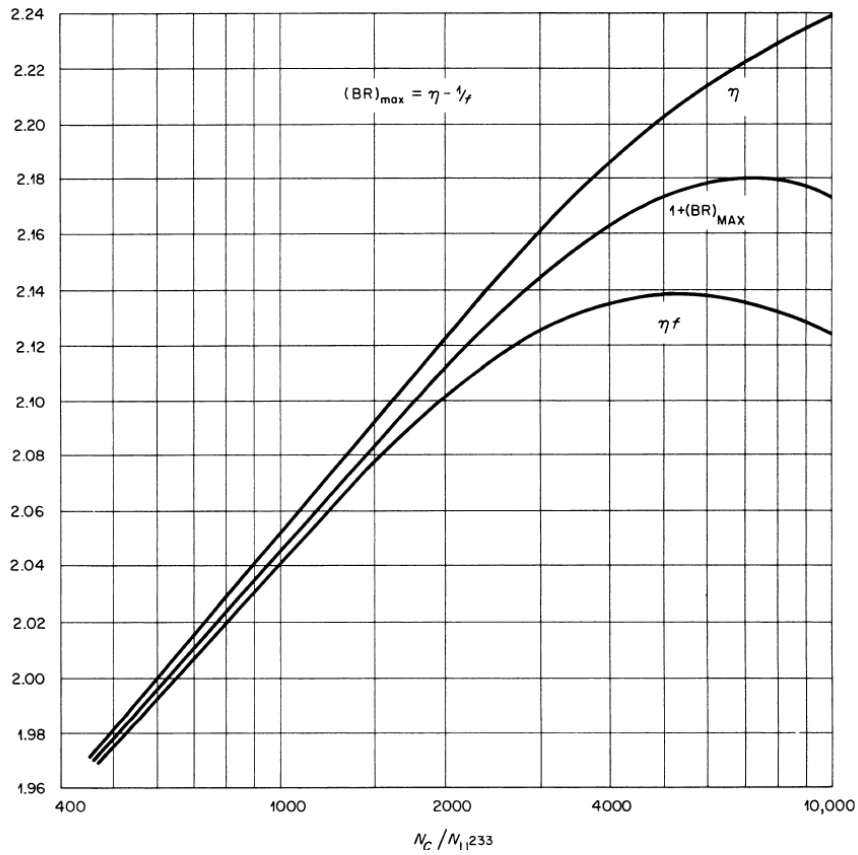


Figure 1.11: Maximum theoretical breeding ratio as a function of moderator to fissile material ratio [35]

## 1.4 Optimization Strategies

Optimization is a process intended to maximize or minimize an objective based on one or more parameters. The desired objective of the system can be referred to as the ‘fitness’ of the system [37]. In many applications, the fitness of the system is the price to purchase or construct the system. In a nuclear engineering context, it could be anything from a dose rate based on shielding or enrichment of fuel for a new reactor core. The fitness of a system can be mathematically stated as

$$\text{Find } X = \begin{bmatrix} x_1 \\ x_2 \\ \vdots \\ x_n \end{bmatrix} \text{ which minimizes } f(X)$$

with the constraints

$$g_j(X) \leq 0, \quad j = 1, 2, \dots, m$$

$$l_j(X) = 0, \quad j = 1, 2, \dots, p$$

where  $X$  is an  $n$ -dimensional ‘design variable’,  $f_k(X)$  are the ‘objective functions’ in a vector of size  $k$ , and  $g_j(X)$  and  $l_j(X)$  are the ‘inequality’ and ‘equality’ constraints. A system is optimized by minimizing the objective functions,  $f(X) = [f_1(X), f_2(X), \dots, f_k(X)]$  using the design variables,  $X = [x_1, x_2, \dots, x_n]$ . The number of variables  $n$  and the number of constraints  $m$  and  $p$  do not need to be related. Inputs to the objective vector can be fixed from the beginning, and these are called ‘preassigned parameters’. For reactor design, preassigned parameters could be materials and general layout of the reactor. The constraints of an optimization problem form a limit on parameters or outcomes. They could be physical constraints such as spatial limits or could be a condition that must be fulfilled such as the  $k_{eff}$  must be greater than or equal to one. However, an optimization problem does not need constraints; in that case, it would be called an ‘unconstrained optimization problem’ [37].

Many factors can be analysed in a nuclear reactor. For example, the optimal geometric distribution and enrichment of fuel can be determined using a design of experiment (DOE) matrix. A DOE matrix can be used to determine how the perturbations of a parameter affect the end result. In this case, the perturbations will affect the geometric layout of the core such as pitch-to-diameter ratios in each region of the core, fuel loading, enrichment, size, and power. If custom macroscopic cross sections are employed, then even the range of viable cross sections can be determined, and from that, the list of possible moderators and coolants. The results of these perturbations can be visualized with Pareto charts, and then a simple gradient method can be applied to the results to determine the trend of the perturbation, and to seek a local optimum.



In addition to the DOE matrix, a more rigorous analysis of the effect of the perturbations can be done with a sensitivity analysis. This is especially useful if determining the fitness is slow or computationally intensive, for instance, in a high-fidelity Monte Carlo simulation. A sensitivity parameter,  $S_{k,N_j}$ , can be defined as a response of the fitness,  $k$ , to the parameters  $N_j$  [39]. Three cases can be analyzed: a nominal case that yields  $k_0$ , an increase in  $N_j$  yielding  $k_{N_j}^+$ , and a decrease in  $N_j$  yielding  $k_{N_j}^-$ . The resulting sensitivity parameter can be defined as

$$S_{k,N_j} = \frac{N_{j,0}}{k_0} * \frac{\delta k}{\delta N_j} = \frac{N_{j,0}}{k_0} * \frac{k_{N_j^+} - k_{N_j^-}}{N_j^+ - N_j^-} \quad (1.9)$$

Multiple cases can be evaluated with this format, changing either the perturbations or the  $N_{j,0}$  to develop a model of how changing a parameter changes the fitness. This can be used to generate a low-cost surrogate model that can be used to determine the fitness, rather than the high cost method used to determine  $k$ .

### 1.4.1 Optimization Methods in the Nuclear Field

There are a number of optimization methods that are prevalent in the nuclear field. Genetic algorithms (GAs), in particular, are already used for optimizing fuel load, reload, and shuffling calculations. They are used for their capacity to yield “sufficiently good solutions in sufficiently short time” [38]. GAs have their roots in the concepts of biological evolution, borrowing the Darwinian concept of survival of the fittest. A unique aspect of GAs is the use of a population of data points, rather than a single design point. The use of a population means that the solution is less likely to be trapped at a local optimum. There are three elements from biology that appear in GAs: reproduction, crossover, and mutation. Reproduction, or selection, is the process of selecting the ‘good’, or most fit, outcomes to be passed on the next generation. Crossover is the mixing of inputs between two randomly selected members of the input population to create a new, potentially more fit member of the new generation. Mutation is the randomized changing of a design variable to a new value. This allows for regions of the design space to be explored that are not already within the population. Again, this helps to prevent trapping the solution at a local optimum. Even though the selection and mutation processes have random elements, GAs are not a random search technique; they are capable of efficiently exploring new combinations within a design space to spawn a new generation with higher fitness than the previous. The

flexibility of GAs also allows them to be a natural fit for problems that include both continuous and integer inputs. While there is no mathematical proof that GAs will improve the fitness of a population over time, they have been shown in practice to converge to optimum solutions [37].

### 1.4.2 Surrogate Modeling

Surrogate models are approximations of the fitness or cost function. A surrogate model is built by exploring the design space of a high cost and high fidelity model. The points of the design space that are explored are determined by the choice of the design of experiment, similar to the DOE referenced for optimization methods. Once the space is explored, a model can be created that replicates the results and generate new results that are sufficiently accurate for points that were not explored in the high fidelity model. Optimization techniques, such as genetic algorithms, can be applied to the new model to efficiently explore for solutions with greater fitness [9]. They are relatively low cost and quick compared to the models or simulations that generate the data needed to create the surrogate model.

## 1.5 Objectives

The objective of this thesis is to determine the feasibility of a thermal spectrum thorium fueled reactor to operate long-term without the use of chemical reprocessing. The ultimate goal is to determine a reactor design that can be initially fueled with a mixture of fissile  $^{233}\text{U}$  or  $^{235}\text{U}$  and fertile  $^{232}\text{Th}$ , but then subsequently refuel with only fertile  $^{232}\text{Th}$ . The feasibility of the thorium fueled breeder reactor can be determined by perturbing parameter values and observing the resulting trends. If a traditional breeder-burner configuration is non-viable, additional perturbations can be explored such as using a swapping scheme or an enriched blanket.

A thorium based reactor needs to have incredibly attractive elements in order to penetrate into the power market. The accumulated operating experience, existing infrastructure for a uranium fuel cycle, and regulatory concerns with less-extensively tested technologies makes significant innovation difficult and expensive. A thorium reactor would have to offer substantial financial benefits over both uranium reactors as well as other methods of power generation like renewable sources or natural gas. In addition to the capital cost, the licensing of the design requires that it is as simple and safe as possible to expedite the process. Since thorium breeder

reactors operate on tight neutronic margins, high-fidelity modeling is required to determine the design space in which such a reactor could operate, if it could operate at all. This may be possible to accomplish with new optimization techniques and modeling methods to speed convergence to an effective design.

## 2 Methods

### 2.1 Introduction

This chapter describes the methods used to determine the feasibility of a thermal spectrum thorium breeder reactor without chemical reprocessing. The code packages and scripts used to facilitate the analysis are described. This section also shows the steps taken to transition from analytic analysis to modeled lattice analysis and then to quarter-core models.

### 2.2 Software

#### 2.2.1 Gnowee Optimization Code

Gnowee is a hybrid meta-heuristic optimization algorithm that was designed for black-box nuclear engineering optimization problems [1]. It was created to help design a material stack that would generate a desired neutron energy spectrum from an incident neutron spectrum. However, the heuristics used are not specific to its original task and Gnowee can be used for any type of problem. A heuristic is defined as a process or method, and meta-heuristics are the selection of one or more heuristics to solve a particular problem. Gnowee is a hybrid method because it does not utilize a single optimization strategy; instead, it uses a genetic algorithm that has several operators with distinct heuristics to create new generations. Many of the heuristics have some degree of overlap in their definitions, and an algorithm or operator can contain several heuristics; each of these operators and heuristics has its own advantages and disadvantages. The heuristics that are employed are:

- Neighborhood Search: New solutions are found nearby current solutions by slightly perturbing one or more inputs. This searches local changes.
- Hill Climbing: A change to an input is only accepted if it leads to an improvement in fitness.
- Accepting Negative Moves: Allows changes to be accepted even if there is a decrease in fitness. This prevents a solution being trapped at a local optimum.

- Multi-Start: Restarts the search after a local optimum is reached. Using a population is considered a form of Multi-Start.
- Adaptive Memory Programming: Past searches are used to guide development and prevent the same area from being explored repeatedly.
- Population Based Search: Many searches are enacted across a population, and information can be shared between each search. This can help accelerate global convergence, as well as prevent converging to a local optimum.
- Intermediate Search: The space between two high fitness solutions is explored. This can find higher local or even global optimums and accelerate local convergence.
- Directional Search: Explores towards established productive directions, such as along gradients or in the vicinity of high fitness solutions.

Gnowee cycles through a bevy of algorithms for each generation, with the members of one generation becoming the ‘parents’ for the next generation of ‘children’. The algorithms used in Gnowee are described by Bevins and Slaybaugh [1]. Table 2.1 shows which heuristics each algorithm employs. The algorithms in Gnowee, in order of execution, are:

- 3-opt: Two re-orderings of the parent’s input sequence are considered. One re-ordering involves swapping two sub-sequences, and the other maintains the positions of the sub-sequences, but inverts the two that have been swapped. The child with the highest fitness replaces the parent if it has a higher fitness than the parent.
- Levy Flight: A parent’s inputs are randomly perturbed, and a Metropolis-Hastings rejection algorithm is used to automatically accept all increases in fitness. A fraction of children that do not improve in fitness over their parents are randomly compared against another parent in the population, and the child replaces that parent if it has better fitness.
- Crossover: Children are created from a random index drawn from the high fitness parents of the previous generation.
- Scatter Search: Parent’s inputs are randomly selected and then perturbed by another randomly selected parents input.

<i>Heuristics</i>	<i>3-opt</i>	<i>Levy Flight</i>	<i>Cross- over</i>	<i>Scatter Search</i>	<i>Mutation</i>	<i>Inversion Cross- over</i>	<i>2-opt</i>
Neighborhood Search	✓						✓
Hill Climbing	✓	✓	✓	✓	✓	✓	
Accepting Negative Moves		✓					
Multi-Start		✓					
Adaptive Memory Programming	✓	✓	✓	✓	✓	✓	✓
Population-Based Search	✓	✓	✓	✓	✓	✓	✓
Intermediate Search			✓	✓	✓	✓	
Directional Search		✓	✓			✓	✓

Table 2.1: The heuristics used by Gnowee algorithms

- Mutation: A simple, random perturbation of an input that selects for higher fitness.
- Inversion Crossover: A portion of a parent is inserted into another to create a unique child.
- 2-opt: Similar to 3-opt, but only a single re-order is considered.

There are several advantages to using Gnowee. Some of them are intrinsic to the methods used, such as the ability to not become trapped at local optimums and the capacity to solve black-box optimization problems. Along with this, Gnowee was written in Python, which is the same language used to create the input files and parse the output files of the transport code. This allowed for direct incorporation of Gnowee with the transport code [1]. Gnowee does not necessarily find a true global optimum in every circumstance. Instead, it can be used as a tool to efficiently explore a design space by searching for high fitness solutions. In these cases, the phrase ‘optimizing’ refers to intelligently searching for higher fitness solutions rather than striving for a true global optimum.

### 2.2.2 SCALE Transport and Depletion Code

SCALE is a code suite comprised of several key programs; the relevant codes to this situation are TRITON, the 1-D through 3-D transport solver, and ORIGEN, the depletion code. TRITON has two sub-codes within it: NEWT, a 1-D and 2-D deterministic transport solver and KENO, a 3-D Monte Carlo transport solver. Both NEWT and KENO use cross sections from nuclear data libraries to calculate fluxes and reaction rates. TRITON’s output flux and materials can be used by ORIGEN to generate a decay-only cross section library that ORIGEN can then use to deplete the given material. Normally, a transport calculation will execute TRITON at

every timestep requested and then use the resultant flux to deplete the material with ORIGEN. However, ORIGEN can retain its cross section library to be used at future timesteps and can be executed independent of TRITON. Using the low cost ORIGEN to deplete over long time intervals may offer significant computational resource savings.

There is a second, significant benefit to using ORIGEN: a built-in material feed and removal function. The designers of ORIGEN included this in the code so that thorium fueled molten sodium reactor models could have on-line fission product removal and thorium addition. This is crucial as many fission products do not require chemical separation to be removed; if the fuel is a liquid, the noble gases and volatile elements will separate from the dense liquid fuel. This allows for fission product venting, which will prove advantageous for the breeding ratio of the fuel, especially since  $^{135}\text{I}$  and  $^{135}\text{Xe}$  will volatilize out. This also has the added advantage of reducing the source term of the fuel in the event of an accident. Several processes are in use or being developed for volatile fission product capture, even up to high temperatures [22].

When TRITON is executed as the main process, ORIGEN's only capability is to be invoked as a subprocess to deplete materials. There are several other features of ORIGEN that can only be used specifically from an ORIGEN input, most important is the fission product removal capability. While the output of a TRITON-only case can be put directly into ORIGEN, the output of an ORIGEN-only case cannot be put into TRITON. The ORIGEN output needs to be put back into TRITON so that  $k_{eff}$  and the flux profile can be resolved. ORIGEN on its own cannot generate a  $k_{eff}$  or a flux spectrum. Cycling from ORIGEN to TRITON required creating a separate script to change the output of ORIGEN into a form that TRITON can read. This script was later expanded to allow the back-and-forth cycle to occur many times over a case, allowing  $k_{eff}$  to be accurately tracked as a function of burnup while still having the fission product removal function.

Every case evaluated in SCALE used the same neutron input of 5000 neutrons per generation for 100 generations with 20 skipped. This produced  $k_{eff}$  uncertainties on the order of  $\pm 0.0015$  for quarter-core geometries and  $\pm 0.0008$  for the infinite lattice cases.

### 2.2.3 Coupling SCALE and Gnowee

A script was written to automate the creation and execution of SCALE's input files, as well as the parsing of the output files. This automation allowed for rapid prototyping and modeling of

the proposed designs. It also allowed for Gnowee to control the input parameters for the file creation and read the output files, giving Gnowee the capacity to operate unsupervised. Three flowcharts are provided to describe the process.

The flowchart in Fig 2.1 outlines the basic Gnowee optimization process. Input boundaries, objective functions, constraint functions, and other parameters are assigned using a Python script. The main loop in *Gnowee.py* creates a population, and cycles through the optimization algorithms until the optimizer has converged on a solution or the iteration limit is reached.



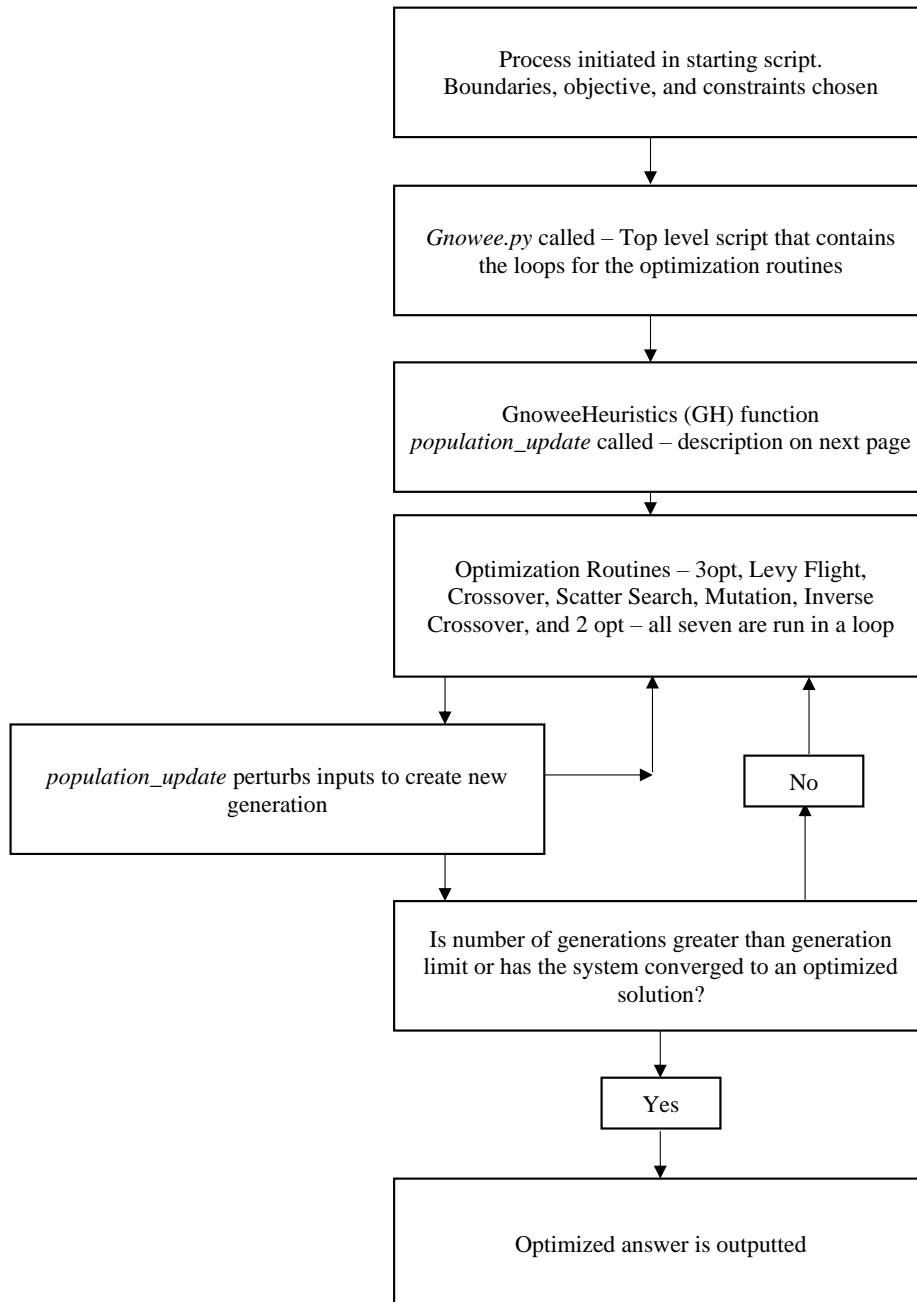


Figure 2.1: A high-level flowchart describing the process that Gnowee uses to optimize a problem.

Fig 2.2 shows the flowchart for the process of translating Gnowee's perturbations into a SCALE input file. When Gnowee updates a population, the parameters of the new generation are passed to a series of scripts that read in the information, as well as information that is constant for all cases. The information for the defined materials is also included at this point. All of the information is collected in one script. Some of the information is sent to functions to determine the layout of the fuel in the core, based on the passed variables and the core geometry selected. The power density or total power is determined once the amount of fuel in the core is determined. The user can dictate whether total power or a power density is used. The geometry, power, and other inputs are fed into a file-creating script that will build the inputs for TRITON and ORIGEN. The resultant files will be checked against other cases that have already been evaluated. If the files are not unique and have been evaluated already, they will not be calculated again and the output of the old calculation is retrieved instead. If the files are unique, the TRITON file is executed. The check for uniqueness is important because Gnowee re-invokes the objective function several times per child in the population. Once TRITON finishes, the output is parsed to update the flux and materials in the ORIGEN input and the ORIGEN file is executed. The output of the ORIGEN file is then parsed for the materials to be put into the final TRITON input file. The output of the last TRITON calculation is then used to determine the fitness and constraints on the system. The script can cycle between TRITON and ORIGEN in order to calculate criticality and the flux profile at each timestep.

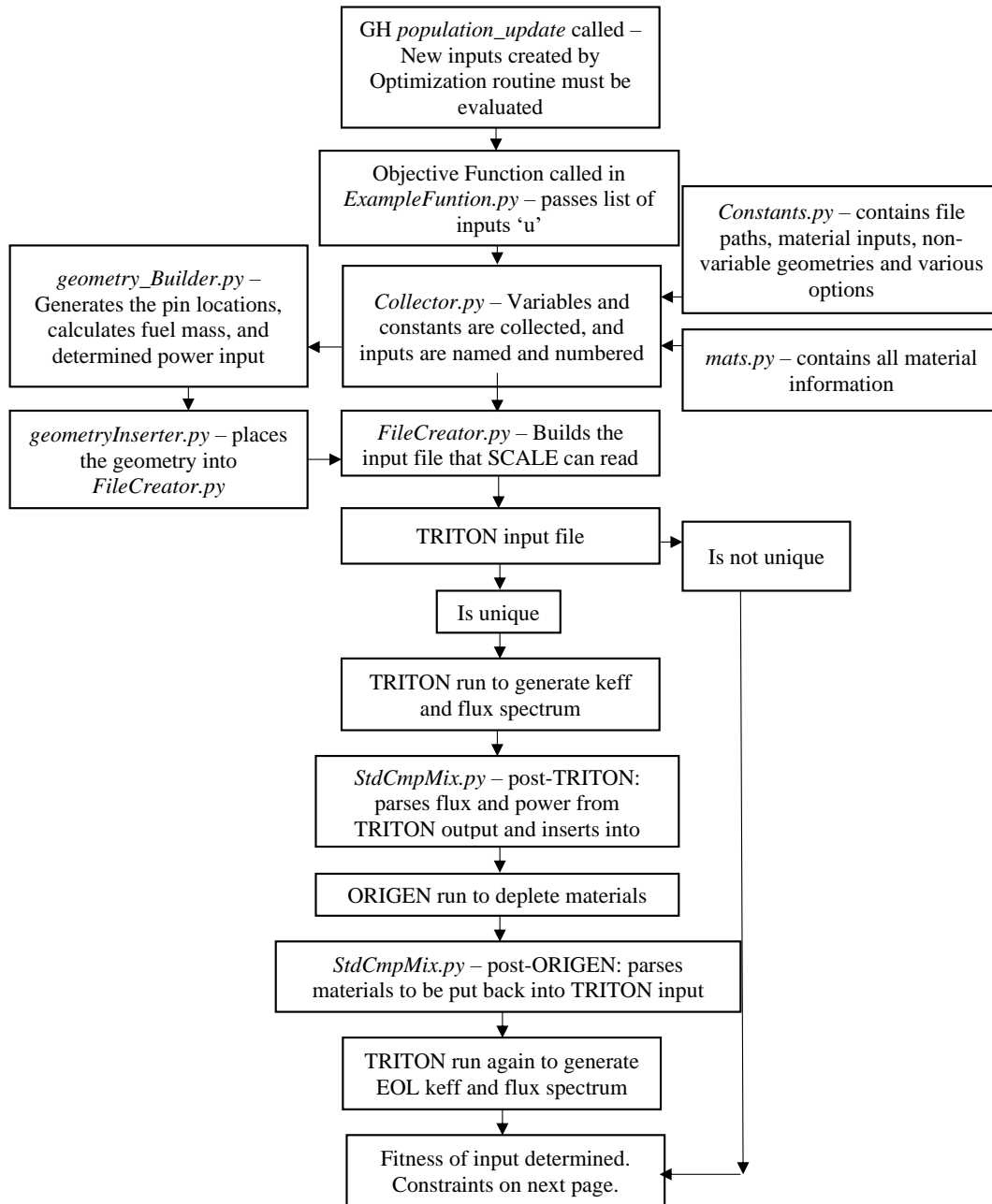


Figure 2.2: A high-level flowchart describing the process that couples SCALE to Gnowee.

Fig 2.3 shows the final step in which the constraints are applied to the problem. If the constraints are not satisfied, the fitness is set to be a large number:  $1E99$  in this case. This means that all cases that violate the constraint are forced out of the population.

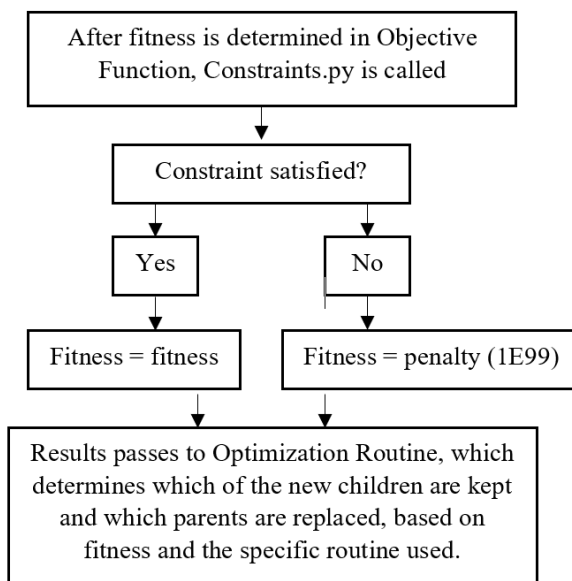


Figure 2.3: A high-level flowchart describing the application of the constraint function after the objective function has been solved.

## 2.3 Engineering Judgments

There are an wide variety of reactor designs and fuels that are potential options for this analysis. Engineering judgments are needed to narrow the scope of the work. These judgments primarily involve maximizing the breeding potential of the design and minimizing the complexity. Addressing the complexity would help to generate a design that is efficient, simple, and potentially cheaper. These judgements come from the past reactor designs discussed in Section 1.3.

The first judgment is that the fuel should be a liquid. A design similar to the Moltex design in which the fuel is a liquid that is contained in a solid walled tube surrounded by coolant and moderator is proposed for the thorium breeder reactor [27]. The fuel is not pumped like it is in MSRs. Liquid fuel is used for a number of reasons:

- Fuel swelling and structural displacements are less of a concern; the problem of structural

damage is highlighted especially in fast breeder reactors which are limited by the burnup of the fuel [12]. Liquid fuel means that fuel swelling is no longer a concern for bursting fuel elements and causing clad failure.

- Gaseous fission products can come out of solution and can be vented out of the fuel tubes. Not all fission products will be able to be removed by this method, but many high-cross section isotopes and their precursors can be removed. An example of this is both  $^{135}\text{Xe}$  and its precursor  $^{135}\text{I}$  are likely to volatilize out or can be removed by non-chemical means [26]. As shown in Fig 1.7,  $^{135}\text{Xe}$  alone causes a substantial reduction in the conversion ratio. Removing volatile fission products has the additional benefit of reducing the source term of the fuel in the event of an accident. Removal of the volatile elements from the fuel means that the remaining fission products are much less mobile, which could potentially result in lower risk to the general populace and smaller emergency planning zones. However, this does pose the risk of also removing some neutron precursors.
- The fuel tubes can be either independent or interconnected. If they are independent, the fuel tubes can be geometrically rearranged or swapped to take advantage of regions of the core that are better at breeder or burning. By this swapping method, thorium can be bred into  $^{233}\text{U}$  where the flux is conducive for breeding and then moved into the locations with a more thermal flux to be burned. This location-specific breeding and burning was the basis of the core design of the LWBR, though it did not include swapping [17]. If the fuel tubes are interconnected, then the liquid fuel can be pumped from location to location like coolant through a radiator. This would result in the same effective fuel swapping, but without the need to manipulate the fuel tubes. Either method would come with its own complexities and costs.
- Modeling a liquid fuel tube could be less computationally demanding than modeling a solid fuel element. If the liquid fuel can flow within its volume, the mesh could be as large as the fuel volume. Solid fuel requires a finer mesh due to depletion varying with fuel depth.

A second engineering judgment is to not use light water as a moderator. Again, this is for several reasons,

- Fig. 1.7 shows the negative impact that water and metal have on the conversion ratio. Decreasing the losses due to hydrogen adsorption could further increase the breeder capability of the reactor.
- The pressure vessel and containment structures for LWRs constitute a substantial portion of the capital cost for the reactor, both in terms of construction time and material costs [43].
- Metallic and salt based coolants, in addition to not requiring high pressures, are not likely to boil away. This reduces the possibility for departure from nucleate boiling (DNB) and other accidents associated with the phase change of the coolant.

Any design feature that can increase safety or reduce risk is beneficial not only due to safety, but also because it will theoretically allow for quicker regulatory approval. However, novel safety methods need special attention and qualification for the regulator to accept them, which can be detrimental to rapid acceptance.

## 2.4 Reduction of Order Method

All numerical methods have some amount of error for any solution that is generated. Deterministic methods can have error due to truncation or convergence criteria, and stochastic methods can have error stemming from statistical uncertainty. In general, the error can be reduced by putting in more work, whether that is in the form of a finer discretization, more simulated particles, or a higher-order method. There is almost always the trade-off between work and accuracy. In the case of coupling SCALE and Gnowee, the cost per evaluation can be quite high, so a reduction of order can be used to exchange the fidelity of the simulation for more rapid execution.

Gnowee solves the given objective function for each member of the population every time the population is updated [1]. Since the proposed method is to use the output of SCALE as the solution to the objective and constraint functions, this means that SCALE will need to be invoked many times. The transport portion of SCALE, TRITON, carries a high computational cost, but there are ways to reduce the overall price. The purpose of this reduction of order method is to decrease computation time required for each step of the optimization process, but at the price of a reduction in accuracy. In this case, the reduction of order will decrease the

temporal fidelity of the flux profile by assuming that the flux profile does not change dramatically over the course of the time-step.

TRITON's output flux and materials can be used by ORIGEN to generate a cross section library that ORIGEN can then use to deplete the given material. Normally, a transport problem will invoke TRITON at regular intervals throughout the prescribed burn length, and then use the resultant flux to deplete the material with ORIGEN. However, ORIGEN can retain its cross section library to be used at future time-steps and can be executed independently of TRITON. A significant savings could be realized if the flux profile was not evaluated at each time-step that the depletion was solved. Instead, the flux profile can be solved for once, and then used to generate a cross section library to be applied to the much faster depletion-only solver. TRITON would then need to be invoked again at the end of the depletion to generate an end-of-life  $k_{eff}$ . A high fidelity case with TRITON evaluated at many short time-steps can be used as the baseline case to compare to the test cases.

This reduction of order method is common for evaluating a traditional  $^{235}\text{U}$  fueled core, but may not work as well for a  $^{233}\text{U}$  fueled core with breeding from  $^{232}\text{Th}$  [10]. This carries the assumption that the flux profile does not change substantially over the course of the depletion. Typical thorium breeder designs have uranium fueled seeds and uranium-less blankets. This means there is the potential that the flux profile could change significantly as fuel is depleted in the seed and bred in the blanket. The purpose of this reduction of order study was testing the possibility that the flux spectrum and isotopics of the reduced case would change from a nominal case.

### 2.4.1 Geometry and Materials

This model utilized one quarter of a cylindrical core 1.5  $m$  in diameter with fuel tubes in a hexagonal lattice. The fuel is a liquid thorium metal alloy enriched to varying levels in  $^{233}\text{U}$  and is burned at a low power density of 2 mega-watts per initial ton of heavy metal ( $MW/ITHM$ ). From the innermost ring outward, the effective enrichments are: 5%, 4.1%, 3.3%, and 2.7%. The fuel tubes are 3  $m$  tall and have a radius of 1.5  $cm$ , with a 5.2  $cm$  center-to-center pitch. The tubes are composed of 2  $mm$  thick molybdenum. The fuel tubes are surrounded by a metallic moderator for moderation. The core is then surrounded by a graphite neutron reflector, a 7  $cm$  thick outer coolant flow path, a 5  $cm$  borated alumina neutron and gamma shield, and then the

5 cm molybdenum reactor vessel wall. The upper portion of the outer flow area homogeneously includes the heat exchanger, and the outer coolant flow path widens from 7 cm to 27 cm while the graphite reflector tapers from 25 cm to 5 cm to make room for the heat exchangers. Above the core is a 5 cm vapor space containing a gaseous argon-hydrogen mixture. Finally, there is 5 cm graphite reflector attached to the bottom of the core barrel. All non-molybdenum materials were coated in 3 mm of molybdenum due to the potentially corrosive nature of the metallic moderator. The modeled core can be seen in Figures 2.4 and 2.5.

The full TRITON case was depleted for 200 days, with the flux solved for at days 0 and 12.5, and then every 25 days after that. The flux was solved for a total of 8 times. The depletion was solved once every 25 days starting at 0 and ending at 200. The reduced case solved for the flux at days 0 and 5 with depletion at days 0 and 10, followed by 100 equally spaced depletion time-steps over 180 days. The follow-on flux calculation was at 190 and 195 days, with depletion at days 190 and 200. The reduced case solved for the flux a total of 4 times. The depletion results at the beginning and end-of-life are seen in Figure 3.1.

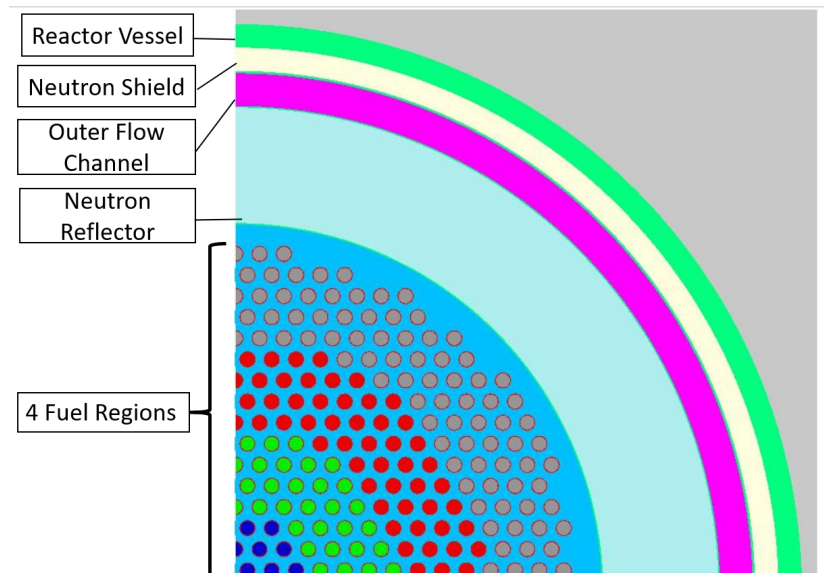


Figure 2.4: Top view of quarter-core model. From the inside out, there are 4 fuel regions within the moderator/coolant, the neutron reflector, the outer coolant flow area, the neutron and gamma shield, and the reactor vessel wall.



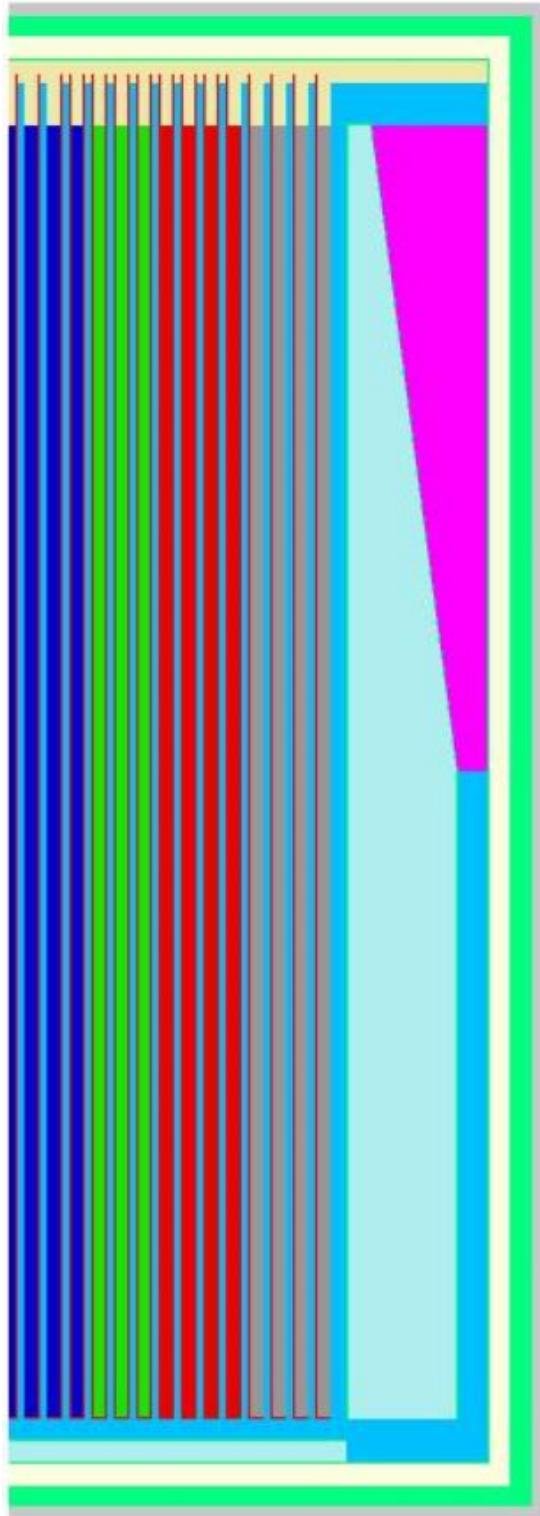


Figure 2.5: Side view of quarter-core model. From the inside out, there are 4 fuel regions within the moderator/coolant, the neutron reflector, the outer coolant flow area, the neutron and gamma shield, and the reactor vessel wall. The purple region is the heat exchanger homogeneously mixed into the outer coolant flow area.

## 2.5 Infinite Homogeneous Model

The first step in determining appropriate materials is a first order comparison of their neutronic properties. This can be used to compare dissimilar materials and narrow the range of materials to be considered in higher fidelity analyses. Parameters such as moderator power and moderating ratio are calculated for all materials that are being considered for further analysis. Light water, while not being considered for this design, is included as a reference point that the other materials can be compared against. The full list of materials is:

- Light Water
- Heavy Water (Pure D<sub>2</sub>)
- Graphite
- Zirconium Hydride (ZrH<sub>2</sub>)
- Liquid Metallic Moderator

The results can be seen in Table 3.3. For unique mixtures, the moderating parameters are calculated by determining the slowing-down power of each material and dividing the sum by the total scattering cross section of the material, shown in Eq. 2.1 [2]

$$\bar{\zeta} = \frac{1}{\Sigma_s} \sum_i \zeta_i \Sigma_s^{(i)} \quad (2.1)$$

The total scattering cross section also had to be determined. The nuclei are generally assumed to be free atoms in the mixture, with no impact from the chemical structures. A common exception to this is for light and heavy water, which have well characterized cross sections in their chemically bound state and have included the effects of the chemical bond. The total scattering cross section is calculated by

$$\Sigma_{s,mix} = \sum_i N_i \sigma_s^{(i)} 1E - 24 \quad (2.2)$$

where  $\Sigma_{s,mix}$  is the scattering cross section of the mixture,  $N_i$  is the number density of material  $i$ ,  $\sigma_s^{(i)}$  is the scattering cross section of material  $i$ , and the units are converted from  $bn$  to  $cm^2$ .

## 2.6 Infinite Lattice Pin Analysis

Additional considerations need to be accounted for in addition to the raw moderating properties. Geometry, depletion, and fission product impacts needed to be analyzed as well. The infinite homogeneous model work that has been done previously can be used to inform the moderators used in an infinite lattice pin analysis. This analysis was done through a series of tests using a single fuel pin of varying diameter surrounded by a moderator. The same moderators selected from the homogeneous moderator study are used in the infinite homogeneous case. Varying the width of the unit cell allowed the effective pitch to be changed. All boundaries were fully reflective to create the infinite lattice. The goal was to determine the pitch-to-diameter ratio that resulted in the best breeding of  $^{233}\text{U}$  in  $^{232}\text{Th}$ , and a different pitch-to-diameter ratio that resulted in the most efficient utilization of  $^{233}\text{U}$  as a fuel. Ideally, there is a range of pitches and radii that allows for both critical operation and breeding to occur within the same pin. If this range does not exist, then the best case from the pin study can be used in a multi-region core model that will have a critical burning region and a sub-critical breeding region. The multi-region core is reminiscent of the design of the Shippingport thorium reactor which successfully demonstrated these burning and breeding regions [32].

If there are no cases that allow for breeding and burning within the same pin, then the fuel must be swapped between locations to take advantage of the different flux spectrums. For the single-region infinite lattice studies, it is assumed that fuel pins are swapped directly, i.e. a fuel pin in a breeder configuration will be placed directly into a burner configuration when it has a sufficiently high enrichment. The burner pin would then either be removed from the core or placed into the breeder region to be bred back to a sufficient enrichment for burning. There are other swapping methods available, such as mixing the liquid fuel from different regions and redistributing it. The dilution and redistribution method of swapping is considered for the two-region infinite lattice.

The fuel pins contained  $^{232}\text{Th}$  enriched to varying weight percents in  $^{233}\text{U}$  mixed into an alloy of interest to NuScale with a melting point of approximately  $780\text{ }^\circ\text{C}$ . The fuel tube is molybdenum. The enrichment was varied to determine the effect of enrichment on breeding, fuel utilization, and excess neutron production. All cases used a power density of  $30\text{ MW/ITHM}$  and a burnup period of 13,000 days with 50 intervals over this period at which flux and  $k_{inf}$  was cal-

culated. This duration was chosen so that the EOL burnup would be nearly 400  $GWd/ITHM$ , which is the maximum burnup analyzed in fast spectrum breeder-burner reactor designs [14].

Some of the moderators analyzed are not likely to be used in a real reactor, but are included in order to explore potential design boundaries. The liquid metallic moderator, which is a hypothetical material that is currently being researched. Materials that cannot act as a coolant as well as a moderator have heat pipe material homogeneously incorporated into the mixture. This applied to the graphite and zirconium hydride. The heat pipe volume takes up 18% of the bulk moderator volume, with five-sixths being void, and one-sixth being molybdenum.

### 2.6.1 Neutron Balance Equation

Part of the infinite lattice analysis is determining the neutron balance of each case, as described in Section 1.3.5. The zero dimension neutron balance equation is

$$N_{ex} = N_{HM} \int_0^{BU} \left[ 1 - \frac{1}{k(BU) * P_{NL} * P_{NRC}} \right] \bar{\nu} dBU \quad (2.3)$$

where  $N_{ex}$  is the number of excess neutrons,  $N_{HM}$  is the heavy metal atom density,  $k(BU)$  is the multiplication factor as a function of burnup,  $P_{NL}$  is the probability of non-leakage,  $P_{NRC}$  is the probability of non-absorption in reactivity control elements,  $\bar{\nu}$  is the average number of neutrons released per fission, and  $BU$  is the burnup of the fuel in terms of fissions per initial heavy metal atoms ( $\%FIMA$ ). In infinite or reflective cases, neutron losses are neglected and  $P_{NL}$  and  $P_{NRC}$  are set to one. In a typical B&B reactor, the minimum burnup required to sustain operation occurs when  $N_{ex}$  is equal to zero, as this represents when the breeding fuel transitions from a time-averaged net sink of neutrons to a time-averaged net source of neutrons [14].

The integral in Equation 2.3 can be discretized and the variables determined from the SCALE output.  $k_{eff}$ , or  $k_{\infty}$  in this case, can be determined by SCALE, as can  $\bar{\nu}$ .  $\bar{\nu}$  is typically on the order of 2.48.  $dBU$  can be determined for each step by calculating the burnup step size between each time step. Since the neutron balance equation is written with  $BU$  in units of percent fissioned initial heavy metal atoms ( $\%FIMA$ ), the calculated burnup must be converted from  $MW/ITHM$  to  $\%FIMA$ . This can be done by calculating the theoretical maximum burnup of complete consumption of the initial heavy metals. This is the burnup achieved if every atom of uranium and thorium was consumed. Dividing the cumulative burnup of the step by the

theoretical maximum burnup yields the fissions that occurred per possible total fissions, which is %*FIMA*. The maximum burnup, in units of *MW/ITHM*, is calculated by

$$BU_{max} = \frac{N_{HM} * 1E24 * \epsilon}{\rho_f} \quad (2.4)$$

Where  $N_{HM}$  is the number density of the heavy metals in the fuel in atoms-per-*bn-cm*,  $\rho_f$  is the fuel density, and  $\epsilon$  is the energy released per fission in *MWd*. This equation calculates the potential energy per unit mass of heavy metals.

### 2.6.2 Fission Product Removal Effects

A study was done to measure the impact of removing the fission products on the reactivity of the system. This study used the infinite lattice geometry, and three test cases were evaluated. In all cases, a cylindrical fuel pin measuring 30 *cm* tall and 0.3 *cm* in radius was placed into a cube of moderator with reflecting boundaries in all directions. The size of the cube gave the infinite lattice an effective square pitch of 1.26 *cm*. The same cladding and fuel was used as was used in the infinite lattice study with a <sup>233</sup>U enrichment of 3wt%. The moderator is the liquid metallic moderator. The fuel is depleted at a power density of 30 megawatts per initial ton of heavy metal (*MW/ITHM*). All cases were depleted for 2060 days, or approximately the duration that previous cases took to reach near-equilibrium.

One case was executed in TRITON with no fission product removal with 20 intervals over the depletion period. This is the control case. The second case was cycled between TRITON and ORIGEN to use the ORIGEN fission product removal feature, also with 20 interval cycles. It had to be cycled back to TRITON in order to calculate  $k_{inf}$  at each timestep. This is the fission product removal case. The third case also cycled between TRITON and ORIGEN, but it only used a beginning-of-life and end-of-life TRITON calculation to replicate the reduction of order method. In the cases with fission product removal, all isotopic species of cesium, xenon, iodide, krypton, and tellurium were removed from the system. These are the same elements that volatilise out of the liquid fuel salt in molten salt reactors [26].

## 2.7 Quarter-Core Analysis

The next step is to use the data gathered from the previous cases to create a heterogeneous core model to determine the breeding potential of a thorium fueled reactor. The Gnowee interface requires that the user defines the upper and lower bounds of the variables to be perturbed. In this case, the variables will be the core height, core radius, fuel radius, fuel pitch, fuel enrichment, core-to-reflector gap thickness, neutron reflector thickness and reflector-to-reactor-vessel gap thickness. The bounds for the fuel radius and pitch are determined using the infinite lattice analysis. The thickness of the ex-core neutron shielding and reactor vessel thickness are held constant during all cases, as shielding calculations are not a concern at this time.

A quarter-core model with reflective boundaries on the truncated axes is used to help decrease the computational time required for each analysis. The fuel radius, fuel pitch, and fuel enrichment will be varied within each region of the multi-region core, i.e. in a four region core, there will be four different fuel radii, fuel pitches, and fuel enrichments. This large number of variables means that Gnowee will need to explore a large initial population and iterate on the variables for a significant period of time.

If there is a core geometry that demonstrates sufficient breeding, the fuel pins can be swapped to breed in one region, and burn in the other. Unless there is a fuel pin geometry that can breed while remaining critical, fuel shuffling will be necessary for the long term operation of a thorium reactor. With an ideal version of this cycle, unenriched thorium will be the only fuel added after the initial core load.

The core geometry is generally the same as the geometry described in Section 2.4. There are multiple fuel regions arranged concentrically, each one containing fuel tubes that are set a certain distance away from each other. The core is bounded by a barrel. Outside the core region is a reflector followed by a coolant flow channel and then the reactor vessel wall with shielding within it. The vessel walls and shielding were not iterated on due to the distance from the core, and the assumption that neutrons that leaked out of the outer coolant flow path would not leak back into the core.

There are three variations that the core can take: circular with fuel regions of equal width, circular with fuel regions that contain roughly the same amount of fuel, and hexagonal with fuel regions of equal width. In the circular cases, there is a radial and an azimuthal pitch between

the elements, which is the distance between ‘rings’ of fuel and then the distance between the elements in the ring. This was done to allow for a tight ring that could be placed a customized distance from the previous ring. For the hexagonal configuration, there is only a single fuel pitch to describe the array that makes up each fuel region. The three core configurations can be seen in Figs. 2.6, 2.7, 2.8. Every case analyzed in this thesis used the circular cases with fuel regions of equal width.

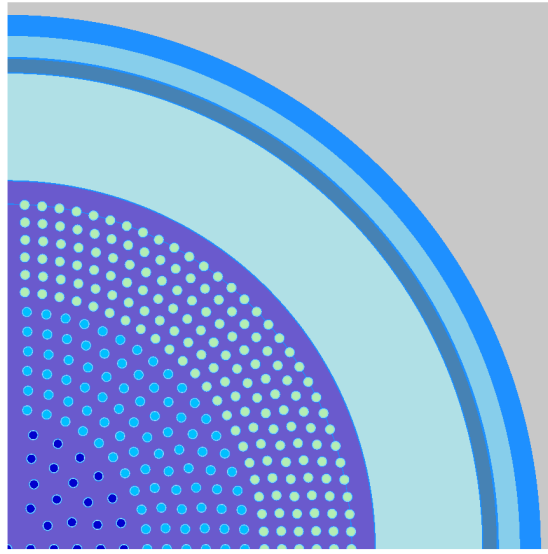


Figure 2.6: Core configuration with circular fuel regions of nearly equal thickness.

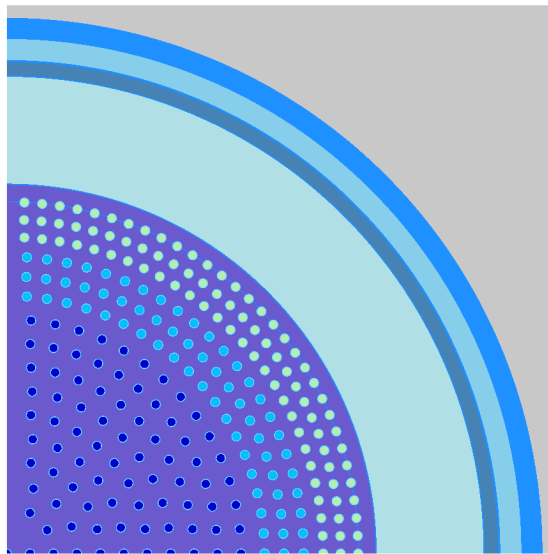


Figure 2.7: Core configuration with circular fuel regions that each contain roughly the same fuel mass.

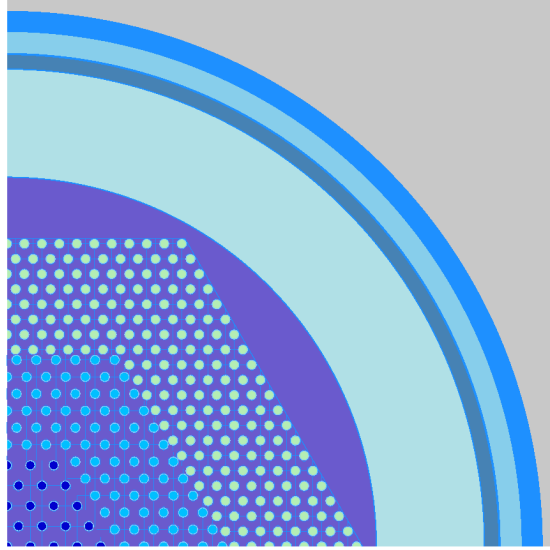


Figure 2.8: Core configuration with hexagonal fuel regions of nearly equal thickness.

The quarter-core model was optimized to maximize the breeding of  $^{233}\text{U}$  in the blanket region, relative to the enrichment of the driver region. Gnowee’s optimization process involves minimizing the objective function, so the objective function of the model was to minimize

$$S = \frac{wt\%_{B,EOL}}{wt\%_{D,BOL}} \quad (2.5)$$

where  $wt\%_{B,EOL}$  is the end-of-life (EOL) enrichment of the blanket and  $wt\%_{D,BOL}$  is the beginning-of-life (BOL) enrichment of the driver. The high fitness outcomes of the objective function should drive the solution to a core geometry and enrichment that breeds the blanket region to a high enough enrichment to be used in the driver region.

## 2.8 Two-Region Lattice

Due to increasing computational costs incurred by the quarter-core model, a simpler model was proposed. This model was comprised of a two-region annular fuel lattice that aimed to create a best-case scenario for breeding. This model was intended to remove as much moderation from the breeding region to harden the flux, while still having moderation in the burner region. This was accomplished by creating an annular burner fuel pin that contained moderator in the center and fuel in the annulus. This pin is encased in a breeder fuel shroud, with reflecting boundaries



outside of the breeder shroud. A pin containing two regions for breeding and burning can also be called a ‘duplex’ pin [41]. The proposed geometry differs from a typical duplex pin by including an internal moderator, which imposed a thermal flux spectrum upon the inner fuel annulus, and a faster flux spectrum upon the outer fuel annulus. Fig 2.9 shows the geometry of the fuel pin. Both of the fuel regions have cladding on the inner and outer faces. The two-region cases will not be evaluated with the neutron balance. The change in enrichment in the breeding region will indicate the breeding efficiency of the system instead. Every case is analyzed at a power density of  $30 \text{ MW}/\text{ITHM}$  for 2000 days. This is similar to the single-region infinite lattice and is long enough to capture when most cases become subcritical. The fuel and structural materials in the two-region lattice are the same as the fuel and structural materials used in the single-region lattice.

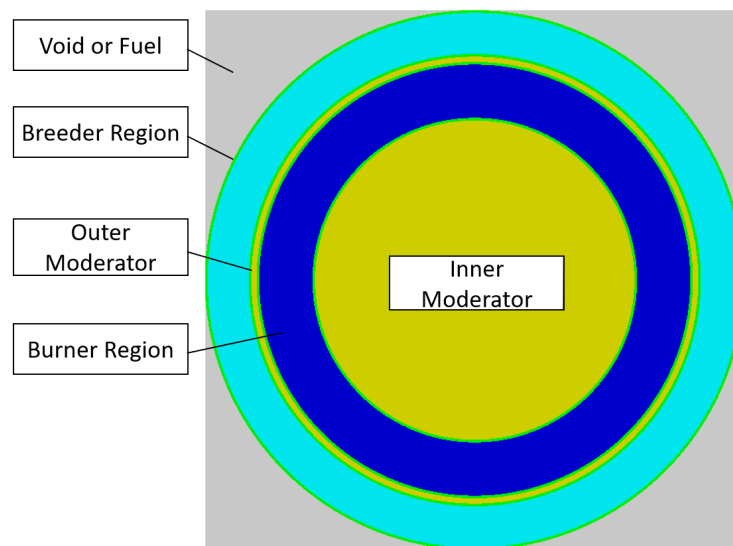


Figure 2.9: The geometry of the two-region, infinite lattice case. From the center outward, the regions are: moderator, burner fuel, a second small moderator region, and then breeder fuel.

For these cases, a different design region was explored than for the single-region infinite lattice case. For the two-region infinite lattice, the outer breeder fuel ring has a higher BOL enrichment than the inner burner fuel ring, whereas the single-region infinite lattice aimed to have a higher BOL enrichment in the burner than in the breeder. A higher enrichment in the breeder region could allow for more power to be generated in that region. The distribution of power between the breeding and burning regions may reduce the thermal gradient and power peaks relative to the gradient and peaks seen in cases that generate power in only one region,

which can be substantial [41]. The swapping method used for these cases assumes that a fraction of the EOL liquid fuel from the burner and breeder regions can be mixed and redistributed to obtain the BOL uranium concentrations in each region. A mass balance can be performed to determine how much fuel must be removed from the burner region and replaced by breeder fuel. The derivation begins at Equation 2.6.

$$M_{Burn,E} - M_{Burn,R} + M_{Add} = M_{Burn,B} \quad (2.6)$$

where  $M_{Burn,E}$  is the mass of  $^{233}\text{U}$  in the burner region at EOL,  $M_{Burn,R}$  is the mass of  $^{233}\text{U}$  removed from the burner region at EOL,  $M_{Add}$  is the mass of  $^{233}\text{U}$  added to the burner region from the breeder region at EOL, and  $M_{Burn,B}$  is the mass of  $^{233}\text{U}$  in the burner region at BOL. These masses can be calculated from the concentration of  $^{233}\text{U}$  in the region, the region volume, and the atomic mass, shown in Equation 2.7.

$$M_{Burn,B} = V_{Burn} C_{Burn,B} A_{U233} \quad (2.7)$$

where  $V_{Burn}$  is the volume of the burner region,  $C_{Burn,B}$  is the  $^{233}\text{U}$  concentration at BOL in *atoms/bn - cm*, and  $A_{233}$  is the atomic mass of  $^{233}\text{U}$ , which is constant across all  $M$  and is canceled out. The masses in Equation 2.6 can be transformed by Equation 2.7, and re-arranged to find the volume of the burner region that must be replaced by breeder fuel, shown in Equations 2.8 and 2.9

$$C_{Burn,E} V_{Burn} - C_{Burn,E} V_R + C_{Breed,E} V_R = C_{Burn,B} V_{Burn} \quad (2.8)$$

$$V_R = \frac{V_{Burn}(C_{Burn,B} - C_{Burn,E})}{C_{Breed,E} - C_{Burn,E}} \quad (2.9)$$

where  $V_R$  is the volume removed,  $C_{Burn,E}$  is the burner  $^{233}\text{U}$  concentration at EOL, and  $C_{Breed,E}$  is the breeder  $^{233}\text{U}$  concentration at EOL. The volume of the breeder region must be replenished after fuel is moved into the burner region. The new fuel should be unenriched thorium and the volume is equal to the volume removed. However, there may be cases where the addition of the fresh fuel dilutes the breeder region  $^{233}\text{U}$  concentration below the BOL concentration. This can be addressed by recycling a portion of the removed burner fuel into the

breeder region with the fresh fuel. The volume of this recycling can be determined with another mass balance, starting with Equation 2.10

$$M_{Breed,E} - M_R + M_{Recycle} + M_{Fresh} = M_{Breed,B} \quad (2.10)$$

where  $M_{Breed,E}$  is the EOL  $^{233}\text{U}$  mass in the breeder region,  $M_R$  is the  $^{233}\text{U}$  mass removed from the breeder region,  $M_{Recycle}$  is the  $^{233}\text{U}$  mass transferred from the burner region to the breeder region,  $M_{Fresh}$  is the  $^{233}\text{U}$  mass added by the fresh fuel and  $M_{Breed,B}$  is the BOL  $^{233}\text{U}$  mass in the breeder region.  $M_{Fresh}$  is unenriched thorium, and has a magnitude of zero. Substituting volume and concentration for mass, the volume of fuel that must be added from the burner into the breeder is shown in Equations 2.11 and 2.12,

$$C_{Breed,E}V_{Breed} - C_{Breed,E}V_R + C_{Burn,E}V_{Recycle} = C_{Breed,B}V_{Breed} \quad (2.11)$$

$$V_{Recycle} = \frac{V_{Breed}C_{Breed,B} - C_{Breed,E}(V_{Breed} - V_R)}{C_{Burn,E}} \quad (2.12)$$

where  $V_{Recycle}$  is the volume of burner fuel that is placed into the breeder region and  $C_{Breed,B}$  is the breeder  $^{233}\text{U}$  concentration at BOL. Since  $k_{inf}$  and  $^{233}\text{U}$  concentration are tracked as a function of time, the EOL data point used does not need to be the last data point from the burnup calculation. The EOL  $^{233}\text{U}$  concentration could be any data point that corresponds to a burnup at which the system is still critical.

## 3 Results

### 3.1 Introduction

This chapter presents the results of the methods outlined in Section 2. The outcome of the reduction of order method is presented first, as it is used throughout every other method that utilized SCALE. The results of the infinite homogeneous moderator model are presented to illustrate the relative capabilities of the moderator candidates. A selection of moderators is chosen from that list to be used in the more thorough infinite pin lattice analysis. The lattice analysis results are used to determine the bounds of the SCALE quarter-core model that is coupled with Gnowee. The quarter-core model explores the design space based on the criteria of the objective function in Gnowee. The results of the two-region infinite lattice model are then presented. These results will be discussed in Section 4.1.

### 3.2 Reduction of Order

Reactor design processes commonly use reduction of order methods that solve for a beginning-of-life flux spectrum and use this flux spectrum to deplete fuel over the course of a core cycle [10]. The results of this study will indicate whether it is appropriate to use a similar method in a core that will deplete fuel in one region, and potentially breed fuel in another. This analysis compares the end-of-life  $^{233}\text{U}$  content of a full TRITON case and a reduced order case. Each case has four regions of fuel, with a different fuel enrichment in each region. Table 3.1 shows the difference between the EOL  $^{233}\text{U}$  of the TRITON case and the reduced order case. Table 3.2 shows the time required to evaluate each case.

<i>Regions</i>	<i>BOL <math>N_U</math></i>	<i>TRITON Case</i>		<i>Reduced Case</i>	<i>% Diff.</i>
		<i>EOL <math>N_U</math></i>	<i>EOL <math>N_U</math></i>	<i>EOL <math>N_U</math></i>	
Region 1	1.36E-03	1.34E-03	1.33E-03	1.33E-03	0.97%
Region 2	1.10E-03	1.09E-03	1.08E-03	1.08E-03	0.74%
Region 3	8.92E-04	8.86E-04	8.92E-04	8.92E-04	-0.75%
Region 4	7.23E-04	7.20E-04	7.25E-04	7.25E-04	-0.75%
Sum of Materials	8.71E-04	8.65E-04	8.67E-04	8.67E-04	-0.30%

Table 3.1: Atom number densities (*atoms/bn – cm*) of  $^{233}\text{U}$ ,  $N_U$ , in the different fuel regions at the beginning-of-life (BOL) and end-of-life (EOL) after 200 days

<i>Case</i>	<i>Time (s)</i>
TRITON Case	2302
Reduced Case	1246

Table 3.2: Computation time comparison

### 3.3 Infinite Homogeneous Model

The infinite homogeneous model is used to compare the moderating properties of different materials. The results of this model can be used to narrow the range of materials that are considered for further evaluation in the infinite lattice and quarter-core models. Light water is included in this list, though no reactor that uses 1000  $K$  coolant would utilize water due to the impractically high pressures required to maintain a liquid state. Instead, light water is used as a reference point to compare to the rest of the materials. The metallic moderator is of interest to NuScale Power. It is hypothesized that the moderator density within the metallic moderator can be adjusted, so a low density case is also presented that has  $\frac{1}{3}$  the moderator density of the nominal case. The two figures of merit, moderating power and moderating ratio, are shown in Table 3.3 for the moderators evaluated.

<i>Moderator</i>	<i>Moderating Power</i>	<i>Moderating Ratio</i>
Light Water	1.16	73
Heavy Water (Pure D2)	0.09	4850
Graphite	0.04	190
Zirconium Hydride (ZrH <sub>2</sub> )	0.30	74
Metallic moderator mixture	0.27	64
Metallic moderator mixture, 1/3 Moderator Density	0.09	53

Table 3.3: The moderating properties of the examined materials, adjusted for a Maxwellian spectrum at 1000  $K$ 

### 3.4 Infinite Lattice Pin Analysis

The infinite lattice analysis was completed for three moderators identified in the infinite homogeneous model: the nominal metallic moderator, the low moderator density metallic moderator, and graphite. The first test of the lattice model was to identify the reactivity effect of removing the gaseous and volatile fission products. The purpose of the following lattice analysis tests was to identify the optimal pitch-to-diameter ratio, fuel enrichment, and fuel radius for the breeding

and burning regions. The next tests determined  $k_{inf}$ ,  $^{233}\text{U}$  enrichment, and net neutron balance as a function of pitch-to-diameter ratio, enrichment, and burnup. The results of these tests were used to develop the bounds of the quarter-core analysis. The infinite lattice cases had uncertainties in  $k_{inf}$  on the order of  $\pm 0.0008$ .

### 3.4.1 Fission Product Removal Effects

The fission product removal study evaluated the change in criticality and  $^{233}\text{U}$  concentration that resulted from removing all isotopic species of: cesium, xenon, iodide, krypton, and tellurium. These are the gaseous and volatile fission products that are able to escape the liquid fuel as vapors, and can be captured without chemically processing the fuel [22]. The effect on reactivity is shown in Fig. 3.1, the effect on  $^{233}\text{U}$  concentration is shown in Fig 3.2, and the comparison between the fission product removal case and the control are shown in Table 3.4. A case solving for the BOL and EOL  $k_{inf}$  and  $^{233}\text{U}$  concentration was included that used the reduction of order method with fission product removal as a second check on the reduction of order method.

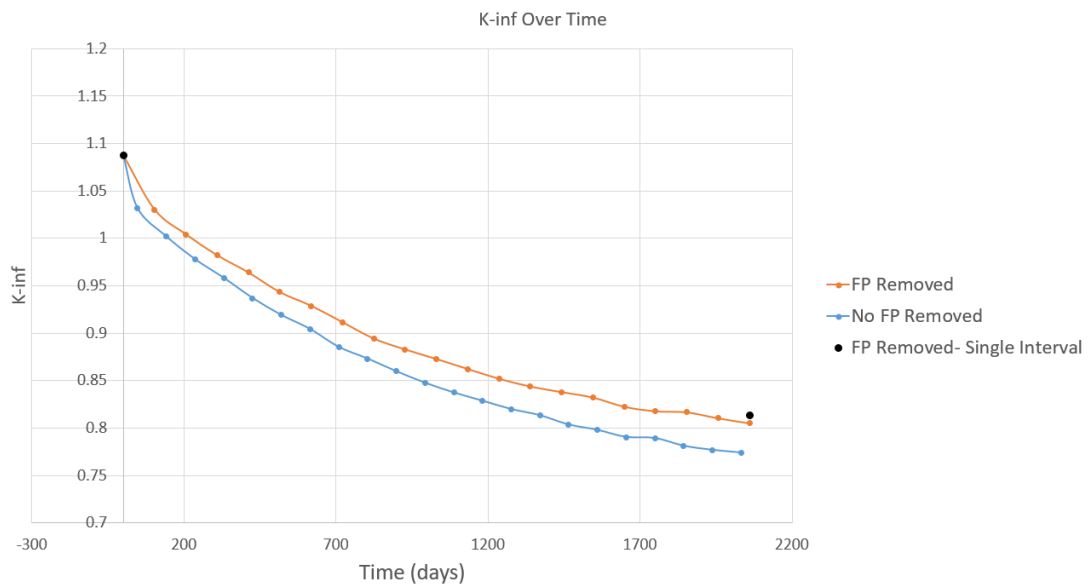


Figure 3.1: Criticality of control case with no fission product removal compared to case with fission product removal.

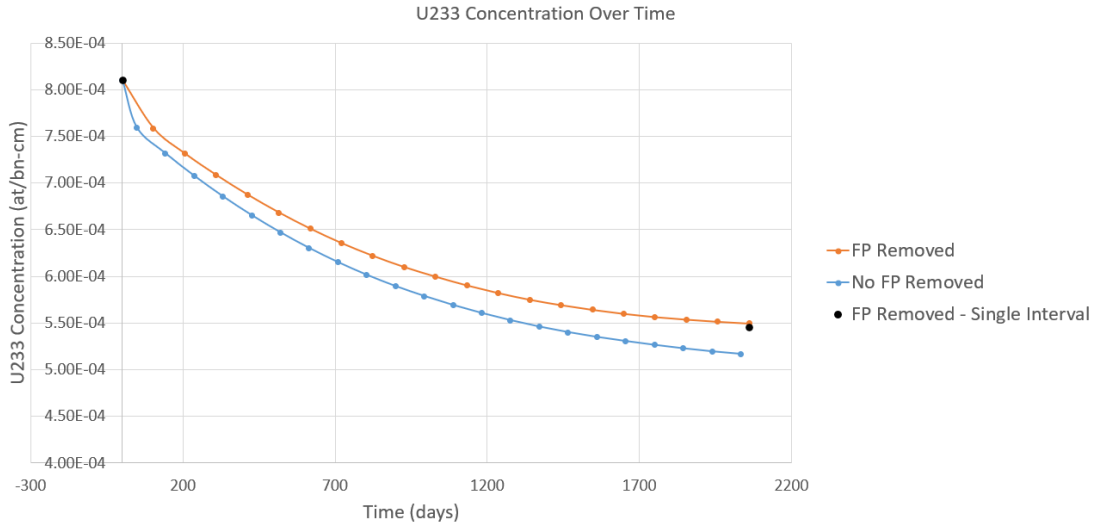


Figure 3.2:  $^{233}\text{U}$  concentration of control case with no fission product removal compared to case with fission product removal.

	$EOL k_{inf}$	$EOL N_U$ (atoms/bn - cm)	Duration $k_{inf} > 1.0$ (days)
Control	0.774	5.17E-4	149
FP Removed	0.805	5.50E-4	225
% Increase	4%	6%	51%

Table 3.4: Comparing BOL and EOL  $k_{inf}$  and  $^{233}\text{U}$  number density of the control to the fission product (FP) removal case.

### 3.4.2 Moderation Curves

The first step of the lattice model is to determine the proper amount of moderator to use to maximize breeding or criticality. There is a limit on the quantity of moderator material a system can contain before the losses due to parasitic absorptions exceed the improvements to criticality due to thermalization of neutrons, and the moderator begins to act as a poison. Fig 3.3 shows the moderation curve as a function of the pitch-to-diameter ratio, and Fig 3.4 shows the moderation curve as a function of the moderator-to-fissile atom ratio. All moderation curves follow a similar shaped peak, so rather than show the entire range for every material from substantially under-moderated to substantially over-moderated, the focus of the plots will be on the peaks.

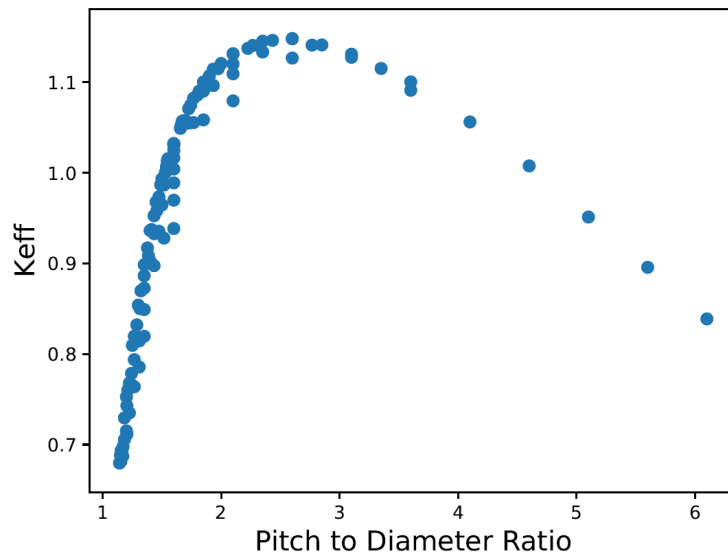


Figure 3.3:  $k_{eff}$  at BOL as a function of pitch-to-diameter ratio

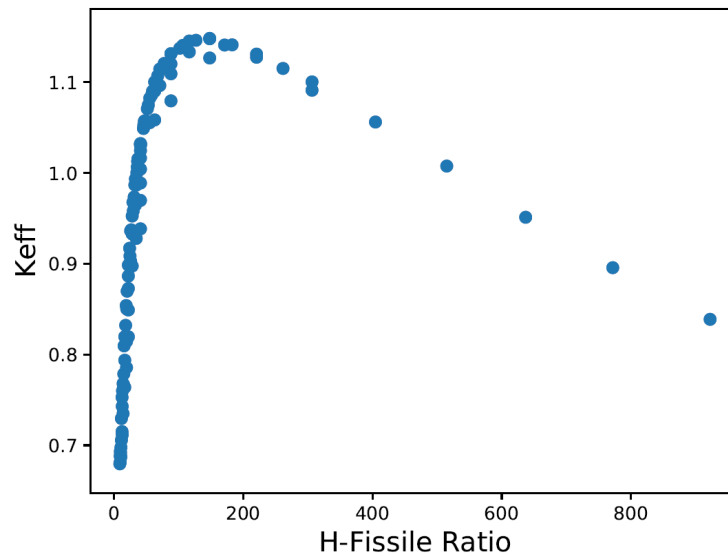


Figure 3.4:  $k_{eff}$  at BOL as a function of H-to-fissile isotope ratio

Moderator-to-fissile ratio and pitch-to-diameter ratio can often be used interchangeably, but they do not always trend together. The overlap between the two can be seen by the high degree of similarity between Fig. 3.3 and Fig. 3.4. There are cases where one ratio is better for



comparing results. For example, varying the enrichment changes the moderator-to-fissile curves, while the pitch-to-diameter trend remains nearly identical, with  $k_{inf}$  increasing with increasing enrichment. This is shown in Fig 3.5. An example of moderator-to-fissile ratio showing a trend better than pitch-to-diameter ratio is when the moderator density or hydrogen concentration in a hydride is not constant. Fig 3.6 shows the trends in  $k_{inf}$  as the moderator density is reduced from the nominal value to 75%, 50%, and 25% of the nominal value. Fig 3.6a shows the change in  $k_{inf}$  as a function of pitch-to-diameter, which has four separate trends for pitch-to-diameter ratio. Fig. 3.6b shows a single trend for moderator-to-fissile ratio, with all cases showing the same peak moderator-to-fissile ratio despite the moderator density changing. In general, pitch-to-diameter ratio will be used unless the moderator-to-fissile ratio is superior for showing data trends in the parameters explored.

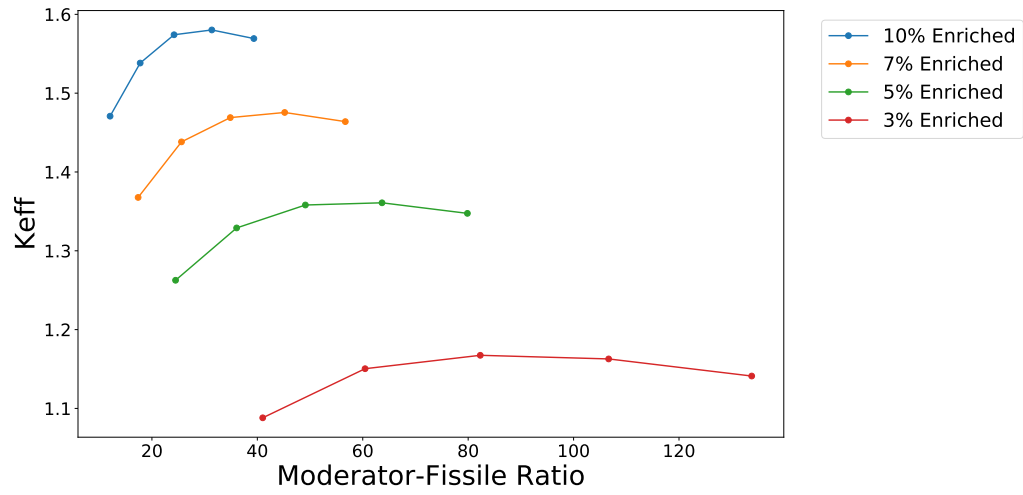
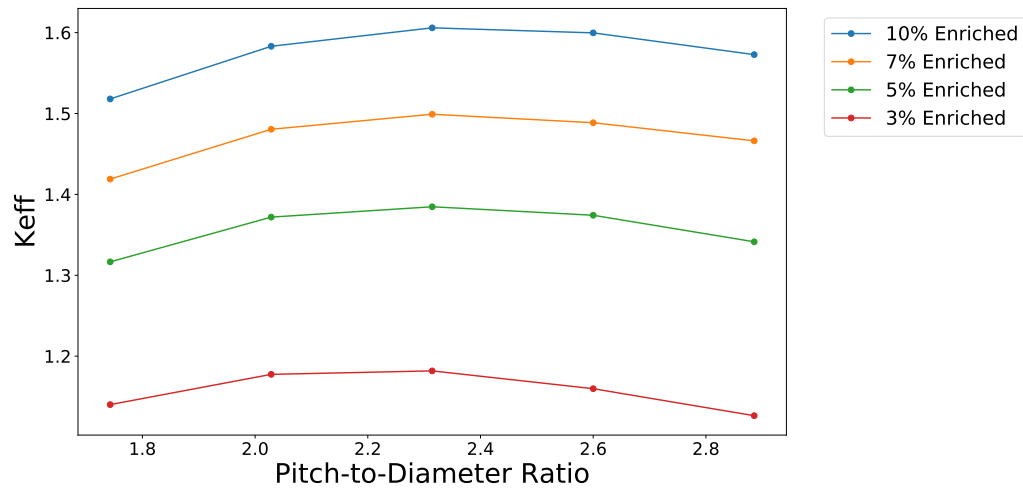
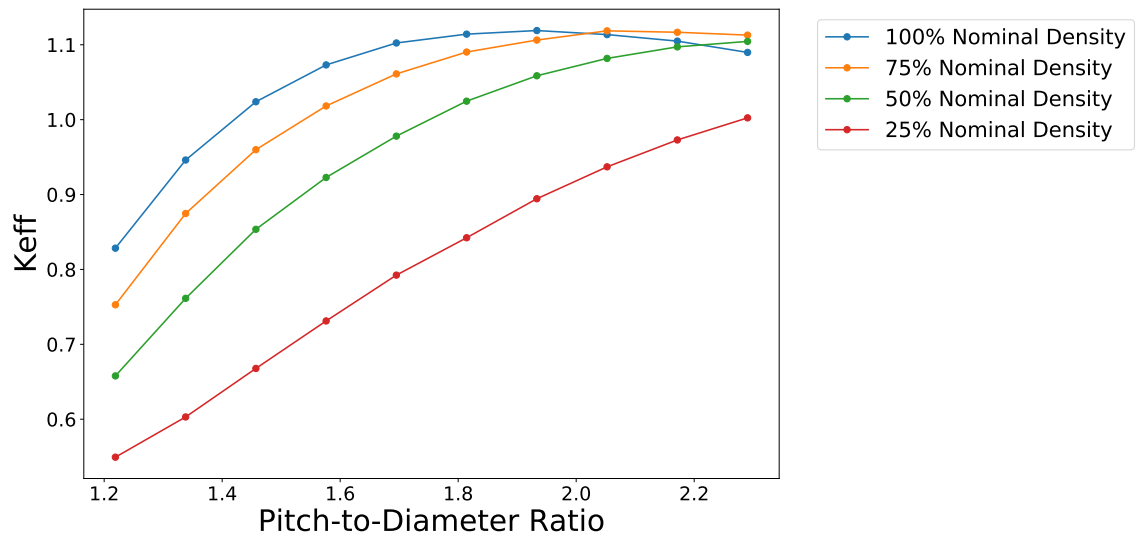
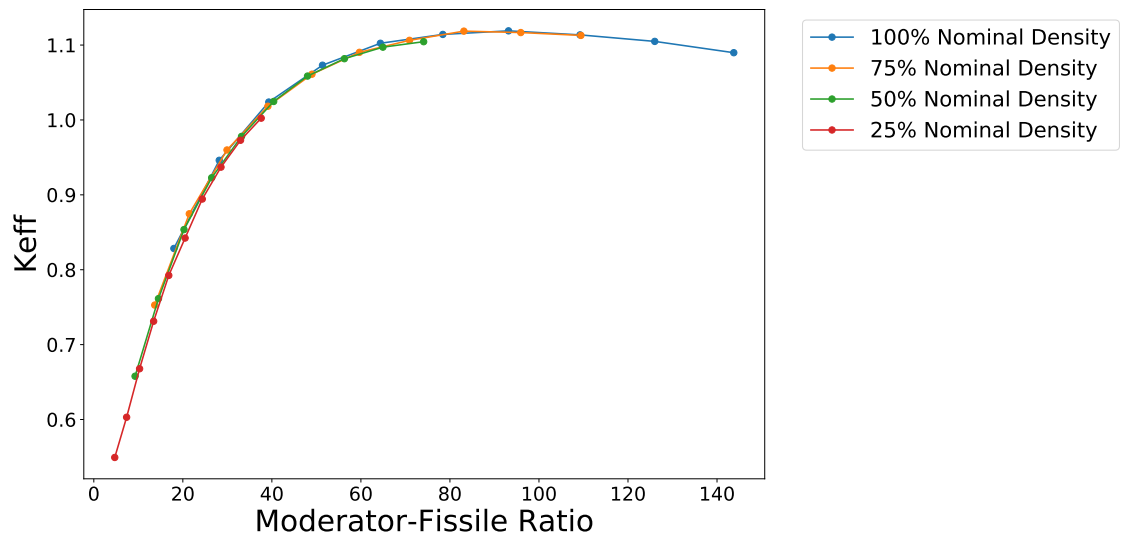
(a)  $k_{eff}$  as a function of moderator-fissile ratio.(b)  $k_{eff}$  as a function of pitch-to-diameter ratio.

Figure 3.5: Comparison of moderator-fissile isotope ratio and pitch-to-diameter ratio for varying enrichment.



(a)  $k_{eff}$  as a function of pitch-to-diameter ratio and moderator density.



(b)  $k_{eff}$  as a function of moderator-fissile isotope ratio and moderator density.

Figure 3.6: Comparison of moderator-fissile isotope ratio and pitch-to-diameter ratio for varying moderator density.

### 3.4.3 Trends for Fissile Isotope Ratio and $k_{inf}$

The lattice analysis was used to determine trends for two important values for a breeder reactor: fissile isotope ratio (FIR) and  $k_{inf}$ . In these cases, a beginning-of-life (BOL) value for  $k_{inf}$  and

and an end-of-life (EOL) value for FIR were determined for a 2060 day burnup. FIR is used to evaluate how well the fuel bred, and  $k_{inf}$  indicates how efficiently the fuel is being used. Only the results for the nominal metallic moderator, low density metallic moderator, and graphite are presented here, in Fig 3.7 through Fig 3.12. The results for light water and zirconium hydride are in Appendix A.3.

### Metallic Moderator

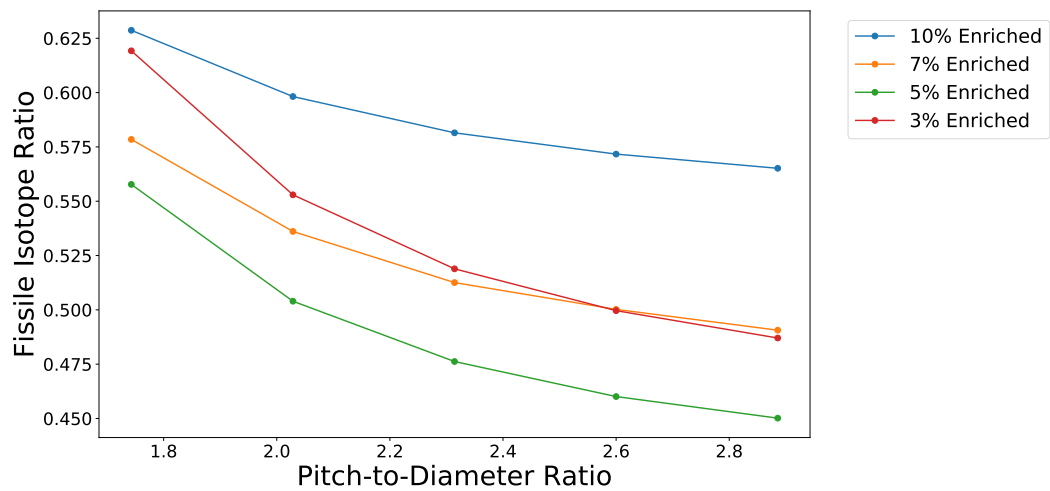


Figure 3.7: FIR at EOL for metallic moderator as a function of pitch-to-diameter ratio

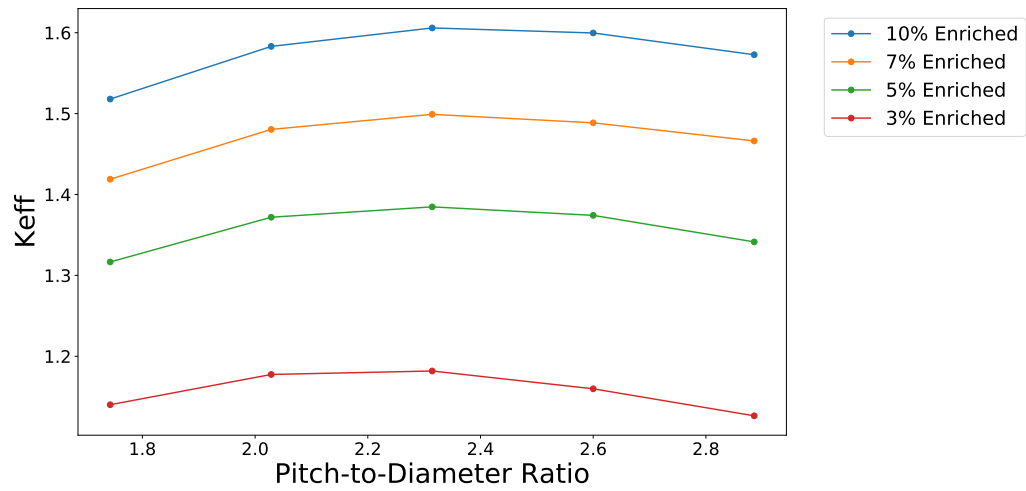


Figure 3.8:  $k_{inf}$  at BOL for metallic moderator as a function of pitch-to-diameter ratio

#### Metallic Moderator, Low Density

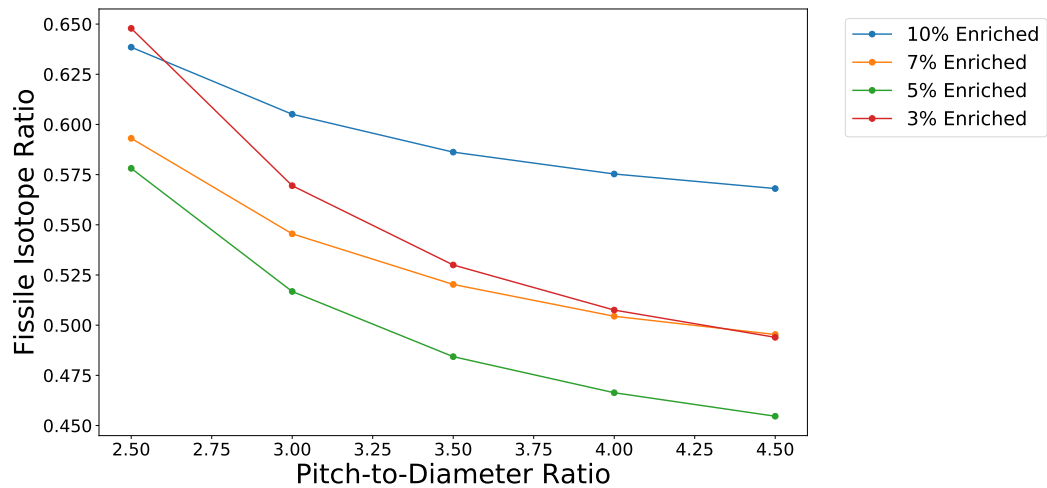


Figure 3.9: FIR at EOL for metallic moderator with low moderator density as a function of pitch-to-diameter ratio.

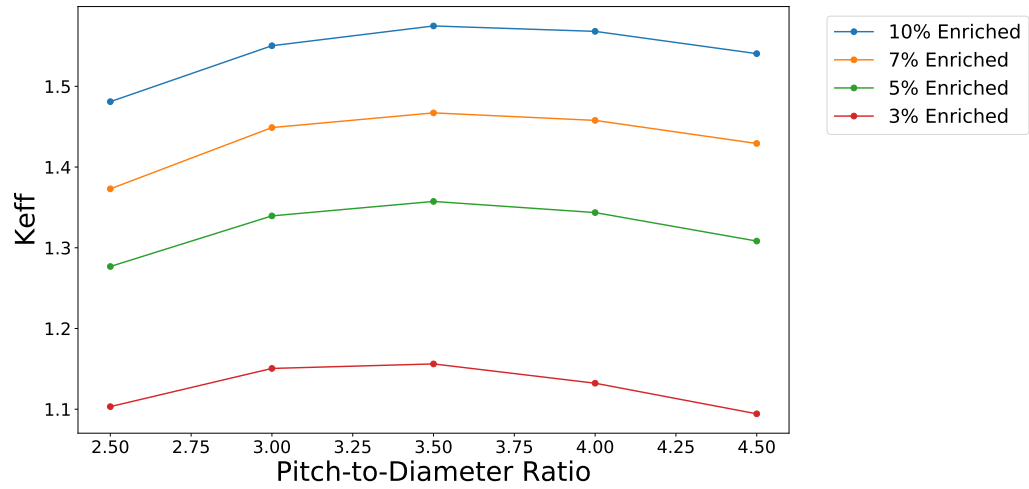


Figure 3.10:  $k_{inf}$  at BOL for metallic moderator with low moderator density as a function of pitch-to-diameter ratio

### Graphite

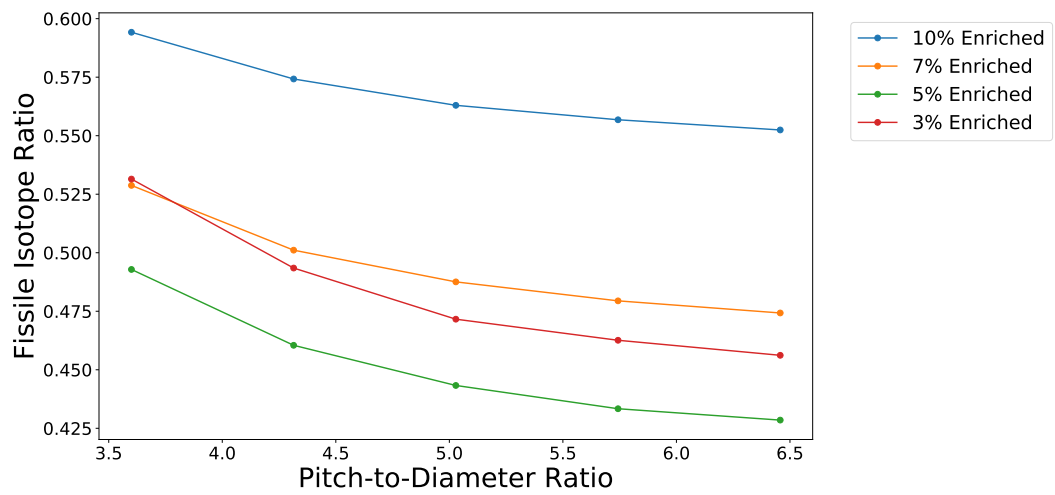


Figure 3.11: FIR at EOL for graphite as a function of pitch-to-diameter ratio

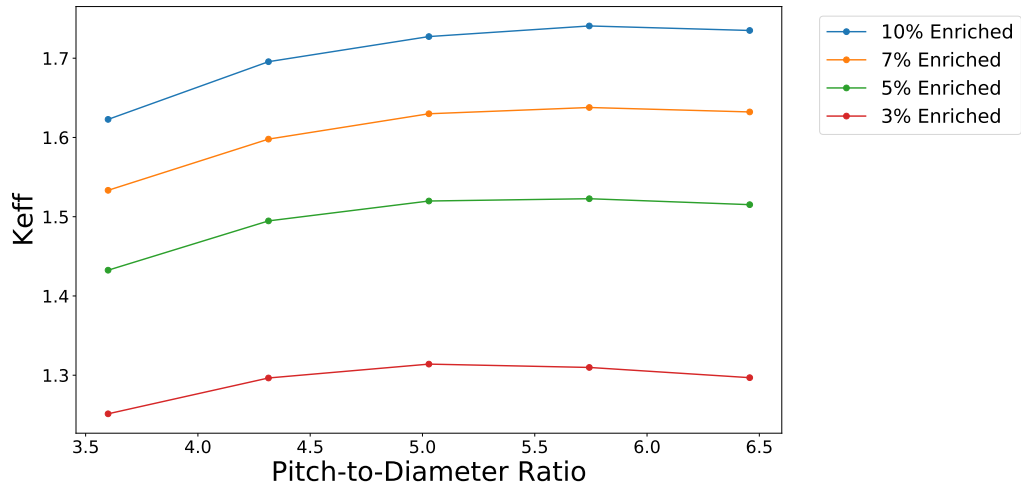


Figure 3.12:  $k_{inf}$  at BOL for graphite as a function of pitch-to-diameter ratio

#### 3.4.4 $k_{inf}$ , $^{233}\text{U}$ Enrichment, and Neutron Balance vs Burnup

These three quantities are presented together due to their interdependence.  $k_{inf}$  and  $^{233}\text{U}$  concentration are not directly coupled, but interpreting the trend of one requires the other to verify if breeding occurs while the system is critical. The neutron balance is calculated using both  $k_{inf}$  and  $^{233}\text{U}$  concentration, so it is directly coupled to both as shown in Eqn 2.3. The plots in Fig. A.1 through Fig. A.9 show  $k_{inf}$ ,  $^{233}\text{U}$  concentration, and neutron balance of all the cases analyzed. The preliminary results indicated that graphite would be the superior moderator for burning fuel, and the low density metallic moderator would be superior at breeding fuel. Graphite and the low density metallic moderator were used for a wider range of analyses than the nominal metallic moderator due to this.

The pitch-to-diameter ratios associated with the peaks identified in Fig. 3.8 and Fig. 3.12 were used as inputs to calculate the values of  $k_{inf}$  as a function of burnup. This is done for a range of enrichments: 0%, 1%, 3%, 5% for all moderators with 7% and 10% included for graphite. The low density moderator was also analyzed at 7% and 9.5%. A wider range of enrichments was used for graphite due to the observation that graphite produced more neutrons than the other moderators for a given starting enrichment. A wider range of enrichments was used for

the low density metallic moderator due to the observation that it required few neutrons to be bred to a given enrichment. These enrichments were chosen to span the range from unenriched to high assay low enriched uranium (HALEU), with the range including the enrichment typical of PWRs and the Shippingport Light Water Breeder Reactor (LWBR). The 9.5% enriched cases for the low density metallic moderator stem from the observation that the 9.5% is where the enrichment of the breeding cases plateaus.

The pitch-to-diameter values were chosen to show the peak and points near the peak of  $k_{inf}$ . A pitch-to-diameter ratio of 1.1 was chosen for the minimum pitch-to-diameter for the metallic moderator. A pitch-to-diameter ratio of 1.1 is the lower limit for pitch-to-diameter ratio in MSRs for heat removal purposes and is extended to these cases [12]. In addition to using pitch-to-diameter ratios that capture the peak of  $k_{inf}$ , a relatively low pitch-to-diameter of 2.0 was used for graphite. The purpose of the low pitch-to-diameter regions is to have a harder flux spectrum and less moderating material that can absorb neutrons. This utilizes the operating experience and design features of the LWBR discussed in Section 1.3.1 that emphasized the importance of a hardened flux spectrum for the breeding region. All cases used a power density of 30  $MW/ITHM$  and a burnup period of 13,000 days, which results in a total accumulated burnup of nearly 400  $GWd/ITHM$ . This is approximately 50% *FIMA*, which is the maximum duration that most B&B studies use [12, 14]. The power density used is close to the power density of LWRs [7].

### Interpreting the Neutron Balance Curves

The neutron balance curve represents the excess neutrons produced by the system up to that time, or the number of external neutrons required by the system up to that time. The peak of the neutron balance curve indicates where the system transitions from critical to subcritical, and the trough indicates where the system transitions from subcritical to critical. This can be seen in Fig 1.8.

A burnup can be found that corresponds to the point where the enrichment in the bred fuel is high enough that the bred fuel is equivalent to the burned fuel at BOL. The neutron balance of the bred fuel can be found for that burnup, and if the number of neutrons required at that burnup is less than the number of excess neutrons supplied, a core composed of those two regions and enrichments could breed the fuel in the breeder region up to the enrichment of



the burner region. The enrichment of the breeder fuel is shown in Fig 3.13, where the horizontal lines represent the enrichments of 3%, 5%, 7% and 9.5%. The burnup required to sufficiently enrich the fuel to the equivalent of the burner fuel at BOL occurs when the enrichment curve crosses the lines drawn in the figure. The burner fuel enrichment is shown in Fig 3.14. The burnup required to enrich the fuel can then be used in Fig 3.15 to determine the number of external neutrons required to reach the required enrichment. Each red dot represents the point at which the enrichment of the breeder fuel crossed one of the lines in Fig 3.13. If the magnitude of this number is less than the peak of the excess neutron curve in Fig 3.16 this indicates that enough neutrons are produced to enrich the breeder fuel. The peak is marked by a red square. This is a very liberal analysis that would indicate whether breeding to high enough enrichments is feasible.

These example plots show one of the major problems of B&B reactors, which is that the minimum burnup required for sustainable operation can be very large. By typical B&B reactor standards, the demonstrated example is non-viable due to the neutron balance never becoming zero after becoming negative. However, swapping from a breeder region to a burner region means that criticality can be achieved at lower enrichments than those required for a fast-spectrum B&B reactor.

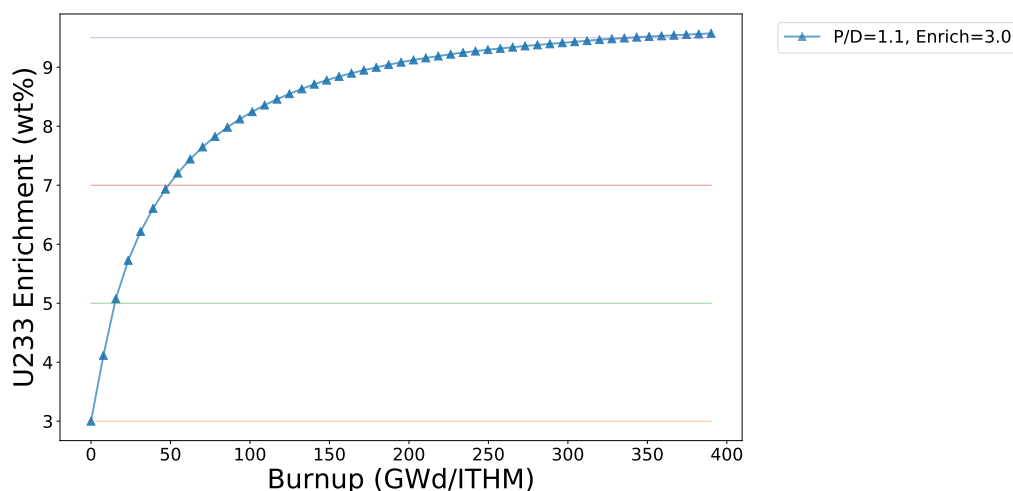


Figure 3.13:  $^{233}\text{U}$  enrichment as a function of burnup in the breeder region.

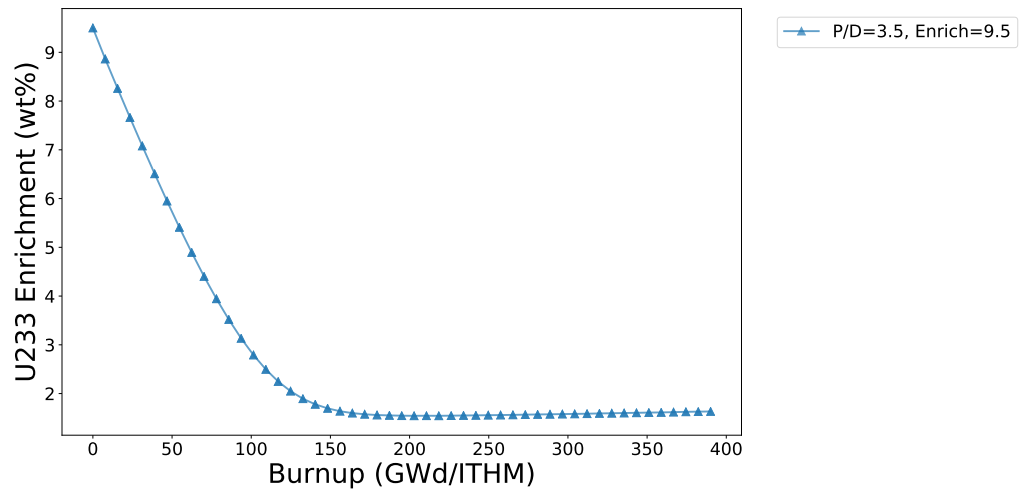


Figure 3.14:  $^{233}\text{U}$  enrichment as a function of burnup in the burner region.

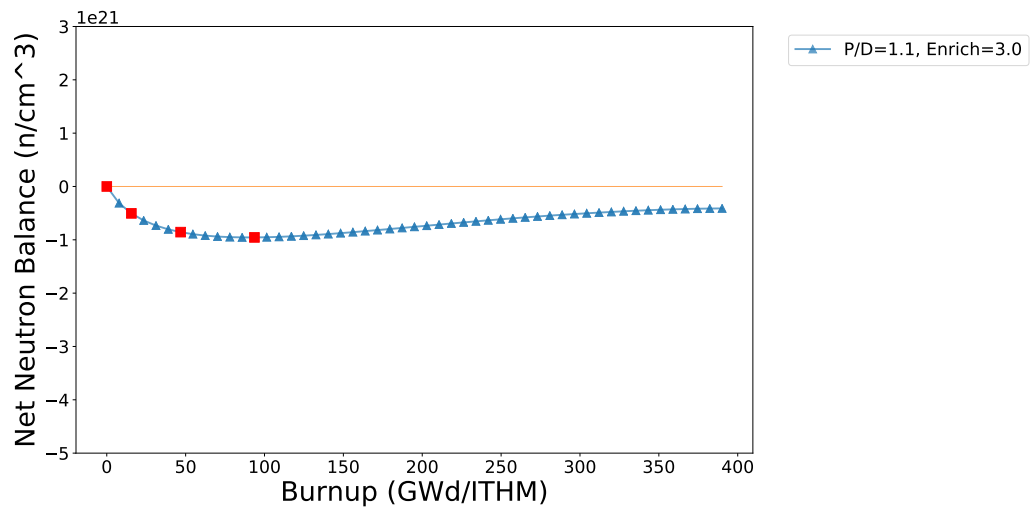


Figure 3.15: Neutron balance as a function of burnup in the breeder region.

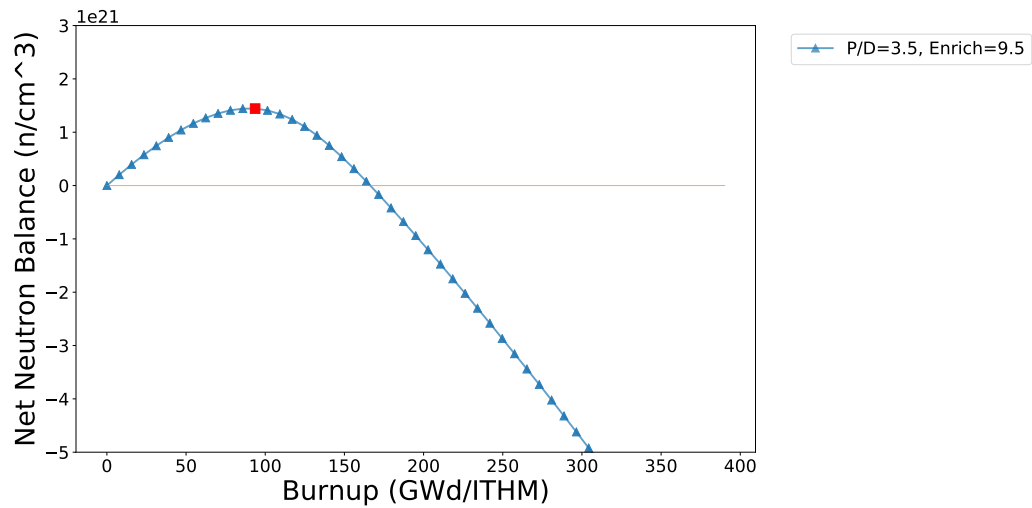


Figure 3.16: Neutron balance as a function of burnup in the burner region.

### Metallic Moderator

The  $k_{inf}$  curve,  $^{233}\text{U}$  enrichment curve, and neutron balance curve are shown for the best breeding cases and the best burning cases found for the metallic moderator cases. The best breeding cases are the cases with a pitch-to-diameter ratio of 1.1, and the best burning cases are the cases with a pitch-to-diameter ratio that corresponds to the highest number of excess neutrons. The best case burner cases had pitch-to-diameter ratios of 2.1. The results of these cases are presented in Fig 3.17 through Fig 3.22. The other cases evaluated are in Appendix A.1. In the figures presented in this section, the best case burning cases have triangular points, and the best case breeding cases have circular points. Lower enriched cases with starting enrichments of 0% and 1% are presented in separate graphs. These cases required shorter timesteps for the first several steps, and could not be plotted on the same graph as cases with different timesteps.

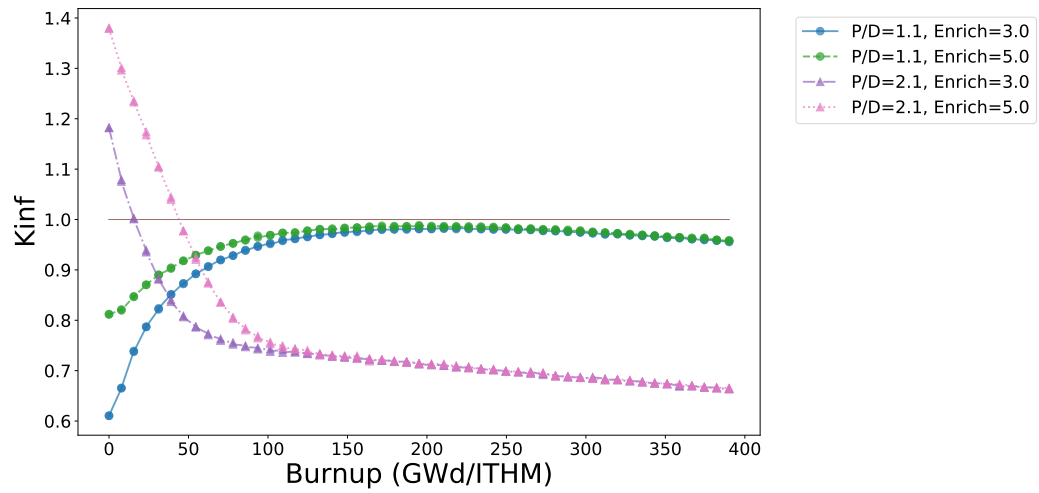


Figure 3.17:  $k_{inf}$  for metallic moderator as a function of burnup, enrichment, and pitch-to-diameter (PD) ratio for higher enrichments.

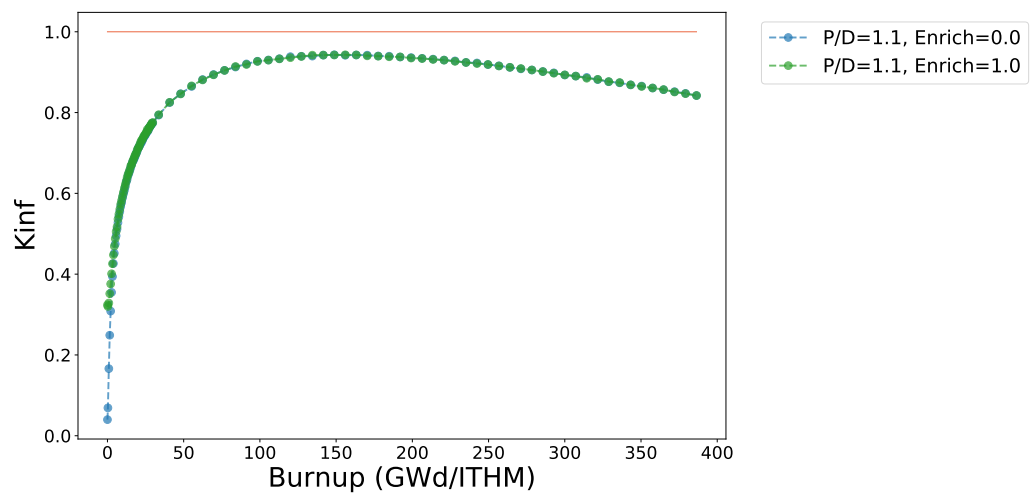


Figure 3.18:  $k_{inf}$  for metallic moderator as a function of burnup, enrichment, and pitch-to-diameter ratio for lower enrichments.

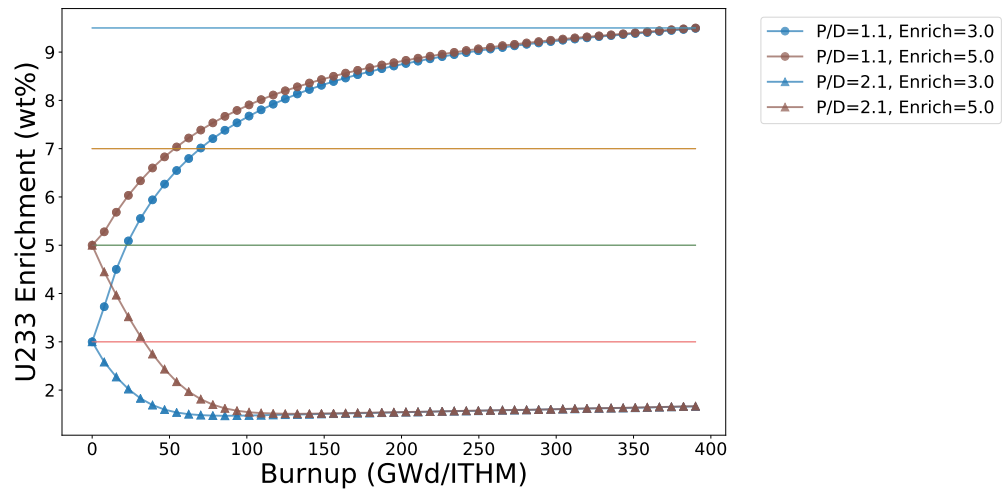


Figure 3.19:  $^{233}\text{U}$  number density for metallic moderator as a function of burnup, enrichment, and pitch-to-diameter ratio for higher enrichments.

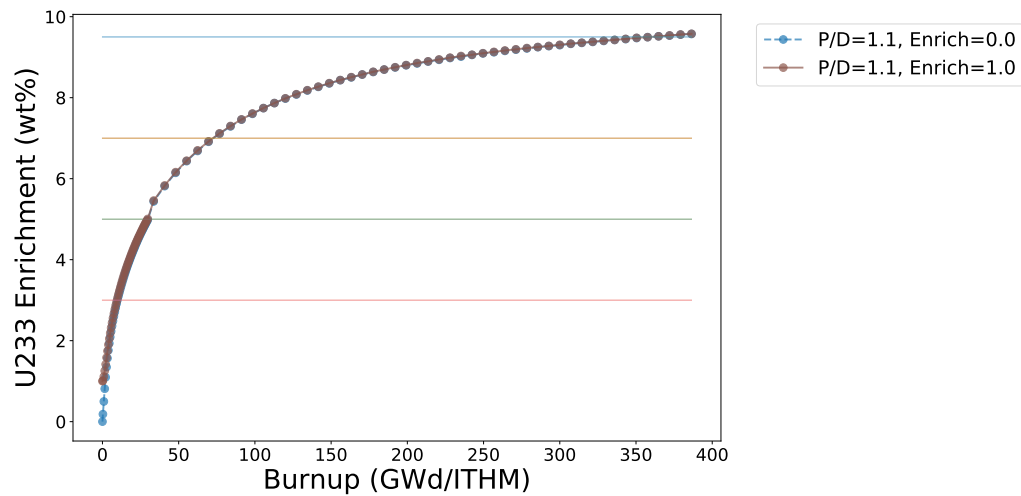


Figure 3.20:  $^{233}\text{U}$  number density for metallic moderator as a function of burnup, enrichment, and pitch-to-diameter ratio for lower enrichments.

In Fig 3.19 and Fig 3.20, the lines across the graph represents the different enrichment cases. Most cases peak and begin to plateau near 9.5%.

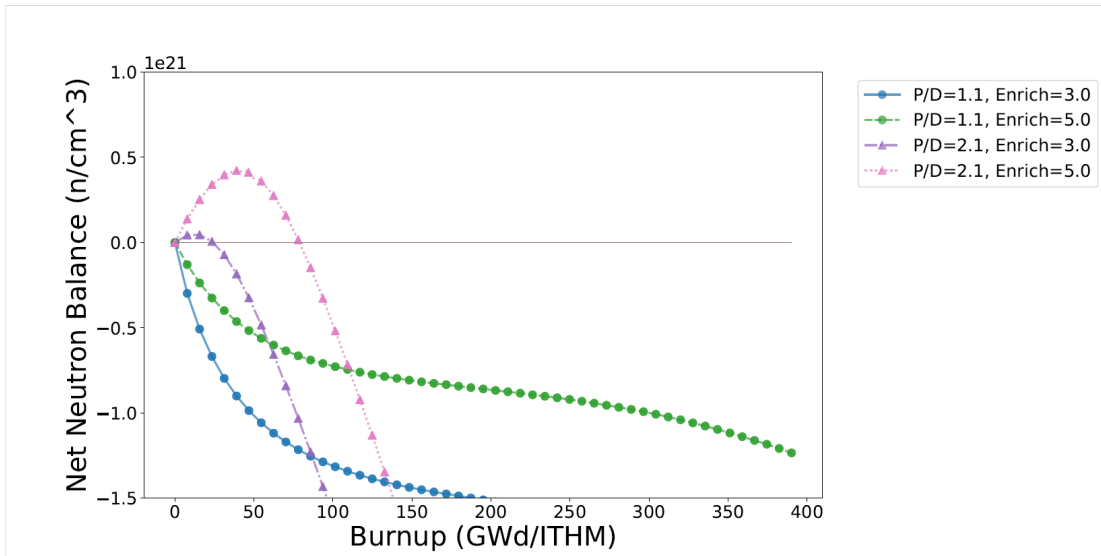


Figure 3.21: Neutron balance for metallic moderator as a function of burnup, enrichment, and pitch-to-diameter ratio for higher enrichments.

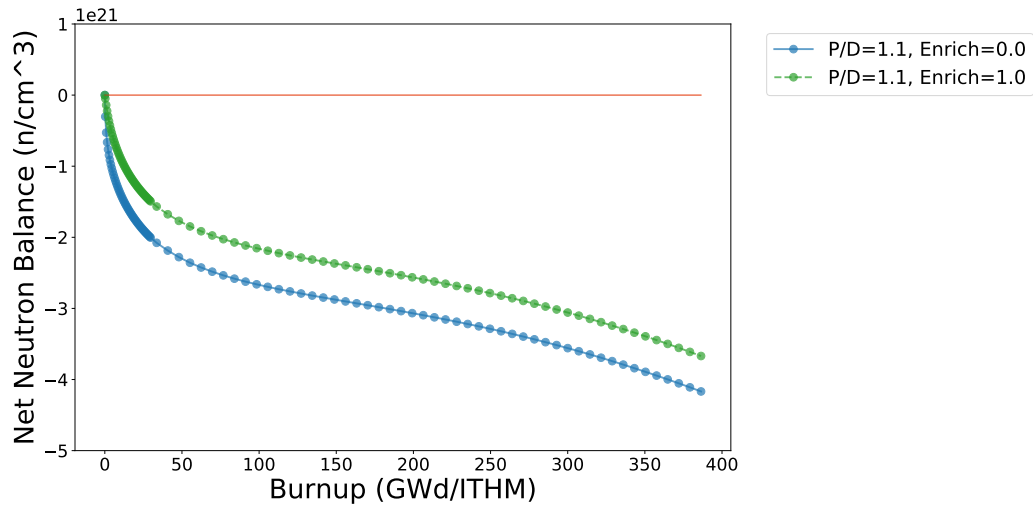


Figure 3.22: Neutron balance for metallic moderator as a function of burnup, enrichment, and pitch-to-diameter ratio for lower enrichments.

### Metallic Moderator, Low Density

The best breeding cases are the cases with a pitch-to-diameter ratio of 1.1 and the best case burner cases have pitch-to-diameter ratios of 3.5, and are presented in Fig 3.23 through Fig 3.28. Similar to the previous cases, the 0% and 1% enriched cases are on their own graphs due

to different time-step sizes. The other cases evaluated are presented in Appendix A.1.

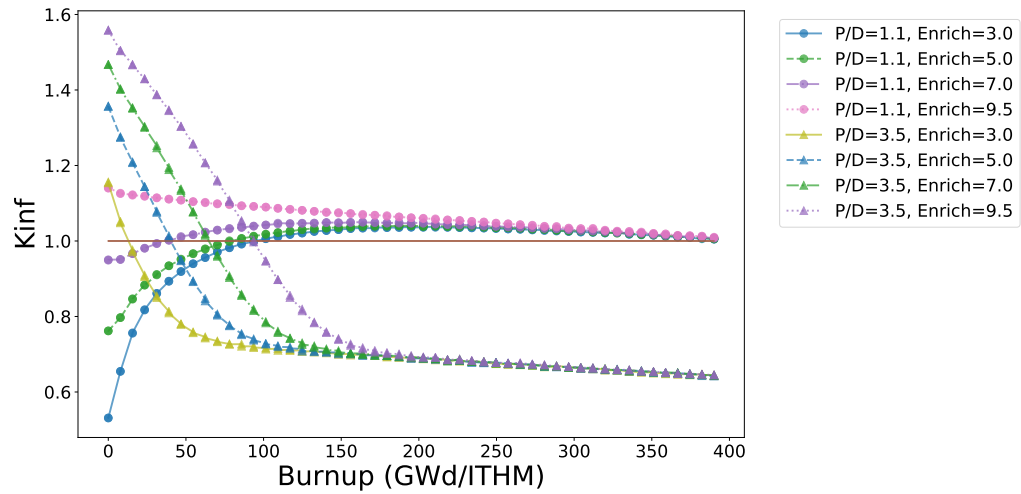


Figure 3.23:  $k_{inf}$  of the best breeder and burner cases for metallic moderator with low moderator density as a function of burnup, enrichment, and pitch-to-diameter ratio for higher enrichments.

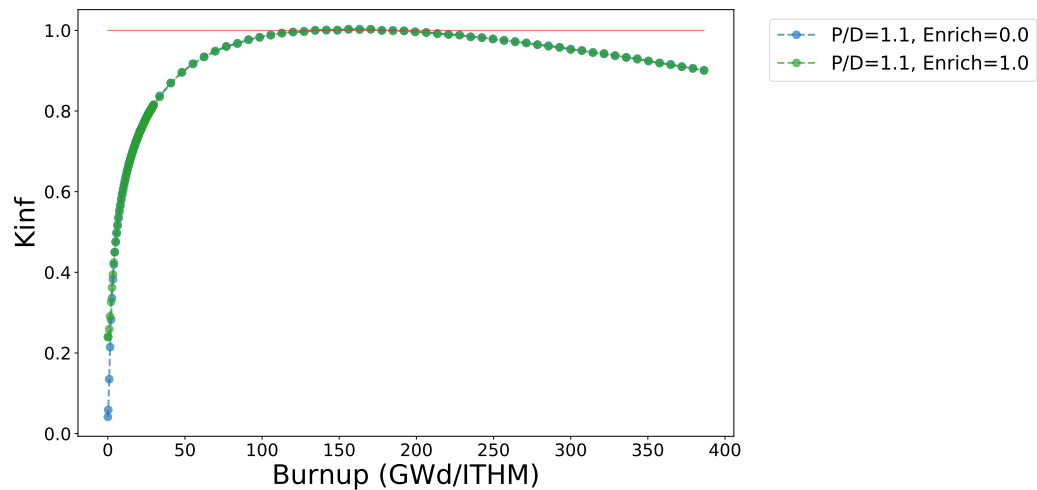


Figure 3.24:  $k_{inf}$  of the best breeder cases for metallic moderator with low moderator density as a function of burnup, enrichment, and pitch-to-diameter ratio for lower enrichments.

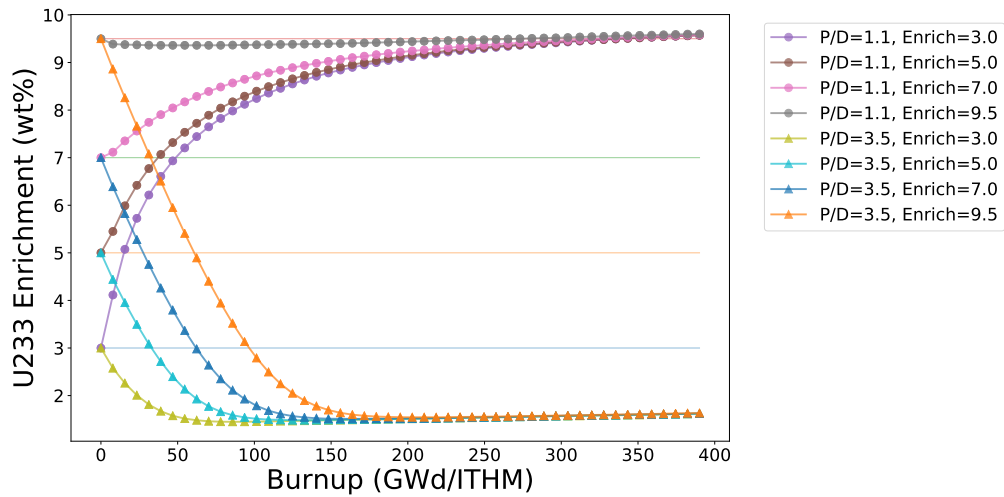


Figure 3.25:  $^{233}\text{U}$  number density of the best breeder and burner cases for metallic moderator with low moderator density as a function of burnup, enrichment, and pitch-to-diameter ratio for higher enrichments.

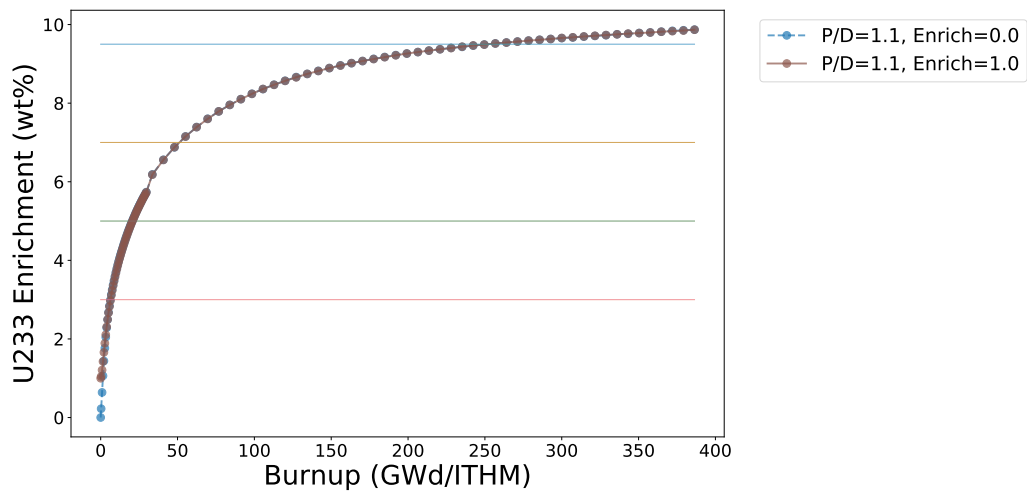


Figure 3.26:  $^{233}\text{U}$  number density of the best breeder cases for metallic moderator with low moderator density as a function of burnup, enrichment, and pitch-to-diameter ratio for lower enrichments.



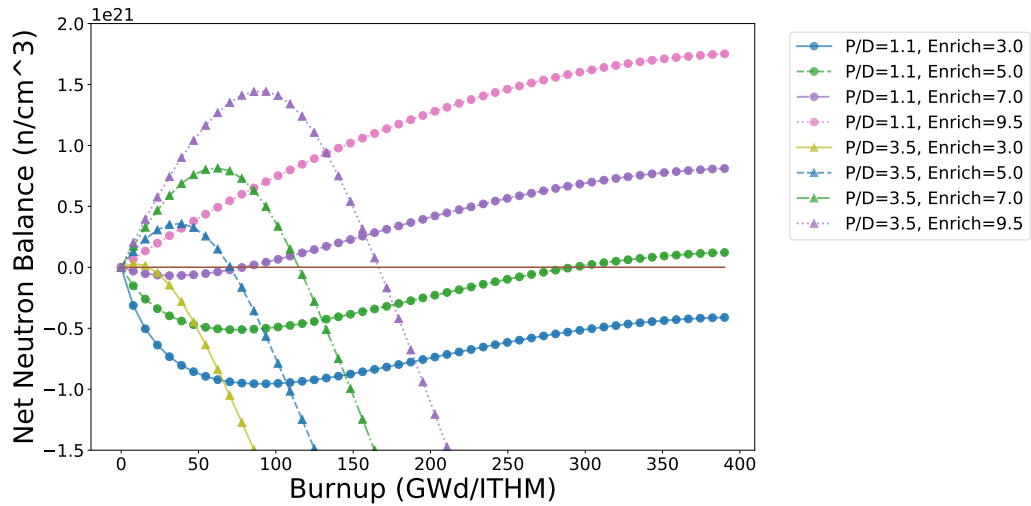


Figure 3.27: Neutron balance of the best breeder and burner cases for metallic moderator with low moderator density as a function of burnup, enrichment, and pitch-to-diameter ratio for higher enrichments.

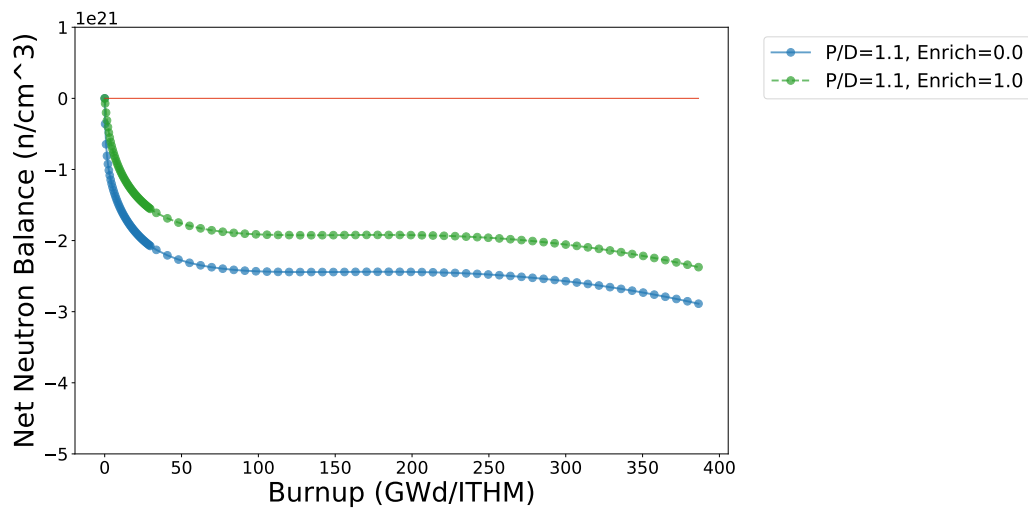


Figure 3.28: Neutron balance of the best breeder cases for metallic moderator with low moderator density as a function of burnup, enrichment, and pitch-to-diameter ratio for lower enrichments.

### Graphite

The best breeding cases are the cases with a pitch-to-diameter ratio of 2.0 and the best case burner cases had pitch-to-diameter ratios of 5.4, and are presented in Fig 3.29, through Fig 3.34.

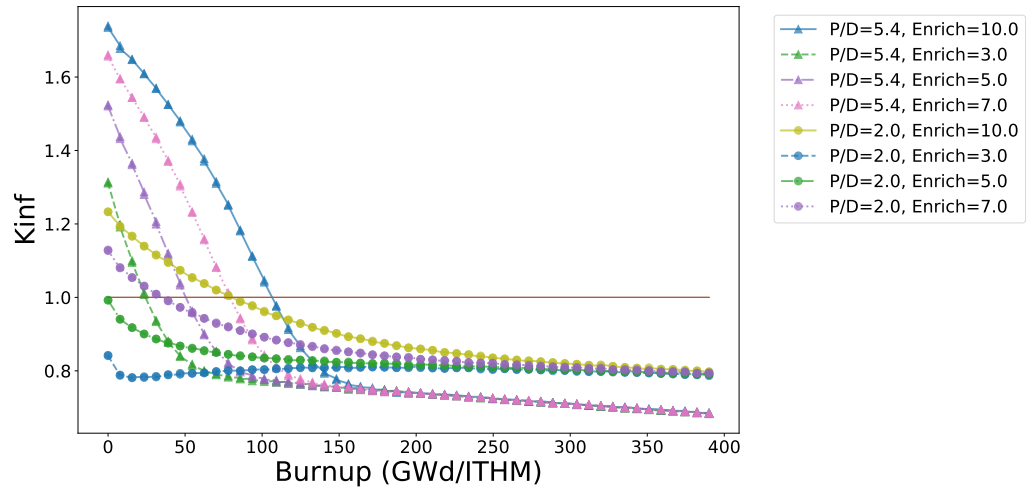


Figure 3.29:  $k_{inf}$  for graphite as a function of burnup, enrichment, and pitch-to-diameter ratio for higher enrichments.

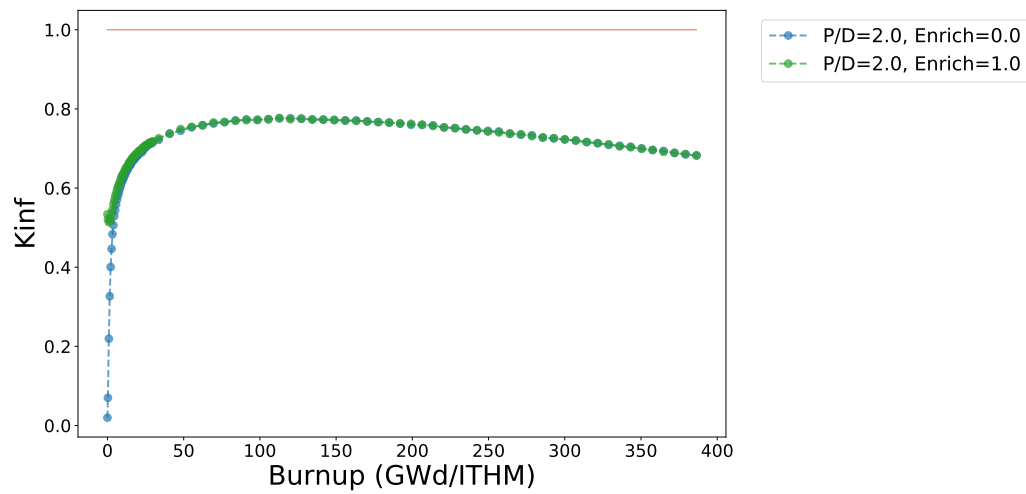


Figure 3.30:  $k_{inf}$  for graphite as a function of burnup, enrichment, and pitch-to-diameter ratio for lower enrichments.

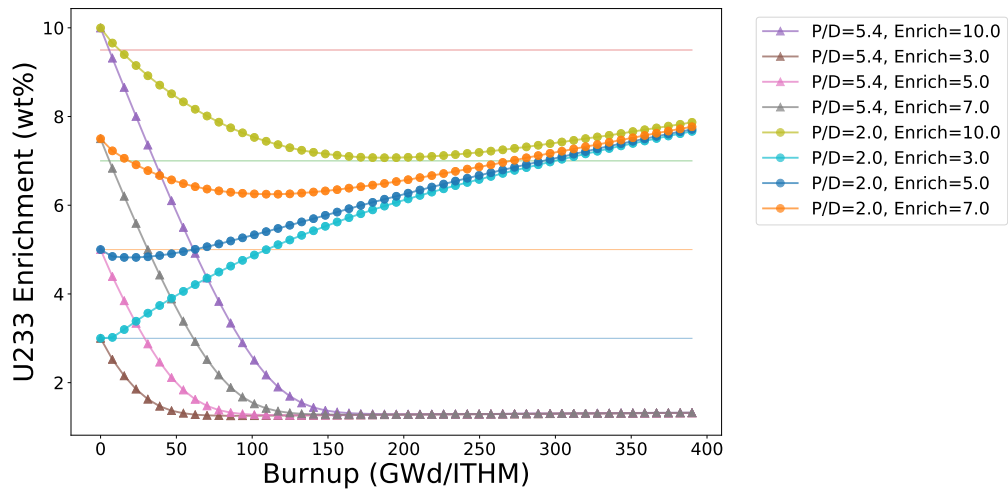


Figure 3.31:  $^{233}\text{U}$  number density for graphite as a function of burnup, enrichment, and pitch-to-diameter ratio for higher enrichments.

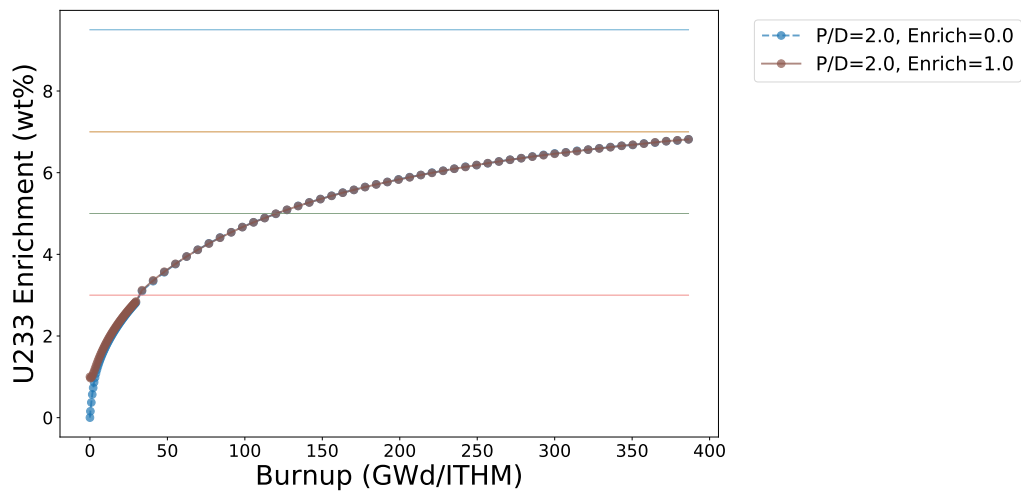


Figure 3.32:  $^{233}\text{U}$  number density for graphite as a function of burnup, enrichment, and pitch-to-diameter ratio for lower enrichments.

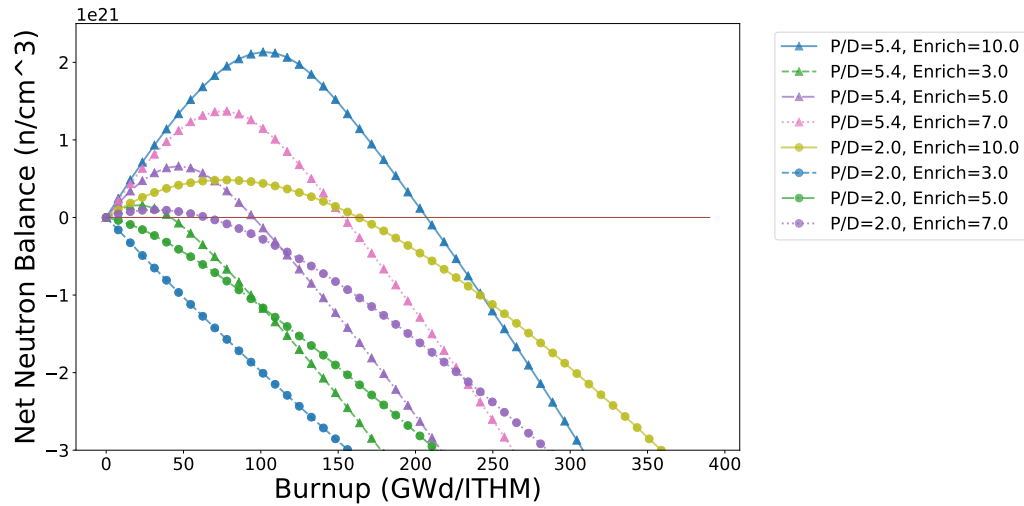


Figure 3.33: Neutron balance for graphite as a function of burnup, enrichment, and pitch-to-diameter ratio for higher enrichments.

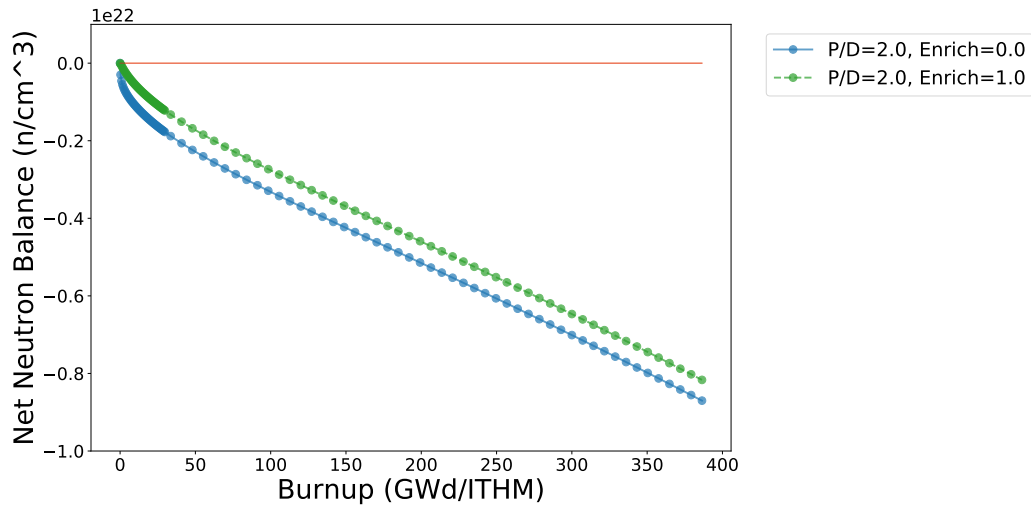


Figure 3.34: Neutron balance for graphite as a function of burnup, enrichment, and pitch-to-diameter ratio for lower enrichments.

### Minimum Required Enrichment

The minimum  $^{233}\text{U}$  concentration required to maintain  $k_{inf}$  above 1.0 can be determined by comparing Fig. 3.17 to Fig. 3.19 for the metallic moderator, Fig. 3.23 to Fig. 3.25 for the low density metallic moderator, and Fig. 3.29 to Fig. 3.31 for graphite. The  $^{233}\text{U}$  concentration

required to maintain criticality is shown in Table 3.5 for the metallic moderator cases, Table 3.6 for the low density metallic moderator cases, and in Table 3.7 for the graphite cases.

<i>P/D Ratio</i>	<i>3wt% <sup>233</sup>U</i>	<i>5wt% <sup>233</sup>U</i>
1.1	N/A	N/A
1.4	N/A	4.23
2.1	2.27	2.74
2.9	2.54	2.94

Table 3.5: Comparing minimum <sup>233</sup>U enrichment required to maintain  $k_{inf} \geq 1.0$  moderated by the metallic moderator.

<i>P/D Ratio</i>	<i>3wt% <sup>233</sup>U</i>	<i>5wt% <sup>233</sup>U</i>	<i>7wt% <sup>233</sup>U</i>
1.1	8.12	7.89	7.74
2.5	2.67	3.22	3.77
3.0	2.61	2.88	3.25
3.5	2.57	2.71	2.98
4.0	2.55	3.00	3.23
4.5	2.99	2.95	3.15

Table 3.6: Comparing minimum <sup>233</sup>U enrichment required to maintain  $k_{inf} \geq 1.0$  moderated by the metallic moderator with low moderator density.

<i>P/D Ratio</i>	<i>3wt% <sup>233</sup>U</i>	<i>5wt% <sup>233</sup>U</i>	<i>7wt% <sup>233</sup>U</i>	<i>10wt% <sup>233</sup>U</i>
2.0	N/A	N/A	6.78	7.87
4.0	1.94	2.31	2.50	2.63
4.7	1.88	2.18	2.29	2.66
5.4	1.85	2.11	2.17	2.51
6.1	1.84	2.08	2.47	2.41

Table 3.7: Comparing minimum <sup>233</sup>U enrichment required to maintain  $k_{inf} \geq 1.0$  moderated by graphite.

### Neutron Balance Results

The neutron balance can be used to compare two cases that have not been subjected to the same neutron fluence, such as a sub-critical case compared to a critical case. Table 3.8, Table 3.9, and Table 3.10 show the largest positive net excess of neutrons for the metallic moderator, low density metallic moderator, and graphite, respectively, as a function of the starting enrichment and pitch-to-diameter ratio. ‘N/A’ in the table indicates that the combination of pitch-to-diameter ratio and enrichment did not result in criticality. These tables are used to determine the best burner enrichment and pitch-to-diameter ratio for excess neutron production. In Table 3.9, the 9.5% case was only analyzed for a pitch-to-diameter ratio of 3.5 as that was the best performing case.

<i>P/D Ratio</i>	<i>n<sup>0</sup> excess, 3wt%</i>	<i>n<sup>0</sup> excess, 5wt%</i>
1.1	N/A	N/A
1.4	N/A	9.76E19
2.1	4.50E19	4.22E20
2.9	1.58E19	3.16E20

Table 3.8: Peak number of excess neutrons ( $n/cm^3$ ) as a function of pitch-to-diameter ratio and enrichment for metallic moderator.

<i>P/D Ratio</i>	<i>n<sup>0</sup> excess, 3wt%</i>	<i>n<sup>0</sup> excess, 5wt%</i>	<i>n<sup>0</sup> excess, 7wt%</i>	<i>n<sup>0</sup> excess, 9.5wt%</i>
2.5	5.65E18	2.64E20	6.58E20	-
3.0	2.65E19	3.51E20	7.97E20	-
3.5	2.92E19	3.59E20	8.14E20	1.44E21
4.0	1.58E19	3.21E20	7.57E20	-
4.5	1.33E16	2.57E20	6.65E20	-

Table 3.9: Peak number of excess neutrons ( $n/cm^3$ ) as a function of pitch-to-diameter ratio and enrichment for metallic moderator with low moderator density. Only the best-case breeder was analyzed at the highest enrichment.

<i>P/D Ratio</i>	<i>n<sup>0</sup> excess, 3wt%</i>	<i>n<sup>0</sup> excess, 5wt%</i>	<i>n<sup>0</sup> excess, 7wt%</i>	<i>n<sup>0</sup> excess, 10wt%</i>
2.0	N/A	N/A	9.87E19	4.83E20
4.0	1.31E20	5.91E20	1.25E21	1.96E21
4.7	1.58E20	6.50E20	1.35E21	2.09E21
5.4	1.60E20	6.6E20	1.37E21	2.13E21
6.1	1.43E20	6.44E20	1.35E21	2.12E21

Table 3.10: Peak number of excess neutrons ( $n/cm^3$ ) as a function of pitch-to-diameter ratio and enrichment for graphite moderator.

Table 3.11, Table 3.12, and Table 3.13 shows the number of neutrons required to breed from a starting enrichment to a greater enrichment. In the cases that become critical as a result of increasing enrichment, the magnitude of the trough will be used as the required number of neutrons. The 10% enriched cases are excluded from Table 3.13 because none of the cases can breed to 10%. ‘N/A’ indicates that a case could not breed up to an enrichment.

<i>Enrichment</i>	<i>n<sup>0</sup> to breed to 1%</i>	<i>n<sup>0</sup> to breed to 3%</i>	<i>n<sup>0</sup> to breed to 5%</i>
0%	7.75E20	1.38E21	2.00E21
1%	0	8.49E20	1.49E21
3%	-	0	3.09E20
5%	-	-	0

Table 3.11: The net neutrons required to breed a fuel of starting enrichment to a new enrichment with metallic moderator

<i>Enrichment</i>	<i>n<sup>0</sup> to breed to 1wt%</i>	<i>n<sup>0</sup> to breed to 3wt%</i>	<i>n<sup>0</sup> to breed to 5wt%</i>	<i>n<sup>0</sup> to breed to 7wt%</i>	<i>n<sup>0</sup> to breed to 9.5wt%</i>
0%	7.65E20	1.36E21	1.89E21	2.28E21	2.44E21
1%	0	8.26E20	1.37E21	1.77E21	1.92E21
3%	-	0	4.80E20	8.45E20	9.56E20
5%	-	-	0	4.25E20	5.11E20
7%	-	-	-	0	6.81E19
9.5%	-	-	-	-	0

Table 3.12: The net neutrons required to breed a fuel of starting enrichment to a new enrichment with low density metallic moderator

<i>Enrichment</i>	<i>n<sup>0</sup> to breed to 1wt%</i>	<i>n<sup>0</sup> to breed to 3wt%</i>	<i>n<sup>0</sup> to breed to 5wt%</i>	<i>n<sup>0</sup> to breed to 7wt%</i>
0%	7.30E20	1.84E21	3.69E21	N/A
1%	0	1.26E21	3.14E21	N/A
3%	-	0	2.07E21	5.53E21
5%	-	-	0	4.45E21
7%	-	-	-	0

Table 3.13: The net neutrons required to breed a fuel of starting enrichment to a new enrichment with graphite moderator

The number of neutrons supplied by the best cases for neutron production can be compared to the most efficient breeder case. The best case producers are P/D=3.5 for the low density metallic moderator and P/D=5.4 for graphite. The most efficient breeding case is P/D = 1.1 for the low density metallic moderator. Fig 3.35 shows the number of neutrons required to breed to each enrichment next to the maximum number of neutrons supplied by that enrichment.



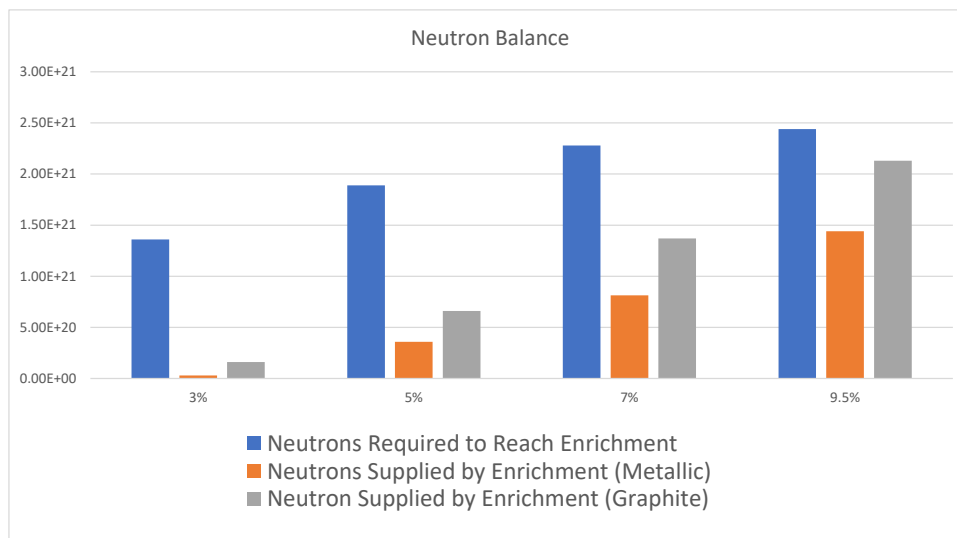


Figure 3.35: Number of neutrons required to reach an enrichment compared to the number of neutrons produced by the enrichment.

### 3.5 Quarter-Core Analysis

The original infinite lattice model contained an error that gave the indication that there were sufficient excess neutrons available to breed from unenriched fuel up to the burner regions enrichment. This was caused by time steps that were too long for the first few steps, which resulted in  $^{233}\text{U}$  breeding faster than is possible and a neutron balance that under-predicted the number of neutrons required to supply the  $^{233}\text{U}$  breeding breeding. This quarter-core model was created under the assumption that breeding up to the burner enrichment was feasible and the purpose of the quarter-core model was to find a geometry that would allow the breeding and burning in a core configuration. Later analysis corrected the error and now indicate that it is not feasible for the pin geometries analyzed. The purpose of this model is to confirm that it is not feasible for the analyzed geometry to operate as a breeder-burner reactor.

The quarter-core model tests if a breeder region could sustain breeding from a burner region to the point that the bred fuel could replace the burned fuel. The quarter-core model is put into the optimization code, Gnowee, using insights and bounds determined from the infinite lattice model. The bounds given to Gnowee to optimize the quarter-core model are in Table 3.14. In this case, Gnowee does not reach a confirmed optimum solution. Instead, Gnowee is used to explore the design space efficiently by using the Gnowee algorithms to search for high fitness solutions. In Table 3.14, the ‘Edge-to-Edge’ parameter is added to the fuel diameter to yield the pitch. It was done to prevent overlapping of the fuel that could occur if the optimizer selected a pitch that was smaller than the diameter of the fuel. The radial pitch is the fuel pin center-to-center distance extending out radially, and the azimuth pitch is the circumferential center-to-center distance of the fuel pins along a common arc. There are two regions defined that will have properties independent of each other. The regions were not given different bounds, so neither region was initially assigned as the breeding region nor the burning region. The alternative to this would be to define which portion of the core each region would occupy, i.e. the center of the core is the burner region. For the purpose of evaluating the objective function, Eqn. 2.5 in this case, the driver region is the region with a higher BOL enrichment. The lower bound of enrichment could not be zero because SCALE cannot interpret a material that composes zero percent of the mass fraction, so a sufficiently low value was put in that would be essentially unenriched. The quarter-core cases had uncertainties in  $k_{eff}$  on the order of  $\pm 0.0015$ .

<i>Parameter</i>	<i>Lower Bound</i>	<i>Upper Bound</i>
Fuel Edge-to-Edge Pitch (Radial) [ <i>cm</i> ]	0.5	6.0
Fuel Edge-to-Edge Pitch (Azimuthal) [ <i>cm</i> ]	0.5	6.0
Fuel Radius [ <i>cm</i> ]	0.5	3.0
Moderator Flow Path Thickness [ <i>cm</i> ]	5	20
Reflector Thickness [ <i>cm</i> ]	5	30
Core Height [ <i>cm</i> ]	250	400
Core Radius [ <i>cm</i> ]	150	200
Fuel Enrichment [ <i>wt%</i> ]	0.001	5

Table 3.14: Parameters and parameter bounds put into Gnowee.

The enrichment ratio as a function of case number is shown in Fig 3.36, and cases with EOL

$k_{eff}$  greater than one are highlighted.

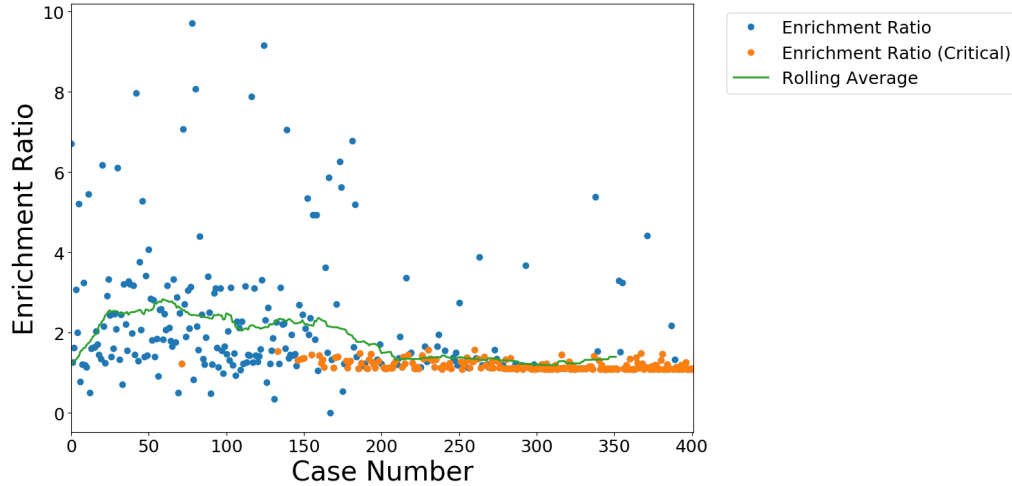


Figure 3.36: Optimizing for an EOL blanket enrichment that is as large as possible, relative to the BOL driver enrichment.

### 3.6 Two-Region Lattice

The two-region lattice was created due to increasing computational costs that prohibited extensive quarter-core modeling. In these cases, the outer breeder fuel ring had a higher BOL enrichment than the inner burner fuel ring. The  $k_{inf}$  and enrichment of the cases are shown in Fig 3.37 and Fig 3.38. The uncertainty in  $k_{inf}$  for the two-regions cases were on the order of  $\pm 0.0014$ . A selection of other analyzed cases are shown in Appendix A.2; the cases that show net breeding in both regions while critical are fast spectrum cases.

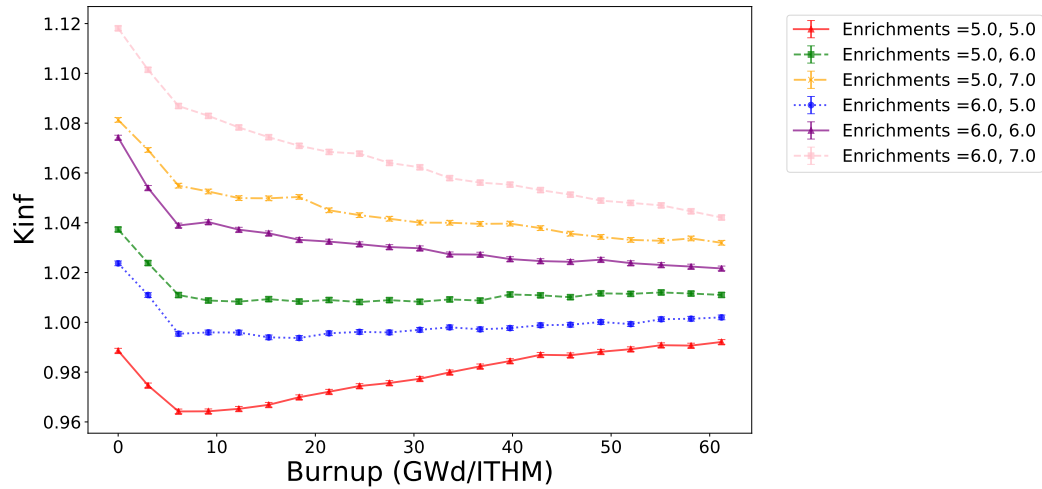


Figure 3.37:  $k_{inf}$  of the high enriched breeder two-region lattice with metallic moderator as a function of burnup and enrichment, with a fuel thickness of 2.5 cm.

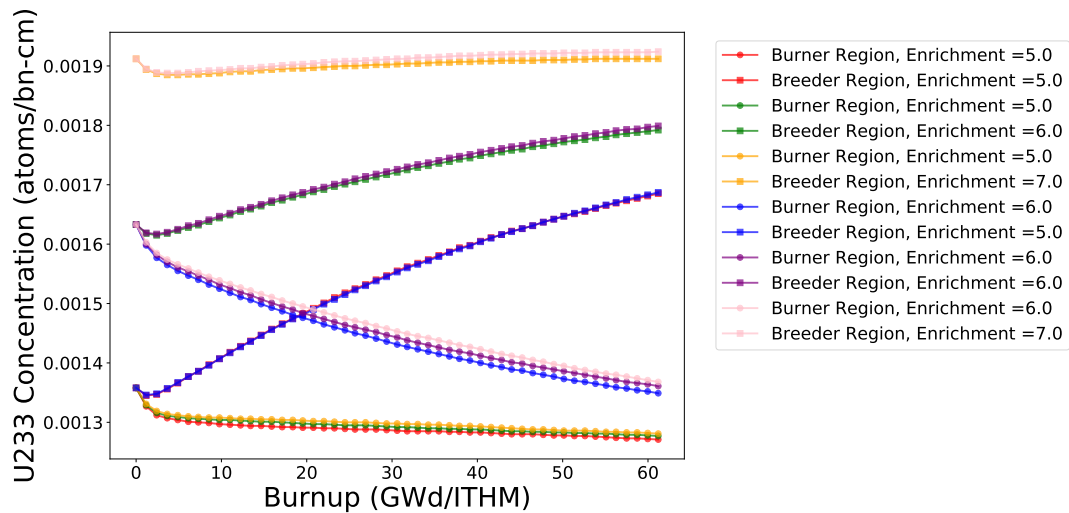


Figure 3.38:  $^{233}\text{U}$  number density of the high enriched breeder two-region lattice with metallic moderator as a function of burnup and enrichment, with a fuel thickness of 2.5 cm.

The best case in terms of breeding while critical had a central moderator radius of 4.5 cm, a burner fuel thickness of 2.5 cm, and an breeder fuel thickness of 3.1 cm. The  $k_{inf}$  of this case was close to 1.0, and the uncertainty was relatively high. This case was executed a second time with more simulated particles to reduce the uncertainty of the result, with 10000 particles per generation for 200 generations with 25 skipped generations. This yielded uncertainty in  $k_{inf}$  on

the order of  $\pm 0.00035$ . The  $k_{inf}$  and  $^{233}\text{U}$  concentration for this case are shown in Fig 3.39 and Fig 3.40.

In addition to a higher fidelity simulation, the fission product removal function was not used for the second analysis of this case. This was done to ensure that no errors were being introduced by the file transformation script and to make the result more conservative. Even without the fission product removal, the system remained critical for the duration of the burnup.

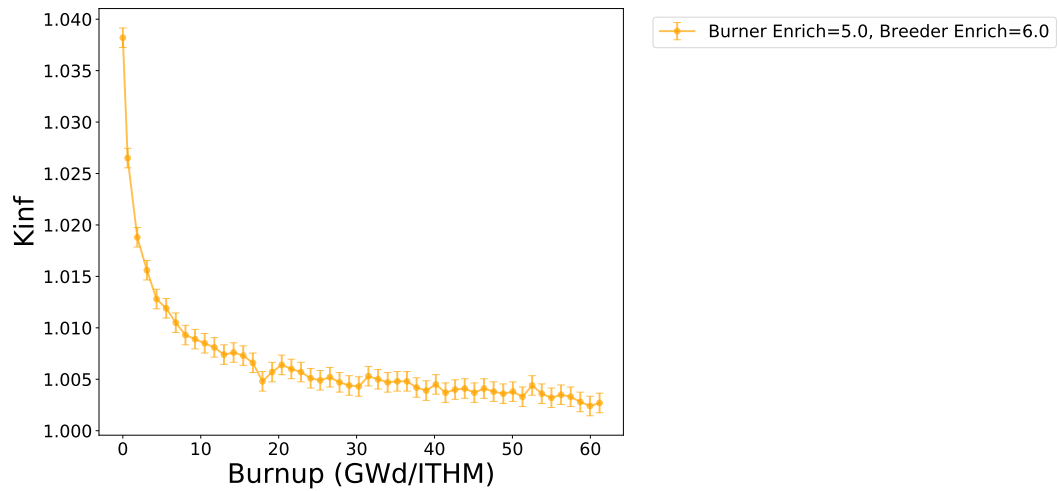


Figure 3.39:  $k_{inf}$  of the high enriched breeder two-region lattice with metallic moderator as a function of burnup for the best case result.

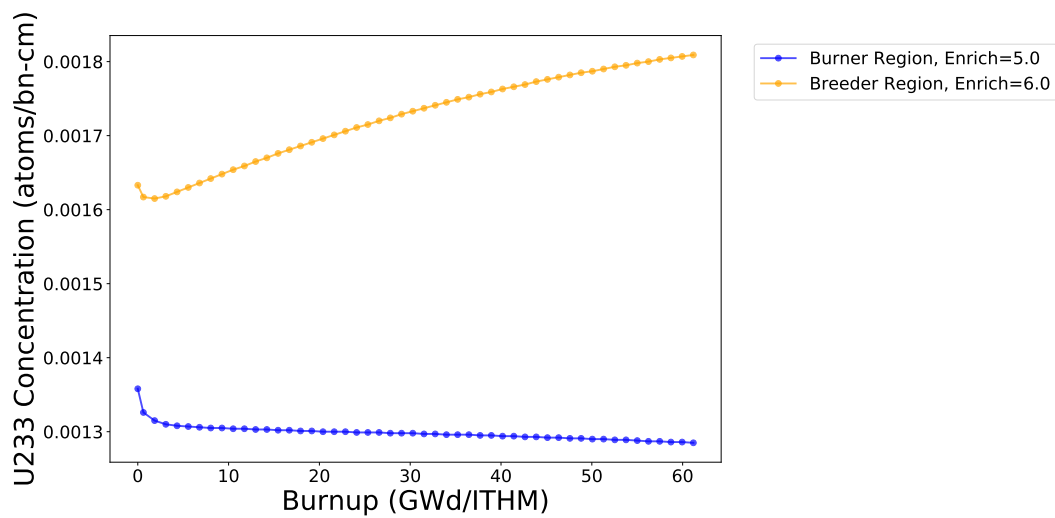


Figure 3.40:  $^{233}\text{U}$  number density of the high enriched breeder two-region lattice with metallic moderator as a function of burnup for the best case result.

The concentrations shown in Fig 3.40 can be placed into Equations 2.9 and 2.12 to determine the volume of fuel that must be exchanged between the regions. Since the model is an infinite lattice, the volumes will be normalized by the burner region volume. The region volumes, concentrations, and swapped volumes are shown in Table 3.15.

A final case was analyzed to ensure that the two-region fuel that displayed breeding while critical was in the thermal spectrum rather than the fast spectrum. Previous cases in the infinite lattice model showed that a sufficiently fast spectrum could support breeding while critical, which means that thermalization must be proven for these cases. This was done by removing the moderating material from the central moderating region in the two-region fuel. Removing the moderator resulted in the  $k_{inf}$  at BOL changing from  $1.03816 \pm 0.00035$  to  $0.91730 \pm 0.00018$ .

<i>Parameter</i>	<i>Value</i>
Volume, Burner	1.0
Volume, Breeder	1.83
BOL Concentration, Burner $[a/bn - cm]$	1.36E-3
EOL Concentration, Burner $[a/bn - cm]$	1.27E-3
BOL Concentration, Breeder $[a/bn - cm]$	1.63E-3
EOL Concentration, Breeder $[a/bn - cm]$	1.80E-3
Volume Removed from Burner	0.19
Volume Recycled into Breeder	0.04
Fissile Isotope Ratio	1.05

Table 3.15: Volumes and  $^{233}\text{U}$  concentrations of two-region lattice.

## 4 Discussion and Conclusions

### 4.1 Discussion

This section will discuss the results presented in Section 3. The focus of this analysis was to determine the feasibility of a thorium fueled thermal spectrum breeder-burner reactor. This analysis was facilitated by the creation of a suite of tools, including scripts that allowed for depletion with fission product removal to be coupled back to a transport code, scripts that coupled SCALE to Gnowee, and automated SCALE input generation and output parsing.

#### 4.1.1 Reduction of Order Study

The reduction of order study was executed first so it could be used with confidence in all follow-on analyses that utilized SCALE. In each region of the core, and over the entire core, there is less than a one percent difference in the  $^{233}\text{U}$  concentration between the high cost TRITON evaluation and the lower cost reduced order evaluation, as shown in Fig 3.1. The lower cost case required approximately half the time as compared to the full TRITON case, as shown in Figure 3.2. The error is low enough that there is confidence that the reduced order cases will produce sufficiently good results for preliminary investigations.

#### 4.1.2 Infinite Homogeneous Model

The goal of the infinite homogeneous model was to compare several materials for their potential as moderators. This is important especially for the metallic moderator as a unique mixture that does not have a well-characterized history as a moderator, unlike the other materials analyzed. The properties of all the moderators will be compared to the properties of light water. The moderating power and moderating ratio are used as the metrics to compare the moderators, and are displayed in Fig 3.3.

Heavy water has an impressive moderating ratio, but a relatively low moderating power. A low moderating power indicates that more of the material will be needed to moderate neutrons. This is problematic because heavy water is very expensive, costing \$1.5 billion or over 20% of the capital cost of a new reactor in 1993 dollars [33]. Heavy water is excluded from further



analysis for this financial reason, rather than its moderating properties.

Graphite is a common, well-characterized moderator and displays good neutronic qualities. However, the low moderating power indicates that a large pitch-to-diameter ratio will be needed to achieve optimal moderation. The downside of this is that the reactor would have to be large and high purity graphite would be required, as mild impurities can have major consequences for a large volume of moderator. However, the properties of graphite are enticing enough that it will be included in further analyses.

The metallic moderator mixture has a moderating ratio similar to light water. This means that neutron losses in the metallic moderator should be roughly the same as those in light water, which should be on the order of the losses shown in Fig. 1.7. The moderating power is lower than water's indicating that a larger pitch-to-diameter ratio will be needed for an optimal case. The metallic moderator is in the research phase of its development, but due to showing moderation qualities that are on the order of light water, it should be a suitable candidate as a moderator. It is expected to have appealing thermal-hydraulic properties that prevent accidents such as departure from nucleate boiling accidents and a negative temperature coefficient. These properties are sufficient to merit further analysis with this material.

Zirconium hydride is another well-characterized moderator, known for its role in the pulsing capability of TRIGA reactors [11]. Zirconium hydride also has a moderating power similar to light water, but may not be suitable for higher temperatures due to hydrogen disassociation. Zirconium hydride will not be considered further as a candidate moderator, as it has similar enough properties to the metallic moderator that analyzing both would likely be redundant.

### 4.1.3 Infinite Lattice Pin Model

#### Fission Product Removal Study

The fission product removal study was performed to measure the impact of removing gaseous and volatile fission products. The results of the study show a clear reactivity benefit in Fig 3.1, with an end-of-life reactivity difference of  $3.8\% \Delta k/k$  between the control case and the fission product removal case. Equilibrium xenon has an effect of roughly  $-2.6\% \Delta k/k$ , so the calculated benefit seems to be reasonable [34]. The fission product removal also has the benefit of extending the duration that the lattice had a  $k_{inf}$  greater than one by 51%. This is summarized in Table

## 3.4.

The results also show that the reduction of order method with 2 time-steps, represented by the two dots at beginning-of-life and end-of-life, has a close agreement with the higher fidelity 20 interval case. There was a 1% difference between the end-of-life  $k_{inf}$  calculated for the reduced order 2 interval case and the high fidelity 20 interval case.

### **Trends for Fissile Isotope Ratio and $k_{inf}$**

The trends for FIR and  $k_{inf}$  are used to determine the peak for FIR and  $k_{inf}$  as a function of pitch-to-diameter ratio. These cases were evaluated before the burnup cases because their computational cost is 4% the computational cost of a burnup case. The peak for  $k_{inf}$  in the metallic moderator is at a pitch-to-diameter ratio between 2.2 and 2.4, the peak for the low density metallic moderator is about 3.5, and for graphite the peak is between 5.5 and 6.0. These values were used to analyze the peak and near-peak cases as a function of burnup. In all cases, FIR increases as moderation decreases.

The results of these trends can be interpreted with the six-factor formula. Referring to Equation 1.7, the probability of non-leakage terms are equal to one due to the infinite medium. Since the reactor is moderated, the fast fission factor,  $\epsilon$ , is expected to remain relatively small and constant. This leaves  $\eta$ ,  $f$ , and  $p$  to change as parameters are adjusted.  $\eta$  will increase as enrichment increases, due to an increased likelihood of a fuel absorption being in  $^{233}\text{U}$ .  $f$  and  $p$  will change with the degree of moderation, with  $f$  growing as neutrons are thermalized. However, at a certain point there will be enough moderator that thermal absorptions begin to happen more frequently in the moderator, decreasing  $f$ . The increasing moderation will likely increase  $p$ , as most moderators do not have substantial resonance integral cross sections and are more likely to down-scatter the neutrons than absorb them. The additions of poisons to the fuel would dramatically change this relationship though, as neutrons in the resonance regions are likely to be absorbed by the poisons.

None of the cases presented in Section 3.4.3 demonstrate a net increase in fissile inventory while also sustaining criticality. The cases that have a high FIR while being subcritical should not necessarily be interpreted to mean that they are better at breeding than the critical cases. For example, a subcritical case with a FIR that is twice the magnitude of the FIR of a critical case is not breeding at twice the rate of the critical case. This is due to the way that SCALE

calculates flux and power. SCALE takes the user input power, given in terms of megawatts per initial ton heavy metal ( $MW/ITHM$ ), with the flux-spectrum weighted cross sections to determine the magnitude of flux needed to achieve a fission reaction rate that would result in the input power. This means that the sub-critical cases are consuming the same amount of fissile material as the critical and supercritical cases, but they are being supplied an ‘artificial’ flux. This artificially supplied flux can be up to an order of magnitude higher than the total flux of the critical cases, and this results in a higher reaction rate with the fertile materials despite having the same burnup as the critical cases. The artificial flux is accelerating the depletion, so the FIR of cases with the same burnup cannot be directly compared. The effects of the artificial flux can be accounted for using the neutron balance equation.

### $k_{inf}$ and $^{233}\text{U}$ Enrichment vs Burnup

The  $k_{inf}$  and  $^{233}\text{U}$  enrichment as a function of burnup plots show that the long-term trends depend on the pitch-to-diameter ratio, with each case converging to a  $^{233}\text{U}$  concentration trend line. These cases show that increasing moderation correlates with less breeding of fuel. This trend is demonstrated in Fig. 3.19, where the cases with pitch-to-diameter ratios of 1.1 show higher rates of breeding and higher steady-state  $^{233}\text{U}$  concentrations than the cases with more moderator. However, the pitch-to-diameter ratio cannot be reduced any further due to thermohydraulic constraints. The flux was able to be further hardened by reducing the moderator density in the metallic moderator.

The rising  $^{233}\text{U}$  concentration required to maintain criticality in Table 3.5, Table 3.6 and Table 3.7 show that fission products are building up in the fuel. This indicates that even if fuel in the blanket can be bred up to the BOL enrichment of fuel in the driver, it may have a concentration of neutron poisons that limit its efficacy at providing neutrons for the next cycle. Fission product poisoning is less of a concern for fast spectrum breeder-burner reactors, but Table 3.7 shows that the higher burnup from the 10 wt% case caused the system to become subcritical at a  $^{233}\text{U}$  concentration that is 43% higher than the  $^{233}\text{U}$  concentration of the 3 wt% case for a pitch-to-diameter ratio of 5.4.

## Neutron Balance

The neutron balance is used to quantify the number of excess neutrons available to the system from a fuel source. A negative value for the neutron balance indicates a sink rather than a source, and can be used to determine the number of neutrons required to enrich fuel when used with the  $^{233}\text{U}$  concentration data. The peak numbers of excess neutrons shown in Table 3.8, Table 3.9, and Table 3.10 are less than the numbers of neutrons required to breed unenriched fuel up to the enrichment of the driver, as shown in Table 3.11, Table 3.12 and 3.13, for all cases analyzed. Fig 3.35 shows that the cases with the highest neutron production do not supply enough neutrons to sufficiently breed the best-case geometry. Even though a graphite case could not have the breeder properties of the low density metallic moderator, the two cases are compared in Fig 3.35 to illustrate the discrepancy between the neutrons required by the best breeding case with low density metallic moderator and the best case for excess neutrons with graphite moderator.

These cases even include non-conservative assumptions. The assumption of an infinite medium means that leakage is discounted, which could be a significant factor. Fig 1.8 shows that leakage and reactivity control losses that total less than 5% are enough to substantially increase the minimum burnup required for operation.

The first iteration of infinite lattice models indicated that there were sufficient excess neutrons provided to enrich the breeder fuel to the BOL driver enrichment. However, the time-step of the original cases was too small for the 1% enriched and unenriched breeder cases. This led to more breeding during the first few depletion steps than should have been possible. New cases were analyzed again with appropriate time-steps and indicated that even in an infinite core there were not sufficient excess neutrons for breeding. However, the quarter-core model had already been created and analyzed. The cases presented in this paper are the more recent, accurate cases.

### 4.1.4 Quarter-Core Analysis

The magnitude of the excess neutrons required by the infinite lattice model was determined to be too large to be feasible. The value of the quarter-core analysis originally was to determine if there are any geometries within the design space of a two-region core with separated burner and breeder regions that are feasible. Now that the infinite lattice indicates that breeding and burning with the assumption of direct swapping is not possible, the value of the quarter-core

model is to show the limitations and in-feasibility of the core model that emphasized non-local breeding.

The infinite lattice model gave insight into efficient geometries for the quarter-core model. Several bounds for Gnowee were determined using the infinite pin lattice analysis. The lower bound of the fuel edge-to-edge pitch was made small to allow for a hard spectrum in the breeder region, and the high bound allowed the pitch to be slightly larger than the values that yielded the optimum pitch-to-diameter ratio in the infinite lattice study. The fuel radius was allowed to be larger than the values evaluated in the infinite lattice study due to the analyses from the LWBR reactor that indicated that larger fuel diameters resulted in a harder neutron spectrum, and better breeding [17].

Fig. 3.36 shows the calculated enrichment ratio between the burner region and the blanket region as a function of case number. The enrichment ratio approached 1.0 with successive generations, but the highest fitness solution had an enrichment ratio of 1.08. This indicates that the blanket cannot be bred to a higher enrichment than the driver, for the parameters explored. This solution is not necessarily the optimum solution, but it is the highest fitness solution that was found within the defined bounds. The reason the enrichment ratio never reached 1.0 is in part because how the bounds of the problem were defined. It is likely that the enrichments were not allowed to become large enough, as they were originally given a 5% enrichment cap. The regions converged to the maximum allowable enrichment when the max number of iterations was reached for the optimization. This indicates that for future cases the maximum allowable enrichment should be increased. Another bound that was over-constrained is the edge-to-edge pitch. This should have been allowed to go to nearly zero in order to capture the very small pitch-to-diameter ratio cases.

This Gnowee evaluation required roughly 20 days to reach its iteration limit, with each case needing between 2 and 3 hours to evaluate a case. The method of defining the geometries of these cases resulted in gaps appearing between the different fuel regions. This was a minor concern when the fuel pitch was larger, but the gaps became substantial relative to the pitch when smaller pitches were used. In order to accommodate cases with small pitch-to-diameter ratios, a different geometry definition was needed in SCALE. The new method removed the gaps, but resulted in much longer computation times due to the new structure definitions. The required computation time changed from between 2 and 3 hours per case to between 24 and 36

hours per case. The two-region lattice became necessary due to computer time constraints.

#### 4.1.5 Two-Region Lattice

The most promising cases in terms of net breeding and sustained criticality were presented in Section 3.6. In these cases, the  $^{233}\text{U}$  content of the system is described by concentration, rather than by enrichment. This is due to the use of concentration in the mass balance equations. These cases explore designs that have a higher enrichment in the breeder region than the burner region. It was originally assumed that a lower enriched breeder region would breed more efficiently than a higher enriched breeder region. However, a higher enrichment in the breeder region allowed for more power to be generated in that region, and the depletion of the burner region was reduced. This meant that less fuel had to be transferred into the burner region. It is also likely that a local source of fast neutrons due to fissions in the breeder region allowed for a better neutron spectrum for breeding. The  $k_{inf}$  and  $^{233}\text{U}$  concentration of the best case analyzed is shown in Fig 3.39 and Table 3.15. The case is both critical and sustaining sufficient breeding that the breeder and burner fuel can be mixed and re-distributed such that each region attains its BOL  $^{233}\text{U}$  concentration. The burnup required for this swapping to occur is around  $60 \text{ MWd/ITHM}$ , which is high for LWR fuel, but relatively low compared to the burnup experienced by fast reactors.

The case was proven to be driven by thermal neutrons. Removing the moderator resulted in the  $k_{inf}$  at BOL changing from  $1.03816 \pm 0.00035$  to  $0.91730 \pm 0.00018$ , indicating that the system relies on the moderator and thermalization of neutrons to operate.

## 4.2 Summary and Future Work

This chapter presented the discussion and interpretation of the results gathered in Section 3. In addition to the direct results of these analyses, a high value item produced for these studies is a software tool that was developed to couple Gnowee and SCALE, with fission product removal. In addition to the optimization capabilities of the coupled codes, the input creation and execution is fully automated outside of Gnowee, so rapid prototyping in SCALE is quick and easy to accomplish. This is a tool that could be used for general core design and shielding calculations.

### 4.2.1 Summary

This section provides a brief summary of the methods and results of this thesis. The first analysis was the reduction of order study, which showed that the reduction of order method provided good agreement with higher fidelity studies, while running in much less time. The homogeneous moderator study was useful for narrowing down candidates for further analysis, and showed that the metallic moderator was a promising option. The infinite lattice analysis determined the optimum pitch-to-diameter ratios for fuel in the burner region of a core, and that less moderation is better for breeding. The fission product removal study, done as part of the infinite lattice analysis, showed that removing the fission products can extend the critical lifetime of a fuel pin by nearly 50% in the case analyzed. The quarter-core model was created with Gnowee using boundaries determined from the infinite lattice study. The optimization succeeded in creating critical cases and improving the enrichment ratio set as the objective function. However, the bounds of the model were over-constrained and no cases were found that allowed for sufficient breeding in the fuel. Finally, the two-region lattice model was created to assess whether breeding and burning could be sustainable. The two-region infinite lattice was able to sustain criticality while also enhancing the breeder region to a sufficient enrichment that both regions were returned to their BOL uranium concentrations. The successful two-region cases were shown to rely on thermalized neutrons by removing the moderator and driving the system to be subcritical.

The results of this thesis indicate the feasibility of a thermal spectrum thorium breeder reactor within the bounds of the analyzed geometry and materials. However, more work is necessary to assess the true viability of this design, including long-term steady state analysis, thermo-hydraulic analysis, and additional material variations.

### 4.2.2 Future Work

All of the studies presented here could be explored in new directions. Different materials could be used in the fuel, moderator, and cladding to potentially achieve better results. Variations of the two-region infinite lattice could also be explored, such as adding a third region, exploring higher enrichments in the burner region, and analyzing the cases for thermal limitations and power density limits.

The next step in the analysis of the two-region lattice is to evaluate multiple cycles of fuel swapping between the regions to determine the long-term effects of fission product build-up. This could give insight into the steady-state swapping scheme and operations. Once the ideal infinite cases are analyzed, a quarter-core model that using the two-region fuel pins could be used to test that the breeding while critical observed in the two-region infinite lattice analysis functions in a finite core geometry. This core analysis could use Gnowee coupled to SCALE to maximize the breeding and investigate critical configurations. The steady-state operation of the core model would also need to be determined, similar to the infinite lattice cases. The ideal product of this would be a core that is confirmed to be a thermal spectrum breeder that has long-term sustainability.





## Bibliography

- [1] J. Bevins and R. Slaybough. Gnowee: a hybrid metaheuristic optimization algorithm for constrained, black box, combinatorial mixed-integer design. Technical report, University of California, Berkley, 2018.
- [2] A. Borio, M. Cagnazzo, F. Marchetti, P. Pappalardo, and A. Salvini. Moderating ratio parameter evaluation for different materials by means of monte carlo calculations and reactivity direct measurements. Technical report, Laboratorio Energia Nucleare Applicata, University of Pavia, Italy, 2004.
- [3] T. Cochran, H. Feiveson, W. Patterson, G. Pshakin, M. Ramana, M. Schneider, T. Suzuki, and F. von Hippel. Fast breeder reactor programs: History and status. Technical report, International Panel on Fissile Materials, 2010.
- [4] J. Cook and et al. Consensus on consensus: a synthesis of consensus estimates on human-caused global warming. Technical report, Environmental Research Letters 11, 2016.
- [5] V. Dekoussar, G. R. Dyck, A. Galperin, C. Ganguly, M. Todosow, and M. Yamawaki. Thorium fuel cycle - potential benefits and challenges. Technical report, International Atomic Energy Agency, 2005.
- [6] P. Denholm, M. O’Connell, G. Brinkman, and J. Jorgenson. Overgeneration from solar energy in california: A field guide to the duck chart. Technical report, National Renewable Energy Laboratory, 2015.
- [7] J. J. Duderstadt and L. J. Hamilton. *Nuclear Reactor Analysis*. John Wiley & Sons, Inc., 1976.
- [8] M. R. Enzo De Sanctis, Stefano Monti. *Energy from Nuclear Fission*. Springer, 2016.
- [9] O. Fabbris, S. Dardour, P. Blaise, J. Ferrasse, and S. M. Surrogates based multi-criteria predesign methodology of sodium-cooled fast reactor cores – application to cfv-like cores. *Nuclear Engineering and Design*, 305:314–333, 2016.
- [10] I. Gauld, G. Radulescu, B. Ilas, G. and Murphy, M. Williams, and D. Wiarda. Isotopic depletion and decay methods and analysis capabilities in scale. *Nuclear Technology*, 174:169–195, 2011.

- [11] General Atomics. Triga advantages. <http://www.ga.com/triga-advantages>, 2020.
- [12] E. Greenspan. A phased development of breed-and-burn reactors for enhanced nuclear energy sustainability. Technical report, University of California, Berkeley, 2012.
- [13] E. Greenspan, F. Heidet, C. Sanzo, S. Qvist, R. Cognet, and S. Gonzolas. Maximum fuel utilization in fast reactors without chemical reprocessing. Technical report, University of California, Berkeley, 2012.
- [14] E. Greenspan and T. Kim. A pebble-bed breed and burn reactor. Technical report, University of California, Berkeley, 2016.
- [15] E. Greenspan, G. Zhang, and M. Fratoni. Improved resource utilization by advanced burner reactors with breed-and-burn blankets. *Progress in Nuclear Energy*, 106:440–454, 2018.
- [16] R. Hargraves and R. Moir. Liquid fluoride thorium reactors: An old idea in nuclear power gets reexamined. Technical report, American Scientist, Vol. 98, No. 4 (July-August 2010), pp. 304-313, 2010.
- [17] H. Hecker and L. Freeman. Design features of the light water breeder reactor (lwbr) which improve fuel utilization in light water reactors. Technical report, Bettis Atomic Power Laboratory, 1981.
- [18] International Atomic Energy Agency. Nuclear power reactors in the world. Technical report, IAEA, 2018.
- [19] International Energy Agency. Global energy and co2 status report - electricity. <https://www.iea.org/geco/electricity/>, 2018.
- [20] International Nuclear Safety Advisory Group. Insag-7, the chernobyl accident: Updating of insag-1. Technical report, INSAG, 1992.
- [21] A. Kasam. Conceptual design of a breed & burn molten salt reactor. Technical report, University of Cambridge, 2018.
- [22] Korea Atomic Energy Research Institute. Trapping technology for gaseous fission products from voloxidation process. Technical report, KAERI, 2005.

- [23] K. Kuwagaki, J. Nishiyama, and T. Obara. Concept of breed and burn reactor with spiral fuel shuffling. *Annals of Nuclear Energy*, 127:130–138, 2018.
- [24] J. R. Lamarsh and A. J. Baratta. *Introduction to Nuclear Engineering*. Prentice Hall, 2001.
- [25] Massachusetts Institute of Technology. The future of nuclear energy in a carbon-constrained world. Technical report, MIT, 2018.
- [26] E. Merle, D. Heuer, M. Brovchenko, and V. Ghetta. Launching the thorium fuel cycle with the molten salt fast reactor. Technical report, Grenoble INP, 2011.
- [27] Moltex Energy. An introduction to the moltex energy technology portfolio. Technical report, Moltex Energy, 2018.
- [28] National Nuclear Science Center. Endf/b-vii.1: Nuclear data for science and technology: Cross sections, covariances, fission product yields and decay data.
- [29] H. Nifenecker, S. David, J. Loiseaux, and M. O. Basics of accelerator driven subcritical reactors. *Nuclear Instruments and Methods in Physics Research Section A: Accelerators, Spectrometers, Detectors and Associated Equipment*, 463:428–467, 2001.
- [30] Nuclear Energy Agency and International Atomic Energy Agency. *Uranium 2018 Resources, Production, and Demand*. Nuclear Energy Agency and International Atomic Energy Agency, 2018.
- [31] Nuclear Regulatory Commission. 10 CFR 50, Appendix A. <https://www.nrc.gov/reading-rm/doc-collections/cfr/part050/full-text.html#part050-appa>, 2020.
- [32] G. Olson, R. McCardell, and D. Illum. Fuel summary report: Shippingport light water breeder reactor. Technical report, Idaho National Engineering and Environmental Laboratory, 2002.
- [33] Ontario Power Generation. Final and total cost of darlington nuclear generating station. <https://web.archive.org/web/20120422220759/http://www.cleanairalliance.org/files/active/0/DarlingtonFOIresults.pdf>, 2004.
- [34] T. Palmer. Lecture notes in nse 452, neutronics analysis ii, xenon and samarium lecture, February 2017.

- [35] A. Perry, C. Preskitt, and E. Halbert. *A study of graphite-moderated Th-U233 breeder systems*. Oak Ridge National Laboratory, 1960.
- [36] A. Perry and A. Weinberg. Thermal breeder reactors. Technical report, Oak Ridge National Laboratory, 1972.
- [37] R. Singiresu. *Engineering Optimization - Theory and Practice*. Wiley and Sons, 2009.
- [38] A. Sobolev, A. Gazetdinov, and D. Samokhin. Genetic algorithms for nuclear reactor fuel load and reload optimization problems. *Nuclear Energy and Technology*, 3:231–235, 2017.
- [39] R. Stewart, C. Pope, and E. Ryan. Fast spectrum reactor fuel assembly sensitivity analysis. *Annals of Nuclear Energy*, 110:1091–1097, 2017.
- [40] N. Takaki. Breeding capability of molten salt reactor (msr), 2018.
- [41] M. Todosow, A. Galperin, S. Herring, M. Kazimi, T. Downar, and A. Morozov. Use of thorium in light water reactors. *Nuclear Technology*, 151:168–176, (2005).
- [42] United Nations. Paris agreement. [https://unfccc.int/sites/default/files/english\\_paris\\_agreement.pdf](https://unfccc.int/sites/default/files/english_paris_agreement.pdf), 2016.
- [43] U.S. Department of Energy. Capital cost estimates for utility scale electricity generating plants. Technical report, US DOE, 2016.
- [44] US Energy Information Administration. Levelized cost and levelized avoided cost of new generation resources in the annual energy outlook 2020. Technical report, US IEA, 2020.
- [45] World Nuclear Association. The harmony programme. <https://www.world-nuclear.org/harmony>, 2018.

# Appendices

## A Additional Moderation Curves

### A.1 $^{233}\text{U}$ Concentration and $k_{inf}$

#### A.1.1 Metallic Moderator $k_{inf}$

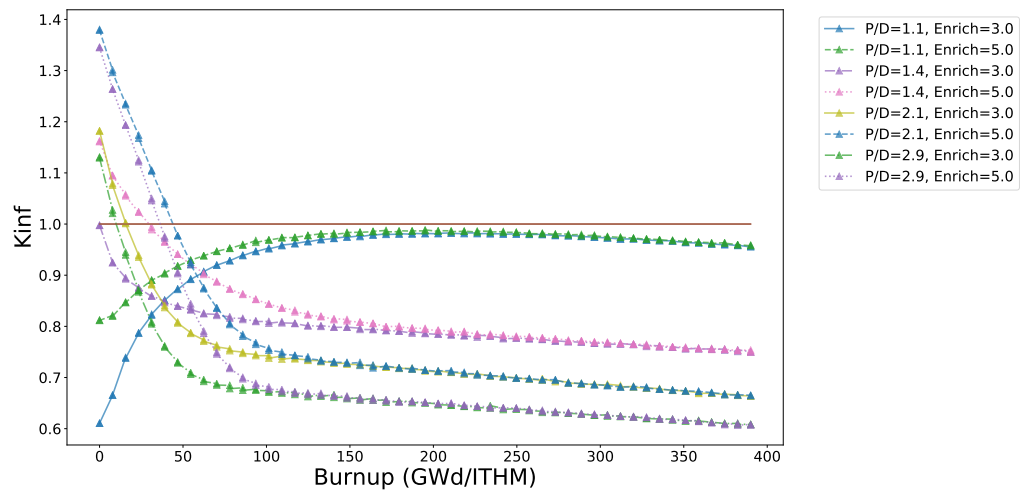


Figure A.1:  $k_{inf}$  for metallic moderator as a function of burnup, enrichment, and pitch-to-diameter (PD) ratio.

### A.1.2 Metallic Moderator $^{233}\text{U}$ Concentration

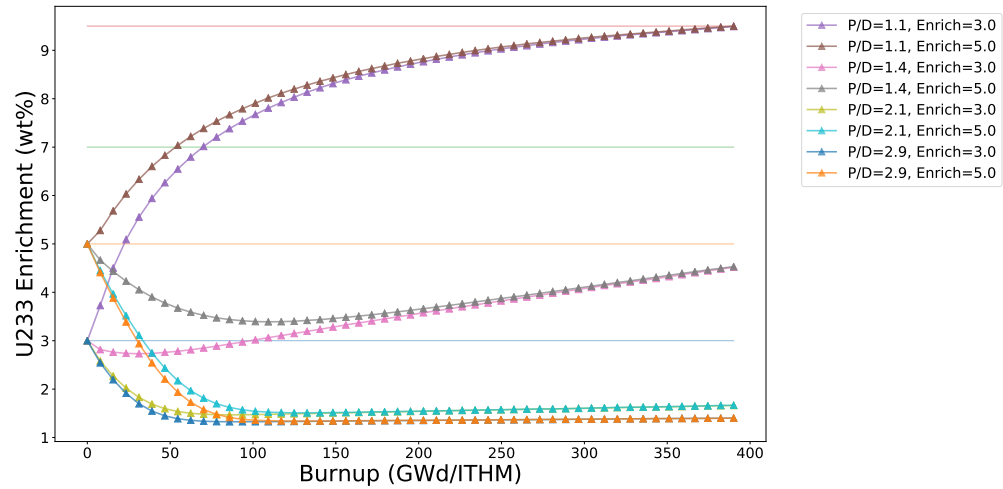


Figure A.2:  $^{233}\text{U}$  number density for metallic moderator as a function of burnup, enrichment, and pitch-to-diameter ratio.

### A.1.3 Metallic Moderator Neutron Balance

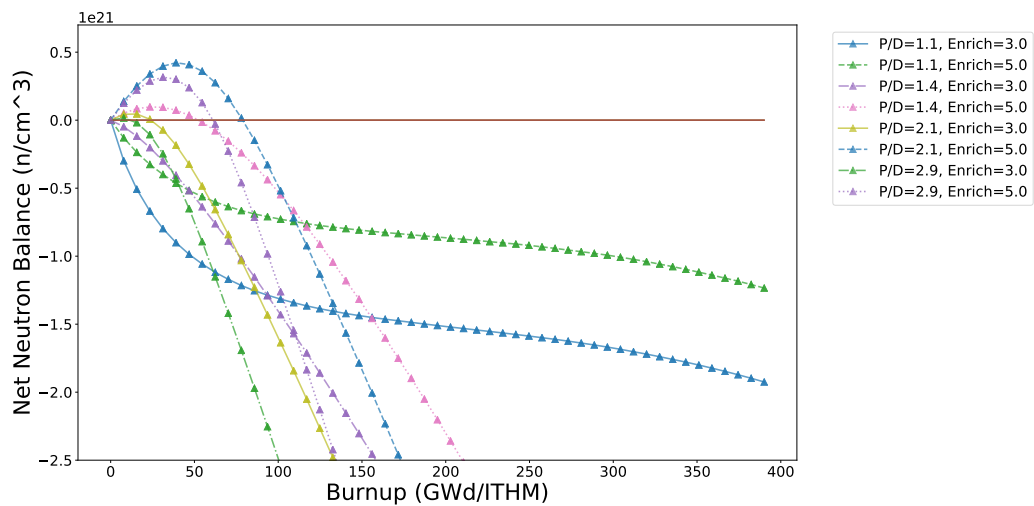


Figure A.3: Neutron balance for metallic moderator as a function of burnup, enrichment, and pitch-to-diameter ratio.



### A.1.4 Low Moderator Density Metallic Moderator $k_{inf}$

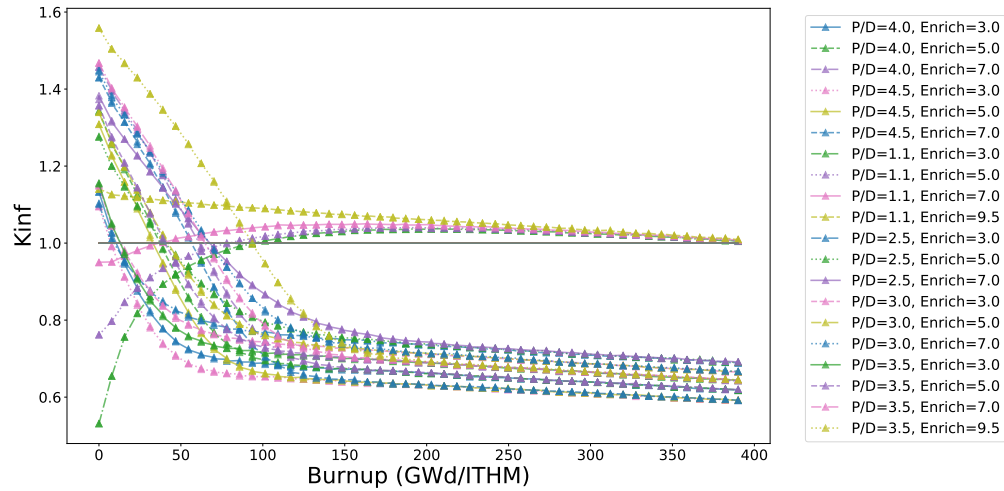


Figure A.4:  $k_{inf}$  for metallic moderator with low moderator density as a function of burnup, enrichment, and pitch-to-diameter ratio.

### A.1.5 Low Moderator Density Metallic Moderator $^{233}\text{U}$ Enrichment

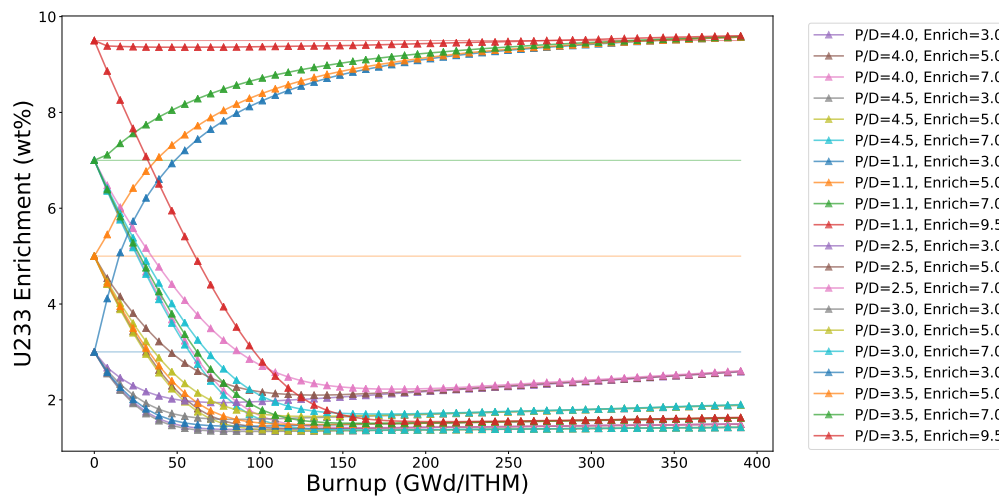


Figure A.5:  $^{233}\text{U}$  number density for metallic moderator with low moderator density as a function of burnup, enrichment, and pitch-to-diameter ratio.

### A.1.6 Low Moderator Density Metallic Moderator Neutron Balance

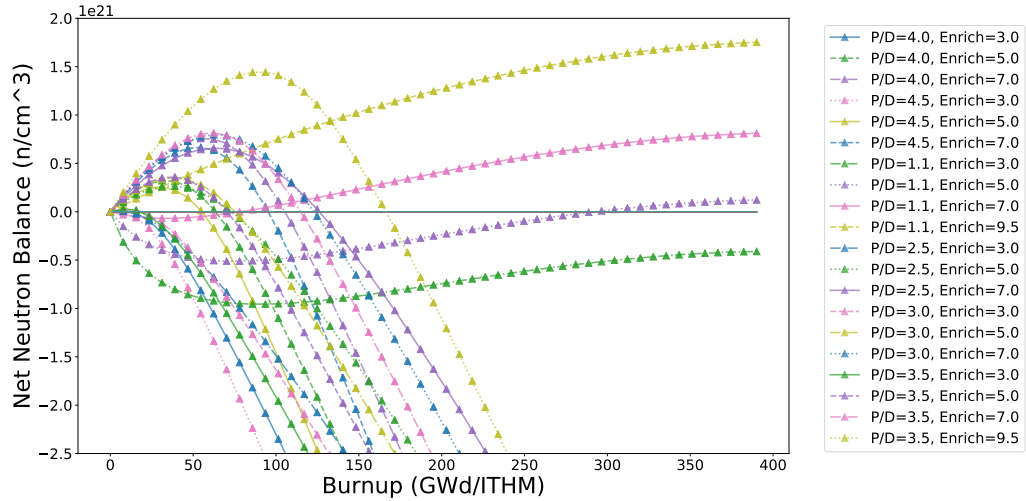


Figure A.6: Neutron balance for metallic moderator with low moderator density as a function of burnup, enrichment, and pitch-to-diameter ratio.

### A.1.7 Graphite Moderated $k_{inf}$

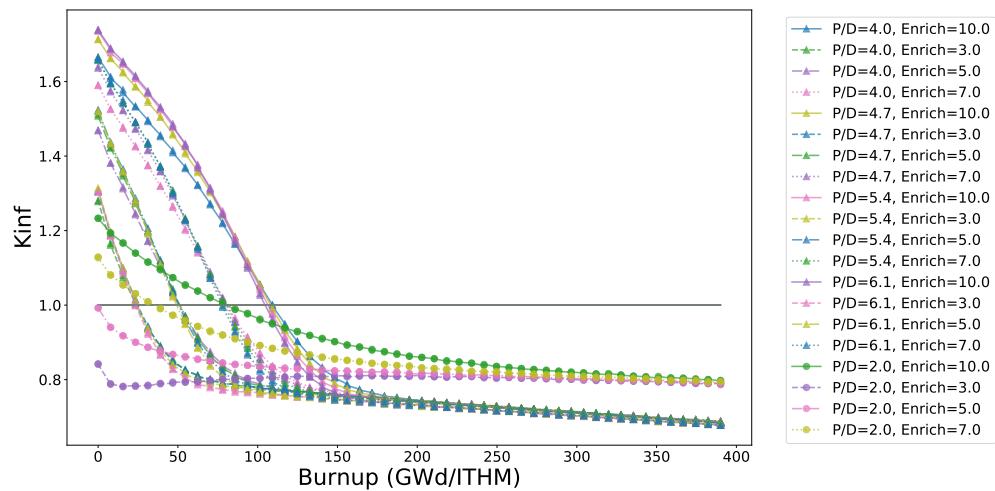


Figure A.7:  $k_{inf}$  for graphite as a function of burnup, enrichment, and pitch-to-diameter ratio.

### A.1.8 Graphite Moderated $^{233}\text{U}$ Concentration

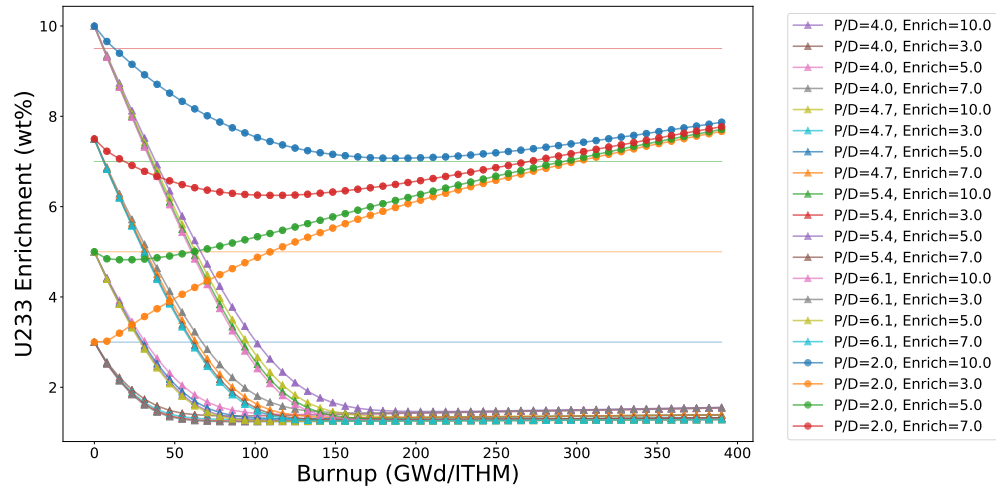


Figure A.8:  $^{233}\text{U}$  number density for graphite as a function of burnup, enrichment, and pitch-to-diameter ratio.

### A.1.9 Graphite Moderated Neutron Balance

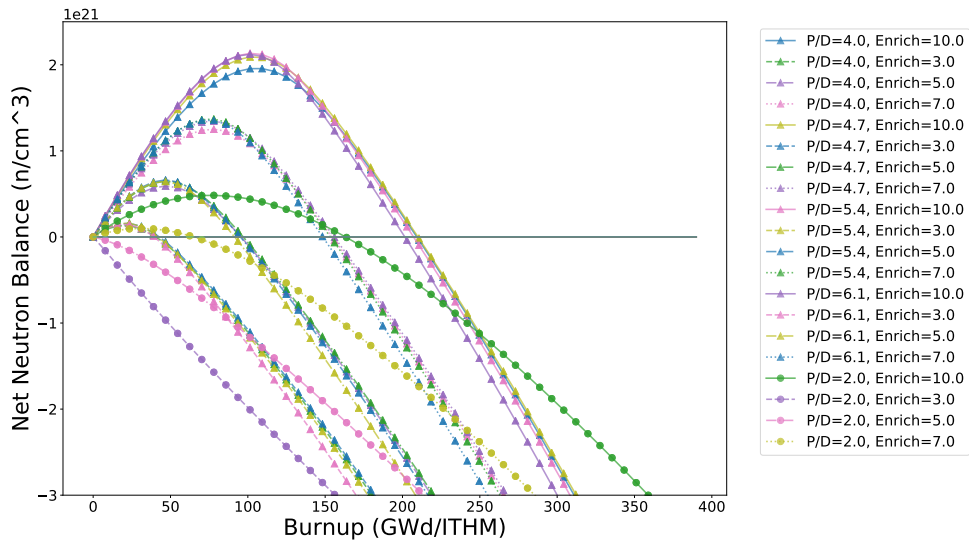


Figure A.9: Neutron balance for graphite as a function of burnup, enrichment, and pitch-to-diameter ratio.

## A.2 Two-Region $k_{inf}$ and $^{233}\text{U}$ Concentration

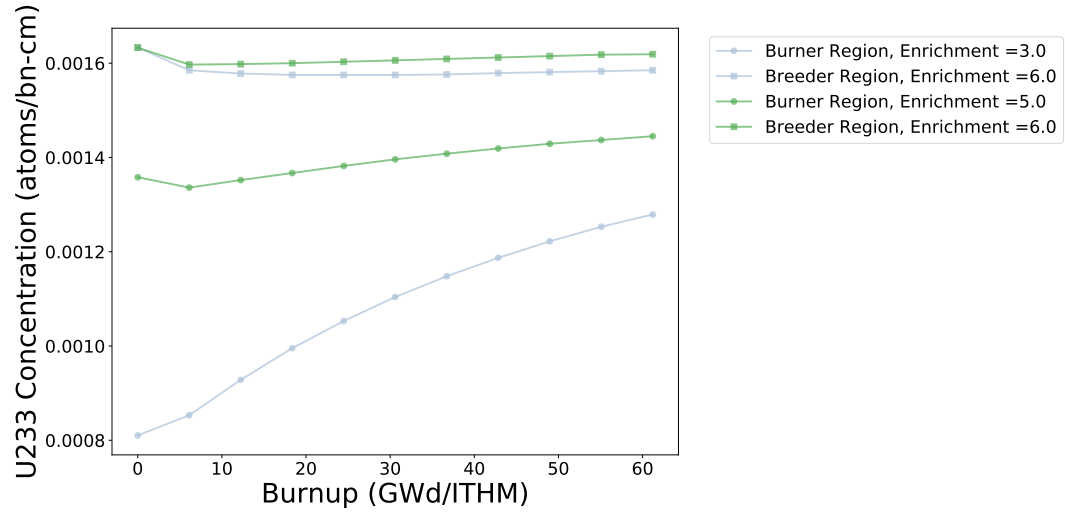


Figure A.10:  $^{233}\text{U}$  number density for metallic moderator in two-region lattice as a function of burnup and enrichment for 1.5 cm moderator radius and 0.5 cm thick inner fuel region.

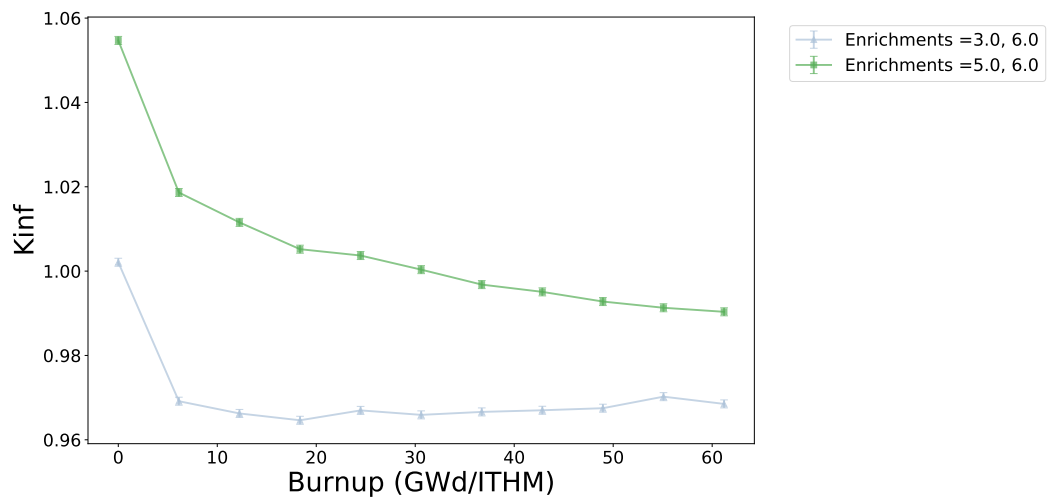


Figure A.11:  $k_{inf}$  for metallic moderator in two-region lattice as a function of burnup and enrichment for 1.5 cm moderator radius and 0.5 cm thick inner fuel region.

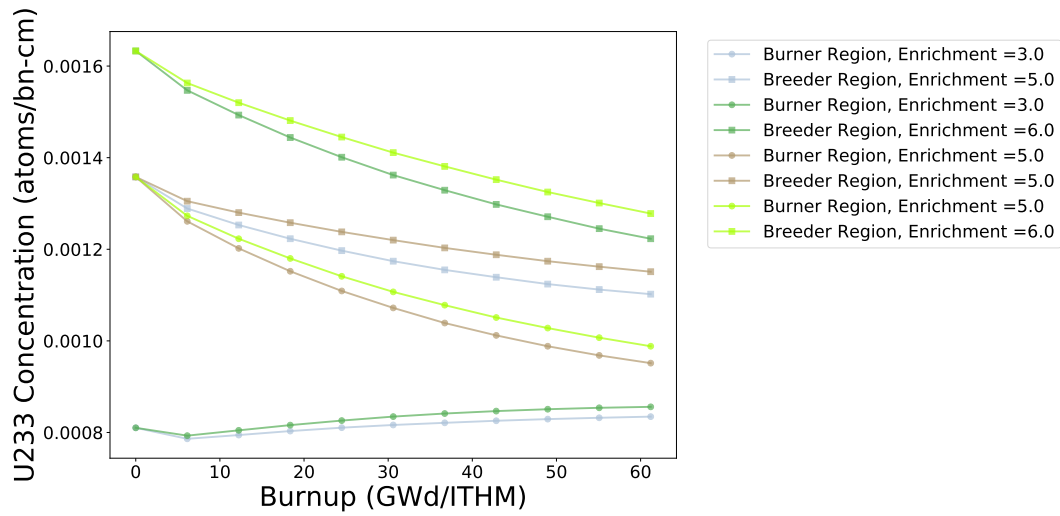


Figure A.12:  $^{233}\text{U}$  number density for metallic moderator in two-region lattice as a function of burnup and enrichment for 3.0 cm moderator radius and 0.5 cm thick inner fuel region.

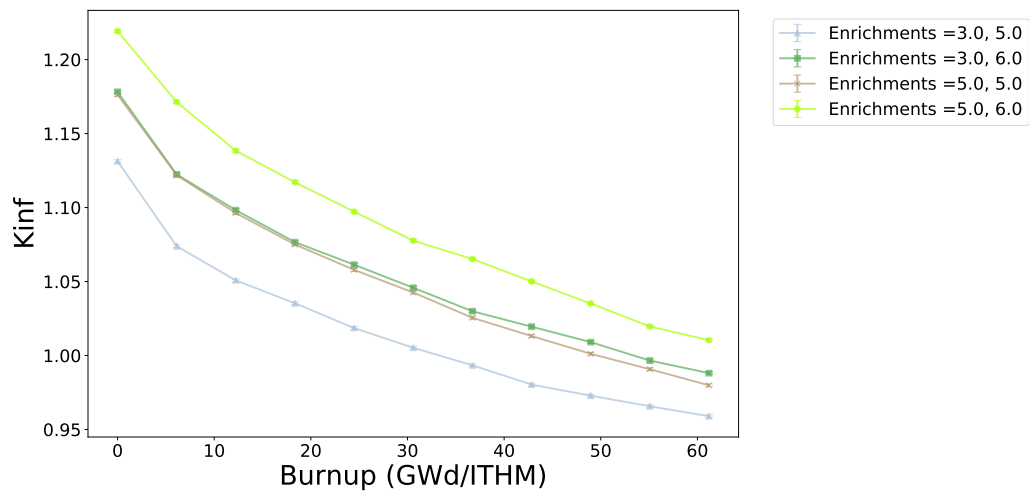


Figure A.13:  $k_{inf}$  for metallic moderator in two-region lattice as a function of burnup and enrichment for 3.0 cm moderator radius and 0.5 cm thick inner fuel region.

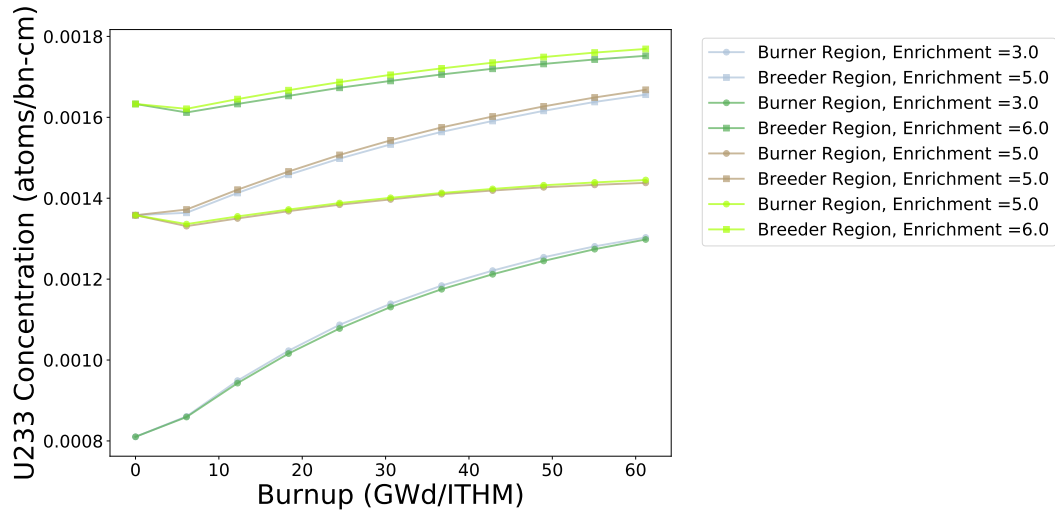


Figure A.14:  $^{233}\text{U}$  number density for metallic moderator in two-region lattice as a function of burnup and enrichment for 3.0 cm moderator radius and 1.5 cm thick inner fuel region.

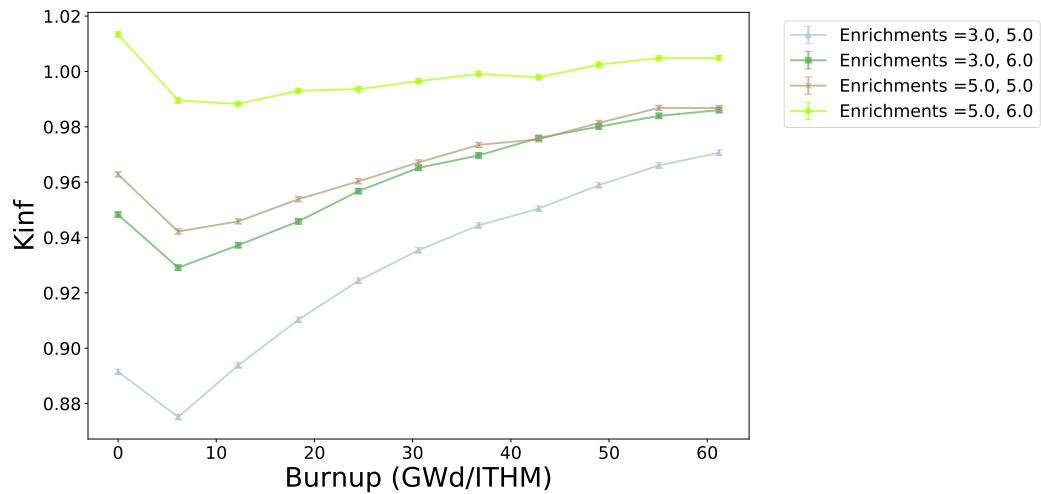


Figure A.15:  $k_{inf}$  for metallic moderator in two-region lattice as a function of burnup and enrichment for 3.0 cm moderator radius and 1.5 cm thick inner fuel region.

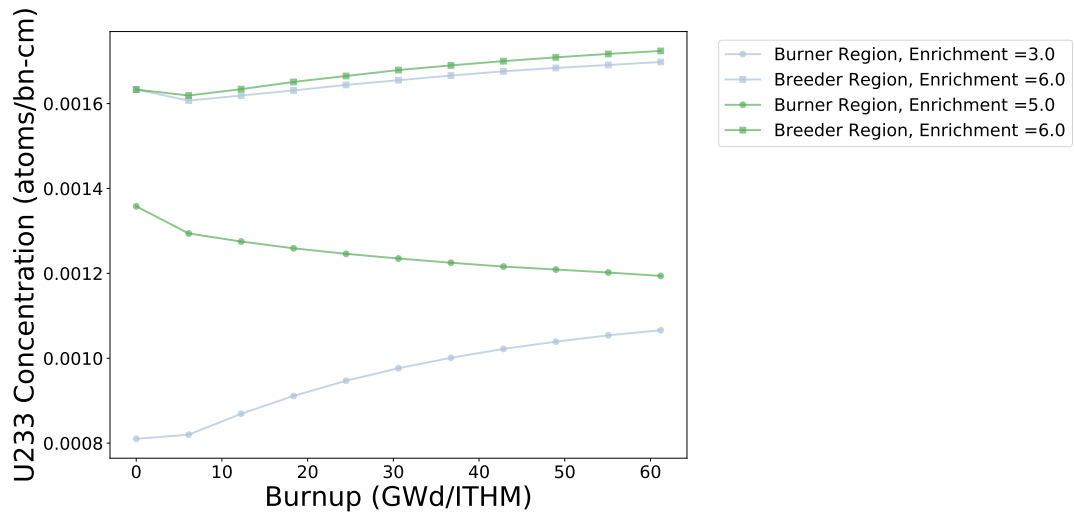


Figure A.16:  $^{233}\text{U}$  number density for metallic moderator in two-region lattice as a function of burnup and enrichment for 4.5 cm moderator radius and 2.0 cm thick inner fuel region.

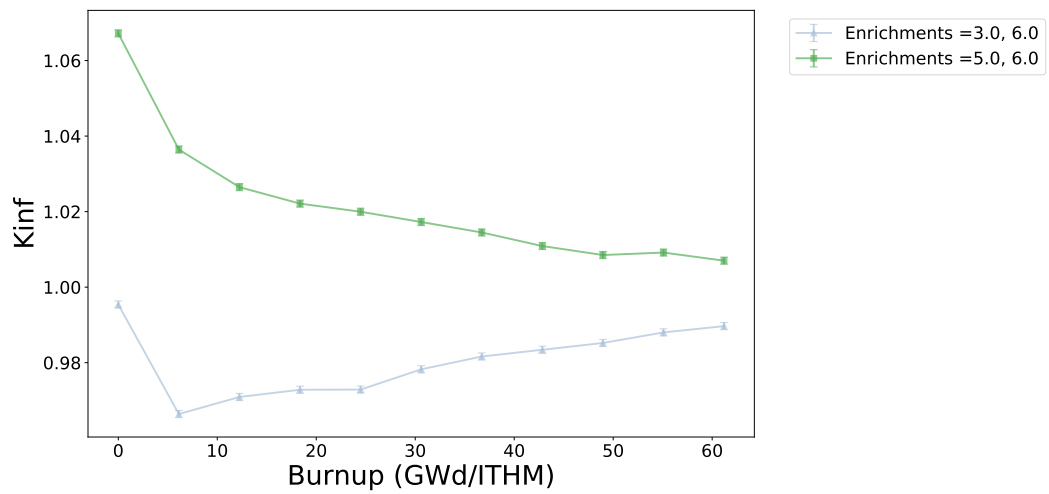


Figure A.17:  $k_{inf}$  for metallic moderator in two-region lattice as a function of burnup and enrichment for 4.5 cm moderator radius and 2.0 cm thick inner fuel region.

### A.3 Other Moderator Curves

#### Zirconium Hydride

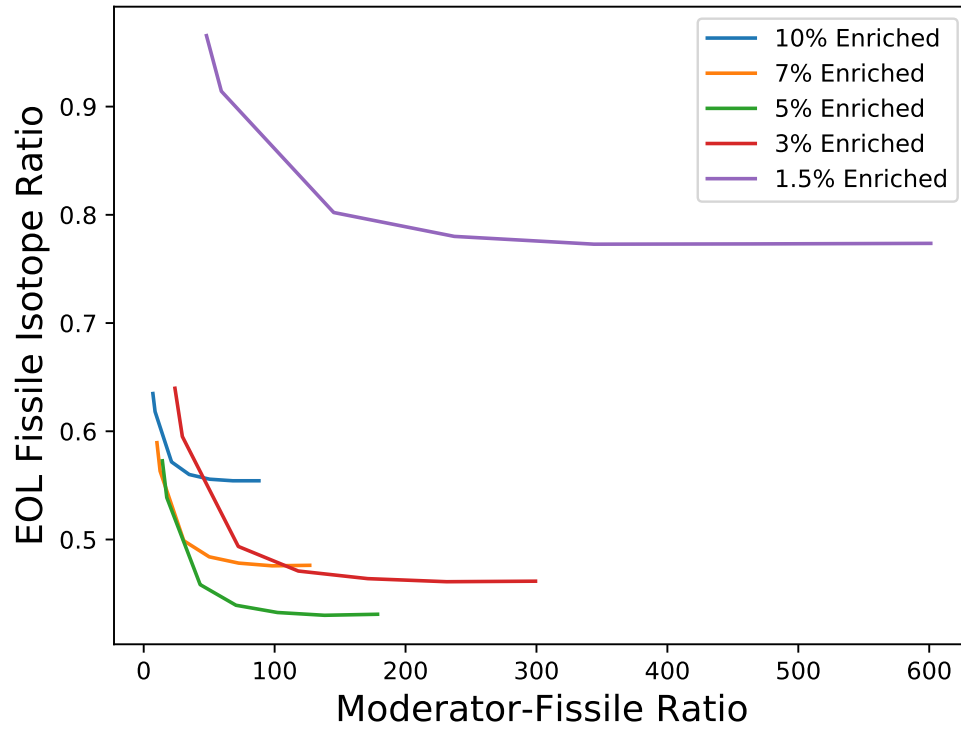


Figure A.18: FIR at EOL for zirconium hydride as a function of moderator to fissile ratio



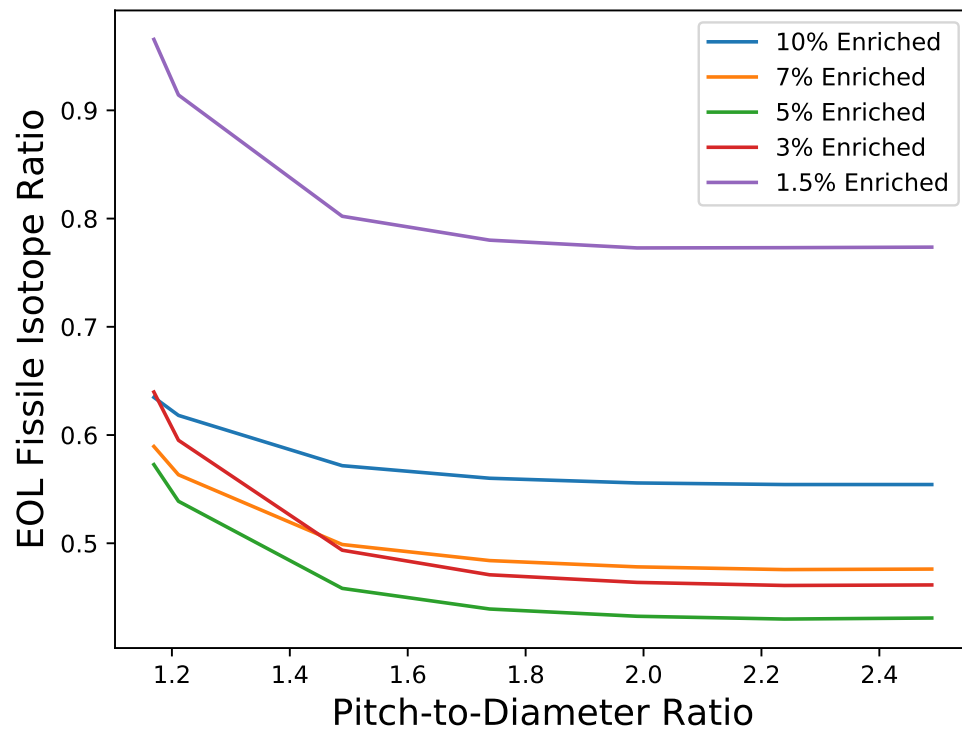


Figure A.19: FIR at EOL for zirconium hydride as a function of pitch to diameter ratio

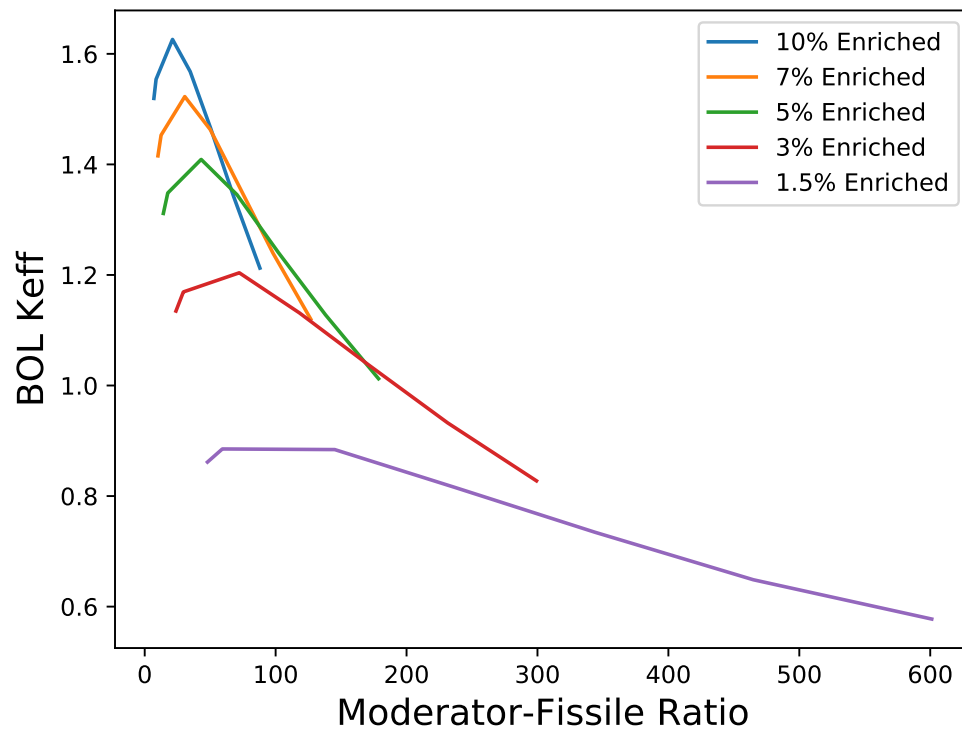


Figure A.20:  $k_{eff}$  at BOL for zirconium hydride as a function of moderator to fissile ratio

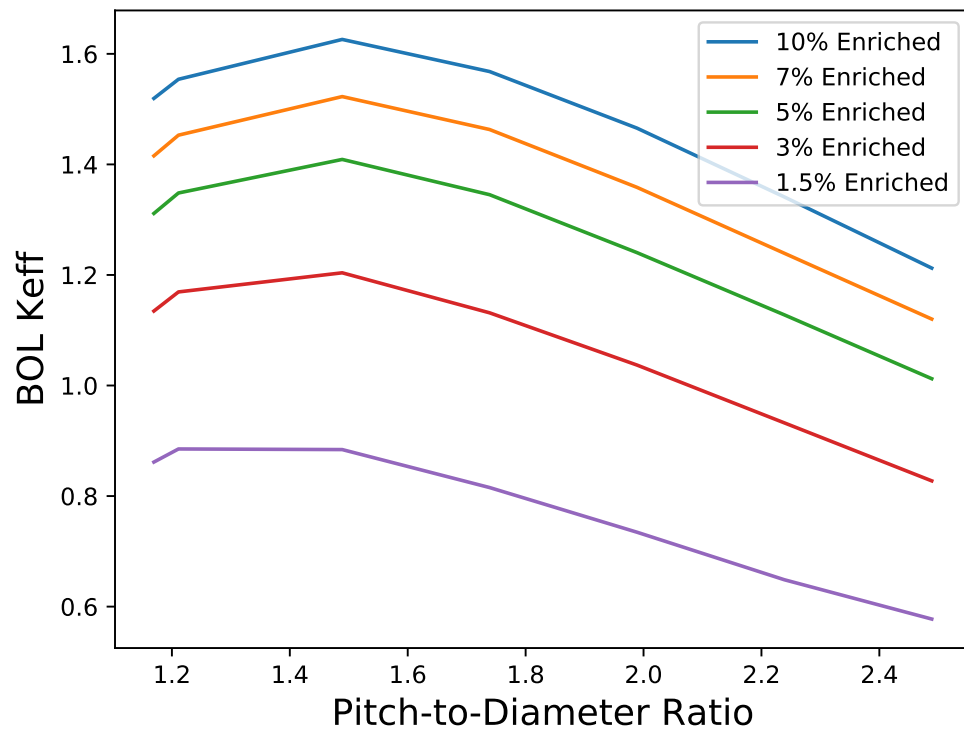


Figure A.21:  $k_{eff}$  at BOL for zirconium hydride as a function of pitch to diameter ratio

## Light Water

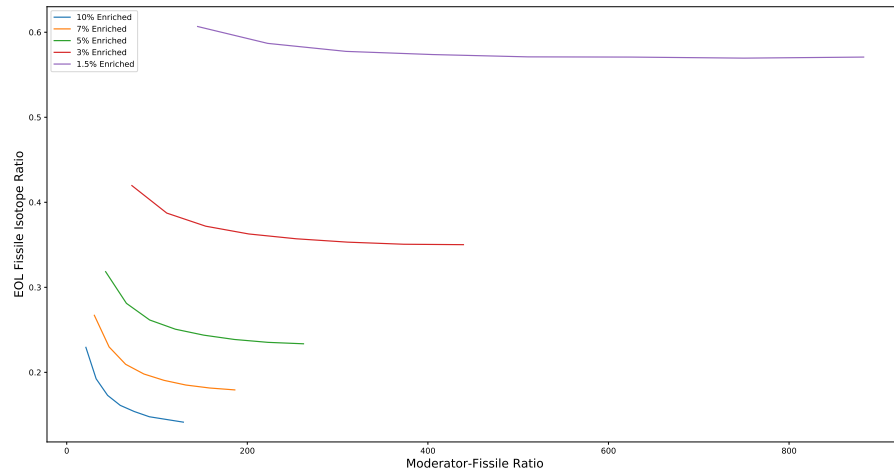


Figure A.22: FIR at EOL for light water as a function of moderator to fissile ratio

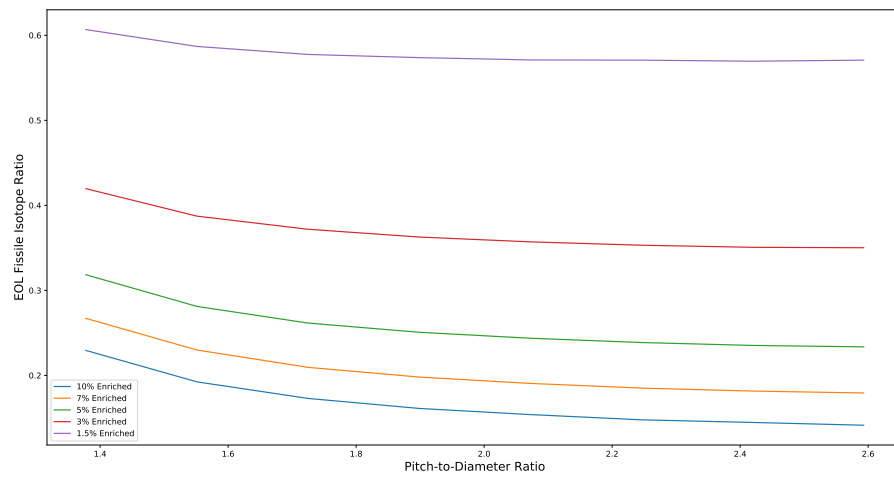


Figure A.23: FIR at EOL for light water as a function of pitch to diameter ratio

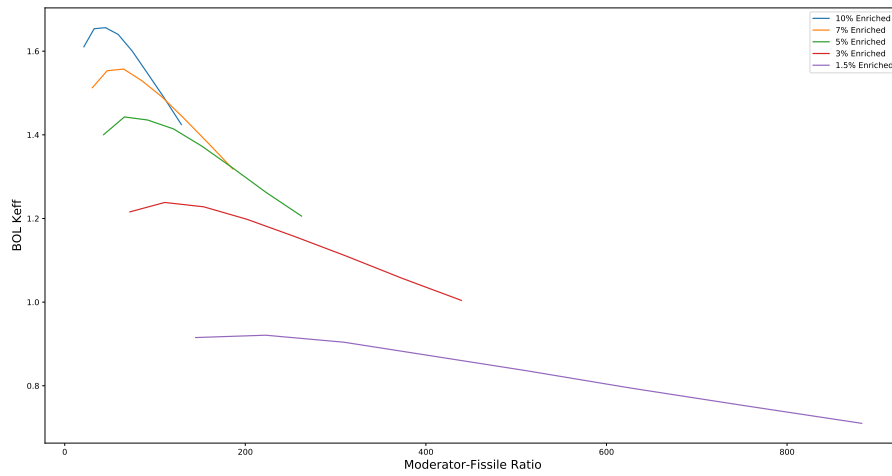


Figure A.24:  $k_{eff}$  at BOL for light water as a function of moderator to fissile ratio

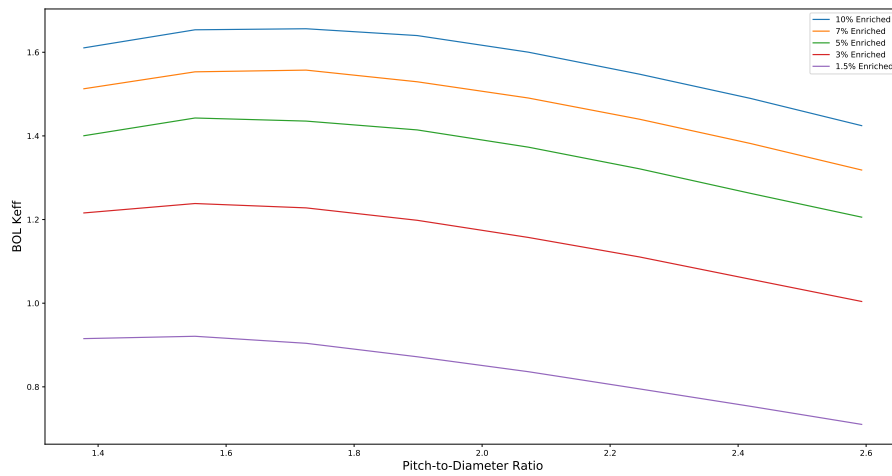


Figure A.25:  $k_{eff}$  at BOL for light water as a function of pitch to diameter ratio